International Journal of Nanomedicine

Dovepress
Taylor & Francis Group

Open Access Full Text Article

REVIEW

Recent Advancement in MRI-Based Nanotheranostic Agents for Tumor Diagnosis and Therapy Integration

Li Zhu[1], Yu Jiang[1], Haijun Tian[1], Yongle Yu[1], Ye Gan[1], Hong Li[1], Mingqing Yuan[1], Xialing Huang[2], Xu Liu[1]

[1]Guangxi Key Laboratory of Special Biomedicine; School of Medicine, Guangxi University, Nanning, Guangxi Zhuang Autonomous Region, 530004, People's Republic of China; [2]Department of Radiology, The First Affiliated Hospital of Guangxi Medical University, Nanning, Guangxi Zhuang Autonomous Region, 530021, People's Republic of China

Correspondence: Mingqing Yuan; Xu Liu, Email yuanmingqing1985@163.com; wedaoliuxu@163.com

Abstract: Cancer remains one of the leading causes of mortality worldwide. Although conventional treatment strategies such as chemotherapy, radiotherapy, and surgery have demonstrated therapeutic potential, their clinical effectiveness is often limited by poor targeting specificity, systemic toxicity, and inadequate treatment monitoring. Magnetic resonance imaging (MRI) has emerged as a powerful diagnostic modality owing to its non-invasive nature, high spatial resolution, deep tissue penetration, and real-time imaging capabilities, making it particularly suitable for guiding and evaluating cancer therapies. Recent advances have led to the development of MRI-based nanotheranostic platforms that integrate diagnostic and therapeutic functions within a single system, enabling precise tumor imaging alongside targeted treatment. This review presents a comprehensive overview of recent progress in MRI-guided nanotheranostic agents for cancer diagnosis and therapy, with a focus on their structural design, functional mechanisms, and biomedical applications in both single treatment approaches such as photothermal therapy, photodynamic therapy, chemodynamic therapy, immunotherapy, and ferroptosis, as well as combined therapeutic strategies. In addition, the contribution of MRI to improving treatment precision through image-guided delivery, real-time therapeutic monitoring, and stimulus-responsive activation is discussed. Key challenges including biosafety, design complexity, and barriers to clinical translation are also examined, along with perspectives on future directions for developing intelligent and clinically viable MRI-integrated therapeutic systems.

Keywords: MRI, diagnosis and therapy integration, nanotheranostic agents, nanomedicine, anti-tumor

Introduction

Cancer is a major global social, public health, and economic burden, accounting for approximately one-sixth of all deaths worldwide. The latest estimates from the International Agency for Research on Cancer (IARC) indicate that nearly 20 million new cancer cases, including non-melanoma skin cancer (NMSC), were diagnosed worldwide in 2022. This figure is projected to increase to 35 million by 2050.[1–3] These alarming figures underscore the need for more precise diagnostic tools and effective treatments. In response, theranostics has emerged as a key biomedicine innovation and research focus.[4] Theranostics integrates diagnostic and therapeutic agents into a single nanosystem, enabling concurrent tumor diagnosis, targeted therapy, and real-time treatment monitoring.[5–7] This integration can revolutionize cancer treatment through personalized, efficient, and effective management.

Magnetic Resonance Imaging (MRI) is a non-invasive, radiation-free imaging modality effective, making it highly valuable for cancer treatment, particularly in diagnosing emerging therapies. Its high-resolution imaging of soft tissues, organs, and blood vessels is essential for advancing integrated theranostic systems.[8–11] MRI contrast agents are essential for improving diagnostics by enhancing tumor-to-normal tissue contrast, shortening imaging time, and improving diagnostic accuracy.[12–15] However, traditional MRI contrast agents face limitations in specificity, sensitivity, and biocompatibility, limiting their efficacy in tumor diagnosis and therapy. To overcome these challenges, researchers are exploring MRI-guided nanotheranostic agents. These innovative agents not only enhance tumor imaging clarity but also facilitate targeted drug delivery and controlled release, enabling precise, targeted, and personalized tumor therapies. Moreover, to further enhance diagnostic precision, some MRI-guided nanoplatforms have been engineered for multimodal imaging, integrating

Received: 18 March 2025
Accepted: 16 July 2025
Published: 29 August 2025

Graphical Abstract

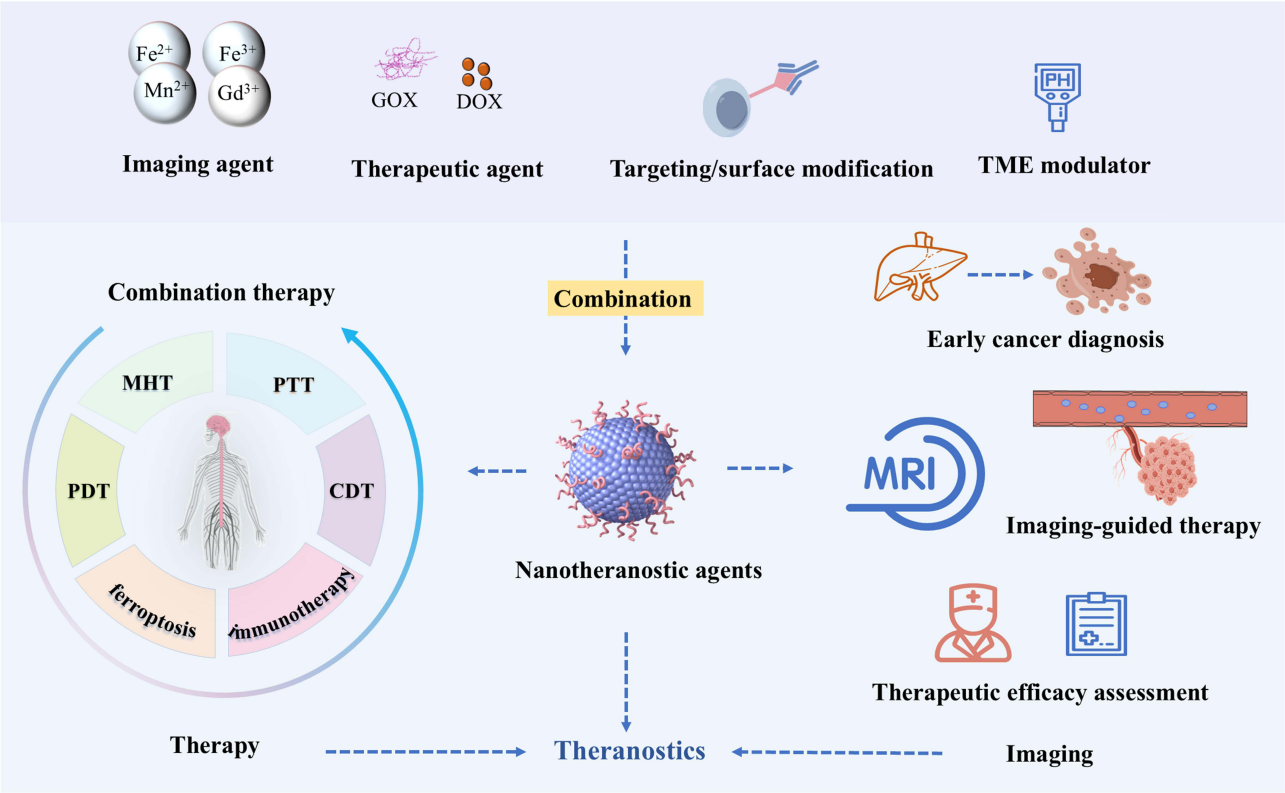

MRI with fluorescence or photoacoustic imaging.[16–18] These dual-modal systems leverage the strengths of MRI's deep tissue penetration and high spatial resolution, while incorporating complementary modalities that offer superior sensitivity or functional readouts.

Traditional cancer treatments, such as surgical resection, chemotherapy, and radiotherapy, remain core strategies in tumor treatment, yet they have significant limitations. Surgical resection is limited by challenges in accurately identifying tumor margins, hindering complete cancer cell removal and elevating recurrence risk. While chemotherapy and radiotherapy can suppress tumor growth, they damage healthy tissues, resulting in substantial side effects.[19–22] A major concern is the risk of tumor cells developing resistance, diminishing treatment efficacy over time. To address these challenges, the medical community is exploring novel cancer treatment strategies. The rapid advancement of nanomaterials and nanomedicine has offered promising solutions. Nanomaterials provide key advantages, such as enhanced drug targeting, better tumor penetration, controlled drug release, tumor microenvironment modulation, and multifunctionality.[23–26] Significant progress has been made in developing nanomaterial-based cancer therapies, including magnetic hyperthermia therapy (MHT), photothermal therapy (PTT), photodynamic therapy (PDT), chemodynamic therapy (CDT), immunotherapy, and ferroptosis therapy. These approaches leverage the unique properties of nanomaterials, paving the way for more effective treatments.

Building on these advancements, researchers have focused on designing MRI contrast agents that effectively combine therapeutic agents (photothermal converters, photosensitizers, and Fenton reagents), targeting agents (targeting ligands or components responsive to external stimuli), and imaging agents (iron oxide, gadolinium, or manganese). These innovations enable the seamless integration of diagnosis and therapy.

Despite the growing number of studies on MRI-guided cancer therapy and the emergence of various MRI-functionalized nanoplatforms, there remains a lack of comprehensive reviews that integrate recent advancements in nanomaterial design,

imaging–therapy coordination, and treatment strategy optimization. Existing reviews often focus on isolated aspects, such as imaging contrast or therapeutic efficacy, without fully capturing how MRI can serve as a central platform for integrating precise diagnosis with targeted, controllable cancer therapy. Therefore, a systematic review that highlights the evolving role of MRI-based nanotheranostics in both monotherapy and combination strategies is timely and necessary.

This article explores the development of nanotheranostics with magnetic resonance imaging (MRI) capabilities and their progress in cancer treatment applications. It systematically examines the construction methods of multifunctional nanotheranostics for various treatment strategies, including magnetic hyperthermia therapy (MHT), photothermal therapy (PTT), photodynamic therapy (PDT), chemodynamic therapy (CDT), immunotherapy, and ferroptosis therapy, both as standalone and in combination (Figure 1). Additionally, the paper provides a detailed overview of their development, application, and future potential. Finally, it discusses the current challenges, opportunities, and key directions for future research in this rapidly evolving field.

Single Cancer Therapy

Single-modality cancer therapies—including magnetic hyperthermia therapy (MHT), photothermal therapy (PTT), photodynamic therapy (PDT), chemodynamic therapy (CDT), immunotherapy, and ferroptosis-based therapy (FT)—employ distinct mechanisms such as localized heating, oxidative stress, immune activation, or metabolic disruption to selectively eliminate tumor cells. Despite their mechanistic diversity, these approaches share several important characteristics that make them highly compatible with magnetic resonance imaging (MRI). First, most of these therapies utilize nanomaterials that can be engineered for enhanced biocompatibility, tumor-targeted delivery, and responsiveness to tumor microenvironment (TME) cues such as acidity, hypoxia, or elevated H_2O_2 levels. Second, many of them rely on the generation of heat or reactive oxygen species (ROS) to trigger cytotoxic effects, which can be spatiotemporally regulated through external stimuli. Third, the nanomaterials used are often amenable to MRI functionalization by incorporating paramagnetic elements (eg, Fe^{3+}, Gd^{3+}, Mn^{2+}) or magnetic structures, enabling high-resolution imaging, real-time tracking, and noninvasive treatment monitoring. By integrating MRI, these therapies benefit from improved precision in agent localization, timing control, and response assessment, which helps to overcome limitations such as nonspecific distribution and delayed therapeutic feedback. This image-guided approach not only enhances safety and

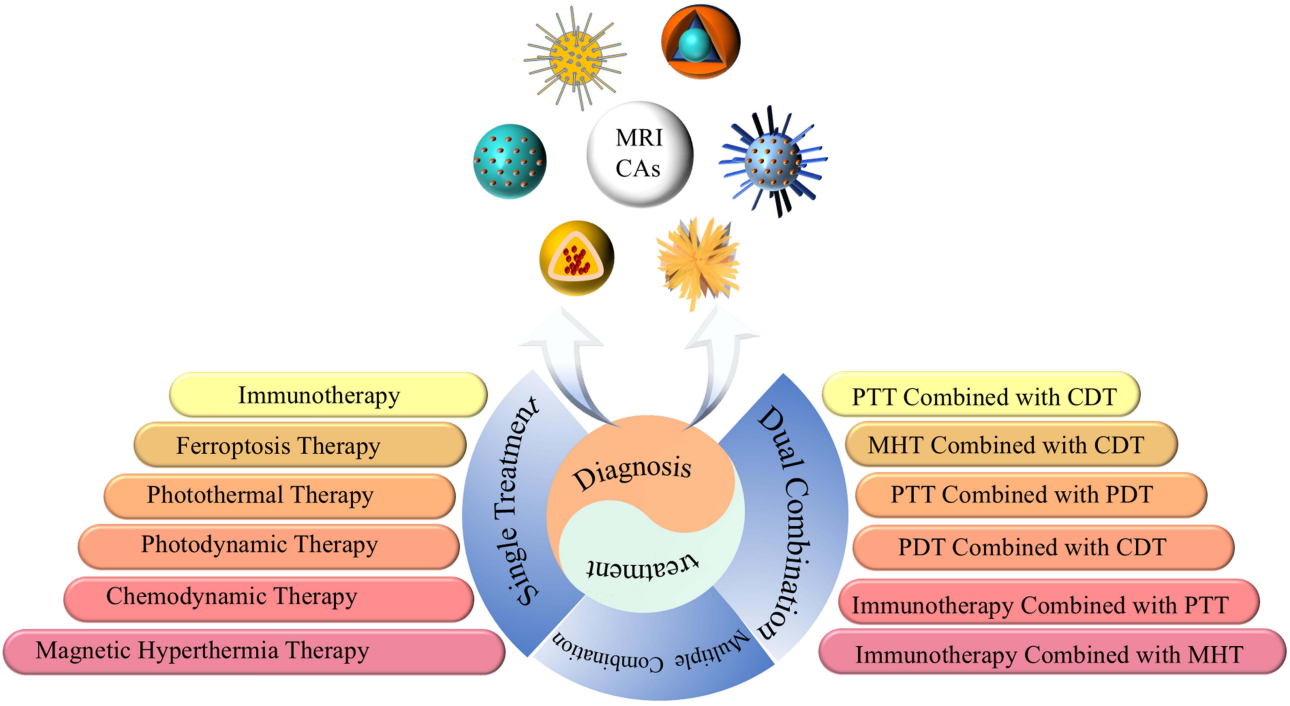

Figure 1 Application of MRI-based nanotheranostic agents in integrated tumor treatment strategies.

https://doi.org/10.2147/IJN.S529003

efficacy but also facilitates the development of theranostic platforms that unify diagnosis and therapy, thereby broadening the clinical potential of single-modality strategies for personalized cancer treatment. The following sections elaborate on each modality's mechanisms, representative materials, technical challenges, and MRI-based enhancements.

Magnetic Hyperthermia Therapy (MHT)

Unlike healthy tissues, cancer cells develop a complex vascular network to support survival and metastasis. It causes slower blood flow in tumors, leading to localized hyperthermia. In contrast, normal tissues maintain regular blood flow and heat dissipation, making cancerous tissues more sensitive to elevated temperatures.[27,28] Studies show that at 41°C to 45°C, cancer cell viability is reduced, while healthy cells survive.[29] This sensitivity has led to hyperthermia-based tumor treatments. Magnetic hyperthermia therapy (MHT) uses an alternating magnetic field (AMF) to heat magnetic nanoparticles.[30–32] Under AMF exposure, these nanoparticles generate localized heat in the tumor, inducing cancer cell apoptosis or necrosis. Moreover, magnetic nanoparticles can be guided to the tumor site and used for MRI under an external magnetic field (Figure 2).[33,34] The main challenge in MHT application is precisely controlling energy delivery to target therapy and avoid non-specific heating of normal tissues.[35]

Superparamagnetic iron oxide nanoparticles (MIONPs) are commonly used in MHT for their excellent magnetic properties and biocompatibility.[36] An example is Fe_3O_4@PLA-PEG, a nanotheranostic agent with a magnetic Fe_3O_4 core and PLA-PEG shell, loaded with ~11% curcumin as an anticancer agent.[37] The PLA-PEG coating enhances Fe_3O_4 @PLA-PEG 's magnetization and heating efficiency, making it an effective T2-weighted MRI contrast agent and hyperthermia transducer. Fe_3O_4@PLA-PEG can rapidly and efficiently release the drug in response to an external magnetic field, combining drug and thermal therapies for tumors, showing significant potential in cancer treatment. The magnetic hyperthermia performance of these nanoparticles is illustrated in.

Ongoing research aims to enhance the magnetic heat conversion efficiency and MRI performance of MIONPs through various strategies. Two effective strategies are doping and controlling nanoparticle shape, size, and surface functionalization. Doping with rare earth elements (eg, Sm^{3+}, Eu^{3+}, Gd^{3+}, Ho^{3+}) influences stress anisotropy, magnetic moment, and other properties of MIONPs, significantly enhancing magnetization strength, improving thermal therapeutic effects and MRI contrast.[38–43] MIONPs with various shapes, sizes, and surface modifications have been developed for advanced

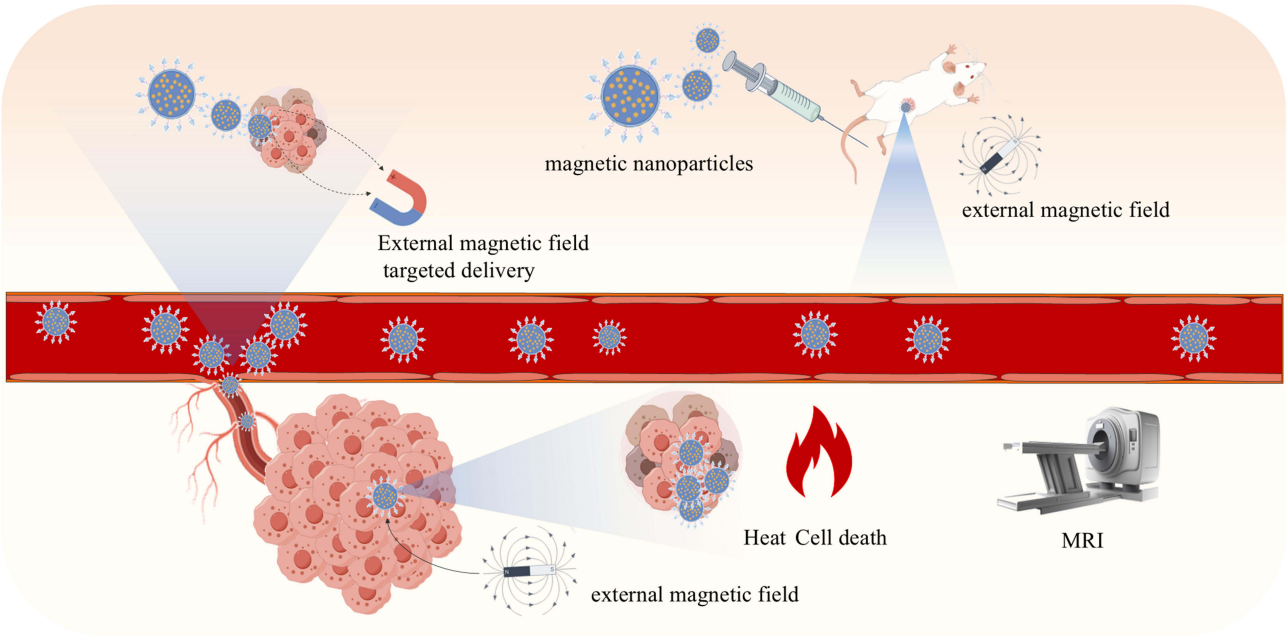

Figure 2 Mechanism of action of magnetic nanoparticles in magnetothermal therapy. By intravenous injection, magnetic nanoparticles can be precisely localized to the tumor area under the guidance of an external magnetic field, where they accumulate in large quantities. Once they reach the target location, they produce a local thermal effect under the action of the magnetic field, leading to the death of tumor cells. In addition, this therapy can be monitored in real time by MRI.

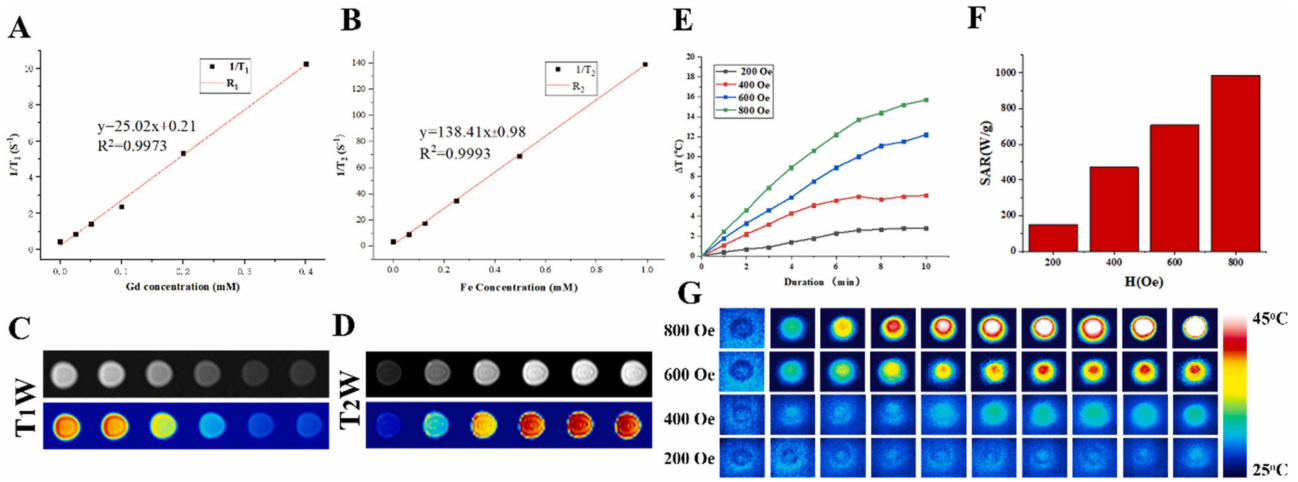

Figure 3 MRI relaxation behavior and magnetic hyperthermia performance of VNFG nanomaterials. (**A**–**B**) Longitudinal (R1) and transverse (R2) relaxation rates of VNFG at different metal concentrations. (**C**–**D**) Axial T1- and T2-weighted MR images showing signal intensity variations. (**E**–**F**) Temperature elevation curves and specific absorption rate (SAR) values under different alternating magnetic fields (AMF). (**G**) Infrared thermal imaging during magnetic heating. Reproduced from Bao JF, Guo SS, Zu XY, et al. Magnetic vortex nanoring coated with gadolinium oxide for highly enhanced T1-T2 dual-modality magnetic resonance imaging-guided magnetic hyperthermia cancer ablation. *Biomed Pharmacother.* 2022;150:112926. Licensed under Creative Commons Attribution-NonCommercial-NoDerivatives 4.0 International License (https://creativecommons.org/licenses/by-nc-nd/4.0/).[45]

nanotheranostics. For example, multi-core magnetic iron oxide nanoparticles, formed by assembling partially melted maghemite (γ-Fe_2O_3) particles into a flower-like structure, show enhanced magnetization while retaining superparamagnetic properties. These multi-core nanoparticles have thermal therapeutic efficiency an order of magnitude higher than single-core nanoparticles under similar conditions, making them promising candidates for next-generation magnetic hyperthermia and T2-weighted MRI materials.[44] Bao and colleagues developed the multifunctional nanotheranostic agent VNFG (Fe3O4@Gd2O3) by integrating these strategies. The nano-ring structure of Fe3O4 enhances magnetic heat conversion efficiency, while the polyethyleneimine (PEI) and Gd2O3 shell minimizes magnetic interference between the core and shell, improving both magnetic hyperthermia performance and T1-T2 dual-modal imaging effects of VNFG 42. As illustrated in (Figure 3), VNFG demonstrates robust MRI relaxation properties (R1 and R2 plots) and provides clear T1-weighted and T2-weighted images across various concentrations, highlighting its diagnostic potential. Furthermore, its excellent magnetic heat capacity, evidenced by time-dependent temperature profiles and heating capacity plots under different alternating magnetic fields (AMF), underscores its strong therapeutic performance in magnetic hyperthermia.[45]

Other iron-based nanoparticles, besides MIONPs, show promise in Magnetic Hyperthermia Therapy (MHT). FePt nanoparticles stand out for their superior magnetic properties and high saturation magnetization, making them effective MRI contrast agents and efficient heat converters. The multifunctional agent, FePt@MMT-MIT, exhibits high saturation magnetization and strong T2-weighted MRI contrast, enabling clear visualization of hepatocellular carcinoma (HCC). It also induces magnetic hyperthermia, effectively destroying tumor cells.[46] The combination of iron and gold elements offers a promising approach. Pearson et al developed flower-like Au@Fe nanoparticles through seed-assisted synthesis. These Au@Fe-PEG nanoparticles serve as contrast agents for MRI and CT, demonstrating excellent multimodal imaging properties. Additionally, these nanoflowers show high thermal conversion efficiency under alternating magnetic fields and near-infrared light, with low cytotoxicity, making them ideal for MHT and PTT.[47] Iron-based hollow nanoparticles offer another exciting avenue for MHT. Their hollow structure allows water molecules to penetrate the center of the magnetic ions, enhancing contrast performance. Additionally, these nanoparticles can be loaded with various therapeutic agents, supporting a range of treatment modalities.[48]

Photothermal Therapy (PTT)

Photothermal therapy (PTT) uses photothermal agents (PTAs) to convert light into heat, raising the temperature at the target and inducing cancer cell death.[49,50] In PTT, near-infrared (NIR) laser irradiation targets tumors or metastatic sites, minimizing damage to healthy tissues, while the method's minimally invasive and remote-controlled nature highlights its significant

potential in cancer therapy.[50,51] Common PTAs include noble metals like Au and Ag, carbon-based materials such as graphene oxide and carbon nanotubes, metal sulfides and oxides like copper sulfide and magnetite, and organic dyes including Indocyanine Green and Prussian blue.[52] Despite their effectiveness, the use of these PTAs is limited by challenges such as their lack of specificity and the inability to visualize drug delivery, internalization, and metabolic processes. These limitations hinder precise targeting and monitoring, which are essential for achieving optimal therapeutic outcomes in cancer treatment.

In recent years, composite nanomaterials combining magnetic nanoparticles (such as iron, manganese, and their oxides) with gold have attracted considerable attention as promising multifunctional agents. These materials exhibit excellent photothermal conversion efficiency and strong magnetic properties. Consequently, they have been widely investigated for various biomedical applications, including magnetic resonance MR imaging, magnetically targeted drug delivery, light-triggered drug release, and PTT (Figure 4a). Liu and colleagues reported a glutathione (GSH)-responsive magnetic gold nanotube (AuNWs) (Figure 4b).[53] The core of this nanoplatform, composed of gold nanotubes (AuNWs), exhibits enhanced photothermal performance due to its gold branches and central pores. The outer shell consists of assembled ultra-small magnetic iron oxide nanoparticles (ES-MIONs). Experimental results have demonstrated that magnetic AuNWs show significantly higher tumor accumulation compared to individual ES-MIONs, with a 2.5-fold increase in T1 imaging signal 24 hours post-injection and greater tumor eradication efficiency. Additionally, Polydopamine (PDA) and mesoporous polydopamine (MPDA) have emerged as promising photothermal agents due to their excellent biodegradability, low long-term toxicity, ease of surface modification, and high photothermal conversion efficiency.[54–56] In PTT, they are often used to functionalize the surfaces of magnetic nanoparticles, enabling both imaging and therapeutic capabilities. For instance, Li and colleagues developed a magnetic nanotheranostic agent using PDA-modified Fe_3O_4, where the PDA shell contributes to enhanced biocompatibility, stability, and efficient photothermal effects.[57] In experimental studies, these nanoparticles exhibited a high transverse relaxivity (337.8 $mM^{-1}s^{-1}$). Moreover, the high photothermal conversion efficiency of PDA enabled the complete eradication of tumors in 4T1 tumor-bearing mice after PTT treatment.

To enhance the efficacy of PTT, researchers are actively developing new multifunctional PTAs and exploring advanced strategies like the use of the second near-infrared window (NIR-II, 1000–1700 nm) and the inhibition of heat shock proteins (HSPs).[58,59] Compared to the first near-infrared window (NIR-I, 700–950 nm), NIR-II offers longer wavelengths, deeper tissue penetration, and fewer side effects, making it particularly advantageous for PTT applications (Figure 5a).[60–62] Zhang

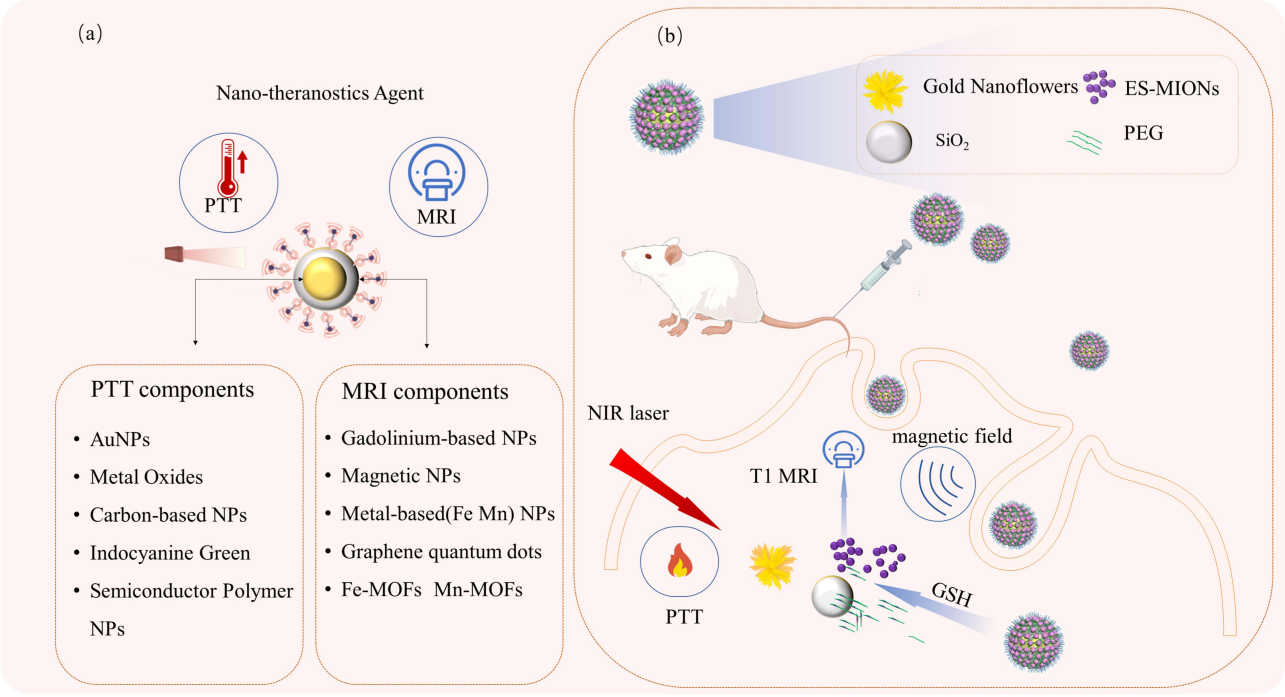

Figure 4 (**a**) Nanotheranostics materials and (**b**) application examples that can be used for PTT and MRI.

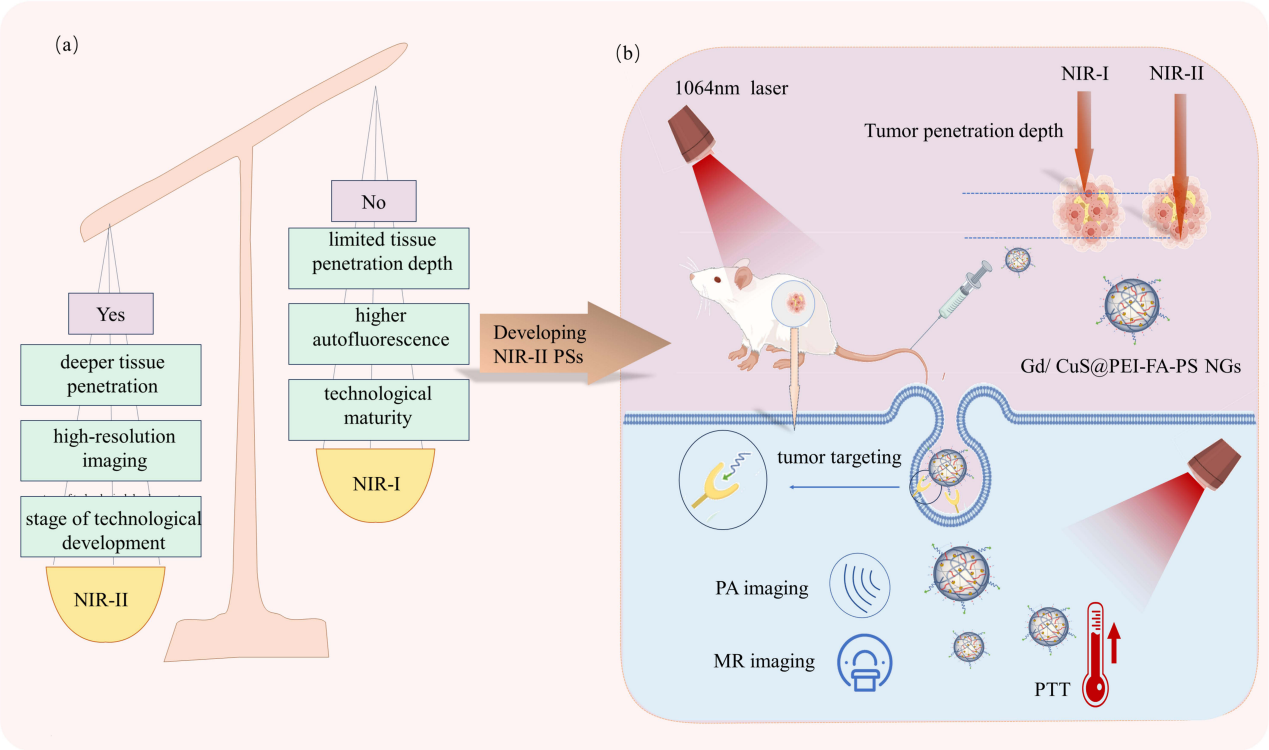

Figure 5 (**a**) Comparison of advantages and disadvantages of NIR-II and NIR-I in PTT, and (**b**) actual application examples of NIR-II in PTT.

et al developed a theranostic agent, Gd/CuS@PEI-FA-PS NGs, for PTT guided by MRI, which leverages the NIR-II absorption properties of copper sulfide (CuS), making it highly promising for precise and effective cancer treatment (Figure 5b).[63] HSPs are overexpressed in tumor cells and can induce thermotolerance by repairing proteins damaged during PTT.[64–66] Therefore, suppressing HSP expression is crucial for improving the therapeutic outcomes of PTT. Yao et al developed $Zn_{0.2}Fe_{2.8}O_4$@PDA@MnO_2 NPs for T1/T2 dual-modality MRI-guided self-enhanced PTT. It releases Mn^{2+} by consuming the high levels of GSH found in tumors, which triggers the Fenton reaction to suppress HSP expression, thereby enhancing the PTT effect. This multifunctional agent offers a promising approach for future PTT drug development.[67]

Photodynamic Therapy (PDT)

Photodynamic therapy (PDT) utilizes light to activate photosensitizers (PSs) in oxygenated tissues, generating cytotoxic reactive oxygen species (ROS) that induce apoptosis or necrosis.[68,69] Additionally, PDT can trigger anti-tumor immune responses by inducing immunogenic cell death (ICD) in tumor cells.[70–72] With high selectivity, minimal invasiveness, low side effects, and precise spatiotemporal control, PDT offers a promising alternative to conventional cancer therapies. However, its broader application is hindered by limited light penetration, insufficient PS accumulation at tumor sites, tumor heterogeneity, and hypoxic conditions. To overcome these challenges, researchers are devising strategies to enhance PDT efficacy. Recent advancements in PDT focus on optimizing light sources, designing novel PSs, and mitigating tumor hypoxia.[73]

Porphyrins and their derivatives, naturally occurring molecules, are essential for light absorption, oxygen transport, and catalysis. Their exceptional light-trapping ability, high singlet oxygen quantum yield, and chemical versatility make them highly efficient photosensitizers.[74–76] Porphyrins act as versatile host molecules, binding with diverse metals like paramagnetic manganese (Mn), copper (Cu), and gadolinium (Gd) to form metalloporphyrin derivatives with strong chelating properties.[77] These derivatives can be encapsulated, grafted onto nanoparticles, or self-assembled at the nanoscale, enhancing phototherapy and MRI performance.[78] Manganese- and gadolinium-porphyrin chelates are the most widely used porphyrin-based nanocomplexes for MRI nanotheranostic.[79,80] For instance, Wang et al reported that incorporating fullerene derivatives into manganese(III) porphyrin with PDT functionality significantly improved water proton relaxation properties, thereby

https://doi.org/10.2147/IJN.S529003

enhancing MRI performance.[81] Similarly, Yuzhakova et al developed multifunctional nanotheranostic agents, GdPz1 and GdPz2, by integrating gadolinium(III) cations into a porphyrin pigment platform. These agents enable fluorescence imaging, MRI, and PDT within a single nanoplatform.[82] Linear P-conjugated Zn(II)-porphyrin dimers complexed with Gd-DOTA serve as MRI-PDT theranostic agents. They effectively induce cell death in experimental studies, and the combination of MRI contrast agents with PDT drugs provides a synergistic effect for drug localization imaging.[83]

Porphyrins and their derivatives, despite being traditional photosensitizers, often suffer from aggregation-induced quenching (ACQ) in physiological environments. This aggregation causes fluorescence quenching and lowers ROS generation. AIE-PSs exhibit high signal-to-noise ratios, minimal self-absorption, and photobleaching resistance, enhancing luminescence and ROS generation to overcome conventional PS limitations.[84–86] To enhance photodynamic therapy (PDT) efficacy, Wang et al developed MUM nanoparticles (MUM NPs) by integrating aggregation-induced emission photosensitizers (AIE-PSs) with upconversion nanoparticles (UCNPs).[87] The UCNPs serve as NIR-to-UV/Vis light converters, effectively exciting AIE-PSs under near-infrared (NIR) irradiation to trigger reactive oxygen species (ROS) generation. This triple-jump energy conversion process not only amplifies PDT effects but also enables dual-modal fluorescence (FLI) and magnetic resonance imaging (MRI)-guided tumor therapy, as illustrated in (Figure 6).

Numerous strategies have been developed to improve oxygenation in the tumor microenvironment and address tumor hypoxia. Fu et al designed a novel nanotheranostic agent, GMCD, by co-loading CAT and DVDMS in Mn-doped calcium phosphate nanoparticles.[88] It catalyzes intracellular glucose consumption via GOx, generating hydrogen peroxide. CAT decomposes hydrogen peroxide into oxygen and water, alleviating hypoxia and facilitating singlet oxygen production by DVDMS. The Mn^{2+}-triggered Fenton-like reaction amplifies oxidative damage, increasing tumor cell death. This process is monitored through

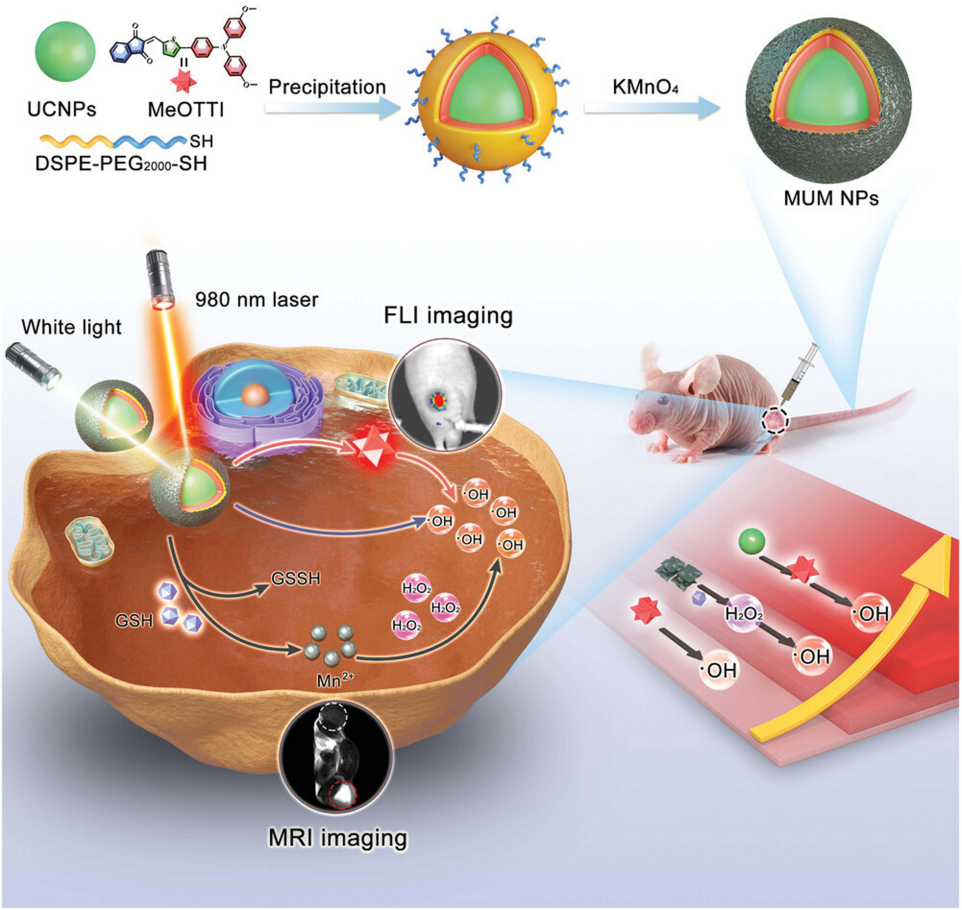

Figure 6 Schematic illustration of MUM NP synthesis and their triple-jump photodynamic process, featuring dual-modal fluorescence (FLI)/magnetic resonance imaging (MRI)-guided photodynamic therapy (PDT). Reproduced from Wang YW, Li YM, Zhang ZJ, Wang L, Wang D, Tang BZ. Triple-Jump Photodynamic Theranostics: MnO2 Combined Upconversion Nanoplatforms Involving a Type-I Photosensitizer with Aggregation-Induced Emission Characteristics for Potent Cancer Treatment. *Advanced Materials*. 2021;33(41).[87]

fluorescence and MRI, offering a spatiotemporally controllable strategy for cancer treatment. Recent research has shifted focus to reprogramming the tumor microenvironment (TME) to enhance PDT efficacy. Researchers, including Yu et al, have reviewed strategies to improve PDT outcomes, such as regulating tumor vascular stroma, disrupting tumor metabolism, and reprogramming immune-suppressive cells. These approaches are guiding the development of next-generation multifunctional PDT nanotheranostics.[89,90]

Chemical Dynamic Therapy (CDT)

Chemical Dynamic Therapy (CDT) is an innovative therapeutic approach that utilizes Fenton or Fenton-like reactions mediated by metal ions (such as Fe^{2+}, Mn^{2+}, Cu^{+}) to consume excess hydrogen peroxide (H_2O_2) in the tumor microenvironment, producing highly toxic hydroxyl radicals (•OH) that induce cancer cell death.[91–93] For efficient CDT, several key conditions must be met: (1) sufficient production of •OH within the tumor; (2) a rapid rate of •OH generation; and (3) the ability of the generated •OH to selectively and effectively target tumor cells.[94] However, the limited availability of H_2O_2 in the tumor microenvironment and the rapid clearance of •OH by GSH present significant challenges to the broader application of CDT in biomedical settings.

Increasing the concentration of hydrogen peroxide in the tumor can effectively promote CDT, and there are two main methods to achieve this (Figure 7a).[95] The first method delivers GOx, superoxide dismutase (SOD), or nano-drugs with catalytic activity to the tumor site, catalyzing in situ generation of endogenous H_2O_2.[96–99] The second approach directly delivers H_2O_2 to the tumor site using liposomes or metal oxides, releasing it in response to the tumor microenvironment or external stimuli, thereby increasing H_2O_2 concentration. Although more direct and effective, the second method risks unintended H_2O_2 leakage from the carrier, potentially causing side effects. Thus, for safety reasons, in situ generation of H_2O_2 with minimal side effects has become the preferred strategy to overcome low endogenous hydrogen peroxide levels. Manganese-based or iron-doped nanoparticles are popular carriers due to their ability to release ions in response to the tumor microenvironment, facilitating both Fenton reactions and MRI. Fu et al successfully developed a biodegradable, pH-responsive nano-diagnostic and therapeutic agent (GOx-MnCaP NPs) through the in situ mineralization of GOx. Even after mineralization, GOx retains its catalytic activity. In the acidic tumor microenvironment, GOx effectively converts glucose into H_2O_2, significantly increasing its concentration within the tumor and

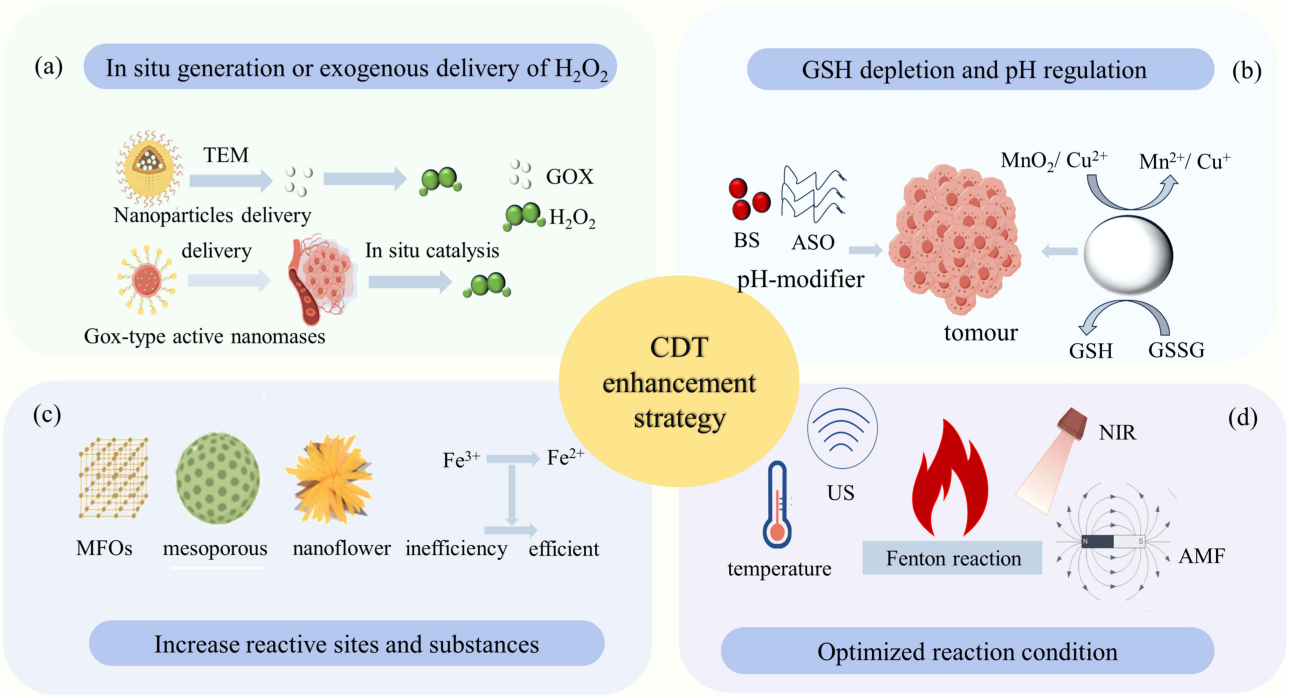

Figure 7 Schematic diagram of MRI-guided enhanced CDT effect strategies. (**a**) In situ generation or delivery of H_2O_2. (**b**) GSH depletion or pH adjustment. (**c**) Increasing reactive active sites. (**d**) Optimizing reaction conditions.

https://doi.org/10.2147/IJN.S529003

promoting Mn^2-triggered Fenton-like catalysis. Additionally, GOx-MnCaP serves as a pH-activated T1 contrast agent, enhancing MRI imaging performance.[100] Another approach involves developing nano-enzymes that mimic GOx activity to increase H_2O_2 concentration in tumors. Jiang and colleagues achieved this by designing MMF-Au nano-enzymes with GOx-like activity, triggering a cascade of glucose oxidation and Fenton-like reactions. In this process, ultra-small Au nanoparticles, which mimic GOx characteristics, catalyze the oxidation of endogenous glucose, generating H_2O_2 and gluconic acid. This leads to a substantial increase in H_2O_2 and a reduction in pH within the tumor microenvironment, further accelerating the decomposition of MMF and the release of Mn^{2+}. The released Mn^{2+} then catalyzes the conversion of the increased H_2O_2 into highly toxic hydroxyl radicals (•OH) via Fenton-like reactions, enhancing CDT. Meanwhile, the Mn^{2+} ions facilitate high-contrast T1-weighted MRI, allowing for precise monitoring of drug distribution.[101]

The second strategy to improve the efficiency of CDT is to modulate the reaction environment at the molecular level, such as lowering the pH and depleting GSH, to reduce the clearance of hydroxyl radicals (•OH) (Figure 7b). Zhu and colleagues developed a macrophage membrane-coated hollow mesoporous iron oxide nanotheranostic agent (HMFe) incorporating CA IX. CA IX, an effective pH-regulating enzyme, acidifies the tumor cell microenvironment, enhancing Fe-mediated Fenton reactions and reducing extracellular acidity to inhibit metastasis. Furthermore, HMFe enables efficient T2-weighted MRI to monitor drug biodistribution and therapeutic progress in real-time.[102] Moreover, antisense oligonucleotides (ASOs) have demonstrated promising pH-regulating properties in manganese-based nanotheranostic agents. ASOs can down-regulate the overexpressed monocarboxylate transporter 4 (MCT4) in tumor cells, thereby blocking lactic acid efflux and reducing the intracellular pH. This not only creates more favorable conditions for CDT catalytic reactions but also enhances the MRI signal.[103]

Besides increasing H_2O_2 concentration and adjusting the reaction environment, continuous and rapid generation of •OH and their precise action in tumor cells are crucial. Key strategies include promoting the conversion of high-valent ions to low-valent states or increasing reactive sites (Figure 7c). Metal-organic frameworks (MOFs), a novel class of porous nanomaterials, are particularly promising for CDT due to their large specific surface area and high porosity, which can significantly increase the number of reaction sites on the catalyst.[104] Moreover, optimizing reaction conditions through external stimuli—such as light, temperature, or ultrasound—can further enhance CDT efficiency (Figure 7d). For instance, integrating Fenton or Fenton-like reagents with photothermal agents or magnetothermal agents can leverage the synergistic effects of PTT or MTT to heat the tumor in situ. This localized heating accelerates the generation of •OH within the tumor, improving the therapeutic efficacy of CDT while minimizing damage to surrounding healthy tissues.

Immunotherapy

Immunotherapy leverages the host's immune system to identify and eradicate cancer cells, aiming to bolster the immune response against cancer while diminishing the tumor's capacity to evade immune surveillance.[105–108] Currently, the most common immunotherapy strategies include immune checkpoint blockade (ICB),[109] tumor vaccines,[110] immunogenic cell death (ICD),[111] and cGAS-STING pathway activation,[112] among others (Figure 8c). Tumor immunotherapy, despite its promise, faces several challenges stemming from the complexity of the tumor microenvironment, tumor heterogeneity, and its inherent mutability. These challenges include immune-related adverse events, pseudoprogression, tumor microenvironment-mediated immunosuppression, and the absence of reliable predictive biomarkers. MRI serves as a pivotal tool in immunotherapy by assessing therapeutic effects, monitoring tumor response, and distinguishing immune-related adverse events from actual disease progression. With advancements in MRI technology, its potential to enhance immunotherapy implementation and evaluation continues to grow.[113–115]

The development of multifunctional theranostic agents, which integrate immuno-oncology microenvironment modulators and/or immunological adjuvants with MRI components, offers a promising avenue (Figure 8a). Among the materials under investigation, manganese-based nanomaterials stand out for their potential in integrating MRI with tumor immunotherapy. These nanomaterials function both as biocompatible carriers for targeted immunotherapeutic drug delivery and as immunological adjuvants, modulating the tumor microenvironment and amplifying immune responses. Manganese-based nanomaterials can activate the cGAS-STING pathway, thereby stimulating the host's immune system. Additionally, they enhance T1-weighted MRI signals, enabling real-time monitoring of tumor immunotherapy outcomes.[116,117]

ICB strategies enhance the immune system's ability to target and destroy tumors by blocking checkpoint molecules such as CTLA-4, PD-1, and PD-L1 on immune cells using specific antibody drugs.[118,119] A bibliometric analysis of

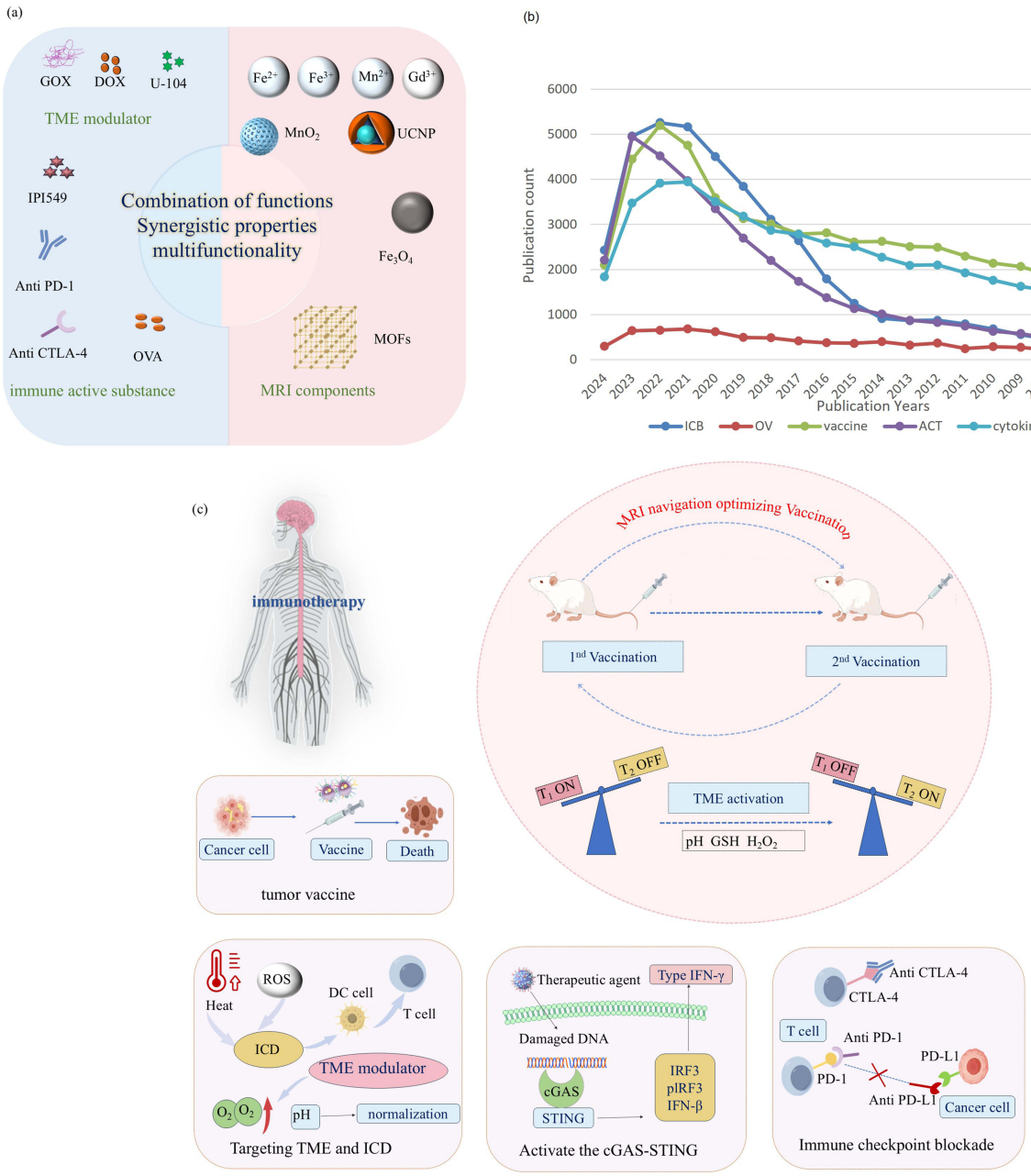

Figure 8 Construction strategies of MRI nanotheranostic agents in immunotherapy and their applications. (**a**) Construction of nano-diagnostic agents. (**b**) Trend analysis of the relevant publication volume of different immunotherapies in the last 20 years (**c**) Mechanisms of action of commonly used immunotherapies and a schematic diagram of MRI-guided immunotherapy, which describes in detail the MRI-guided vaccination cycle and the control of T1-addition through the mechanisms that control the switching of T1-weighted and T2-weighted MRI signals in response to TME.

literature in the Web of Science database reveals that ICB has become the most prominent topic in immunotherapy over the past two decades (Figure 8b). However, the acidic and hypoxic conditions within the tumor microenvironment can impair the effectiveness of ICB. These conditions reduce T cell activity and proliferation and hinder their infiltration into tumors through various mechanisms.[120–122] To overcome these challenges, researchers have developed the MRI-guided MRGIT strategy, which uses the pH-responsive nanotheranostic agent APPAM@U-104 to normalize the acidic tumor microenvironment and restore ICB's anti-tumor efficacy.[123] It generates a T1 "on" MRI signal in acidic environments, which switches to a T2 "on" signal upon neutralization of the tumor microenvironment, allowing real-time monitoring of tumor acidity, indicating reduced immunosuppression, and guiding anti-PD-L1 therapy timing. To address tumor hypoxia, Meng et al developed a multifunctional nano-regulator named BMI, based on bovine serum albumin (BSA),

https://doi.org/10.2147/IJN.S529003

which encapsulates MnO_2 particles and the PI3Kγ inhibitor IPI549.[124] Following intravenous injection, BMI accumulates extensively at the tumor site, where it utilizes manganese dioxide to consume hydrogen peroxide and generate oxygen, thereby alleviating hypoxia. Concurrently, BMI releases IPI549, which downregulates PI3Kγ expression in myeloid-derived suppressor cells (MDSCs). This action prompts a shift in macrophages from an immunosuppressive M2-like phenotype to a pro-inflammatory M1-like phenotype, restoring tumor sensitivity to ICB. BMI also serves as a tumor-specific MRI agent, enabling real-time monitoring of therapeutic outcomes. As additionally demonstrated in (Figure 9),

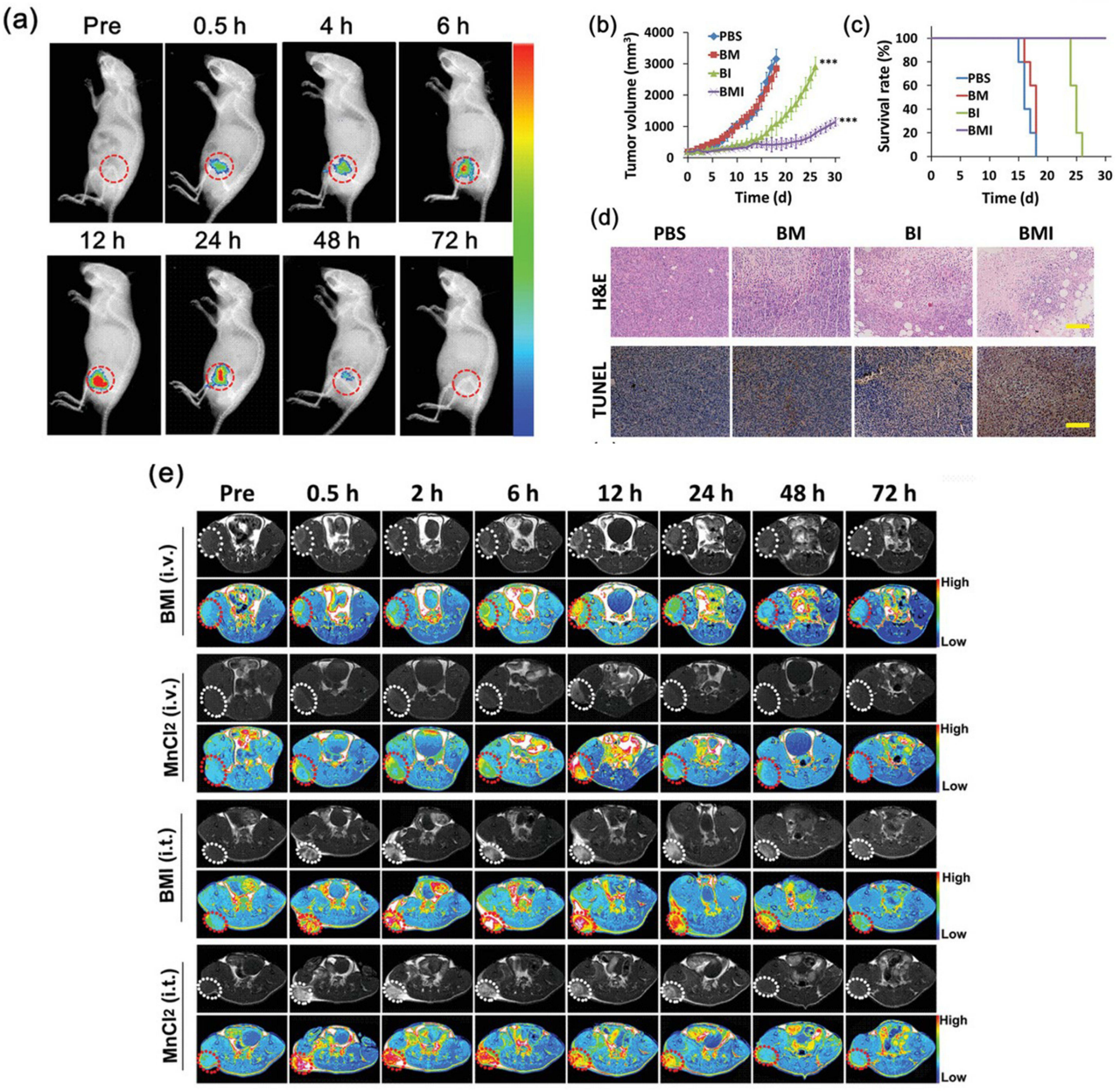

Figure 9 In vivo imaging, therapeutic efficacy, and histological analysis of the BMI nanoregulator for tumor immunotherapy. (**a**) In vivo fluorescence imaging (FLI) of 4T1 tumor-bearing mice at various time points (0–72 h) after intravenous injection of BMI. (**b**) Tumor growth curves of 4T1 tumor-bearing mice under different treatments (PBS, BM, BI, BMI. Data are presented as mean ± SD (n = 5). Significance between the treatment groups and control group during the medication treatment (0–18 d) was calculated using unpaired two-tailed Student's *t*-test. **P* < 0.05, ***P* < 0.01, ****P* < 0.001. (**c**) Survival rates of 4T1 tumor-bearing mice under the same treatment conditions (n = 5). (**d**) H&E and TUNEL staining of tumor sections from each treatment group. Scale bar in (**d**) represents 100 μm. (**e**) In vivo T1-weighted MRI tracking of BMI (i.v. and i.t.) and $MnCl_2$ (i.v. and i.t.) in 4T1 tumor-bearing mice over 72 h. Adapted from Yu M, Duan XH, Cai YJ et al. Multifunctional Nanoregulator Reshapes Immune Microenvironment and Enhances Immune Memory for Tumor Immunotherapy. *Advanced Science*. 2019;6(16), licensed under CC BY 4.0 (https://creativecommons.org/licenses/by/4.0/).[124]

in vivo imaging confirmed the favorable biodistribution of BMI and its strong TME-responsiveness in MRI, highlighting its accumulation and activation within the tumor. Moreover, further in vivo experiments in 4T1 tumor-bearing mice revealed significant enhancement of immunotherapeutic efficacy and negligible systemic toxicity following intravenous administration, supporting the clinical translational potential of this nanoregulator. Similarly, another nanotheranostic agent, NanoMnSor, was developed to combat hypoxia-driven tumor escape and suppress hepatocellular carcinoma. NanoMnSor co-delivers manganese dioxide and the anti-angiogenic drug sorafenib, combining the benefits of oxygen generation and anti-angiogenic therapy to enhance the overall effectiveness of cancer treatment.[125]

Combination therapy with immune checkpoint inhibitors and agents that activate the cGAS-STING pathway also has shown significant efficacy.[126] Recognizing the role of manganese in activating the cGAS-STING pathway, Huang et al developed a novel nanotheranostic system known as MCCS. This system is composed of manganese ions (Mn^{2+}), silk sericin (SS), a tumor-targeting pentapeptide (CREKA), and an anti-CTLA-4 antibody (aCTLA-4).[127] Studies have shown that MCCS effectively targets tumors, enhances T1-weighted MRI signals for precise imaging, and increases reactive ROS levels in tumor cells, activating the cGAS-STING pathway. This activation stimulates immune responses by promoting $CD8^+$ and $CD80^+$ T cell activity, reducing regulatory T cells, and boosting the secretion of interferon (IFN-γ) and granzyme. As a result, autophagy and apoptosis are induced in tumor cells both in vitro and in vivo. The addition of the anti-CTLA-4 antibody in MCCS further enhances the immune response by blocking immune checkpoints, enabling a more effective tumor attack. The combination of precise MRI imaging, immune modulation, and direct tumor cell killing makes MCCS a promising tool for integrated cancer diagnosis and treatment.

Cancer vaccines that use tumor-associated antigens or whole-cell components to stimulate the immune system's recognition and destruction of cancer cells are widely used immunotherapies. These vaccines induce long-term immune memory, enabling the immune system to recognize and respond to the same antigen in future encounters. However, free antigens are prone to degradation by enzymes in the bloodstream, limiting their effectiveness. To address this, some studies have focused on integrating nanomaterials with imaging capabilities to protect antigens and enable real-time therapeutic monitoring. For example, Xiao et al developed a multifunctional nano-vaccine (OMPN) by combining ovalbumin (OVA), MnO_2, and polydopamine.[128] In this formulation, MnO_2 serves as both an MRI contrast agent and an immunological adjuvant, allowing for real-time monitoring of the immunization process through MRI tracking, while also enhancing the immune response. Similarly, Huang et al designed a self-navigating nano-adjuvant composed of manganese carbonate integrated with a nano-vaccine. This nano-adjuvant degrades in the acidic environment of immune cells within lymph nodes, producing both T1 and T2 MRI signals to guide vaccination strategies.[129]

Ferroptosis Therapy (FT)

Ferroptosis, a form of cell death driven by iron-dependent lipid peroxidation, has emerged as a significant area of research in recent years.[130–133] This type of cell death is regulated by multiple factors, including the activity of glutathione peroxidase 4 (GPX4), the uptake and metabolism of iron ions, and the supply and synthesis of fatty acids.[134–136] While ferroptosis shares similarities with CDT, its therapeutic strategies differ. Ferroptosis plays a dual role in cancer treatment. On one hand, ferroptosis effectively eliminates tumor cells, stimulates the immune system's attack on cancer, and helps overcome drug resistance in tumor cells.[137,138] On the other hand, it can also release pro-inflammatory factors that trigger inflammatory responses, alter the tumor microenvironment, and reduce the immune susceptibility of tumor cells.[139] However, several factors limit the effectiveness of ferroptosis, including low intracellular concentrations of iron and H_2O_2, as well as the enhanced antioxidant defense mechanisms within tumors. The high levels of glutathione present in the tumor microenvironment further reduce the efficacy of ferroptosis by neutralizing ROS. To address these challenges, researchers have explored iron-doped and iron-based hybrid nanostructures, iron-organic frameworks, and iron oxide nanoparticles as potential ferroptosis inducers.[133,140–142] Recent advancements have led to new inducers that effectively target the ferroptosis pathway in cancer cells by promoting lipid peroxidation (LPO) or ROS accumulation. These inducers can also disrupt the ferroptosis defense mechanisms in cancer cells, enabling better control of the process (Figure 10).

Professor Zhe Yu Shen's team at Southern Medical University, inspired by the "cyclotron" principle in physics, proposed an innovative strategy to accelerate the generation of ROS within tumor cells. They developed a self-assembled

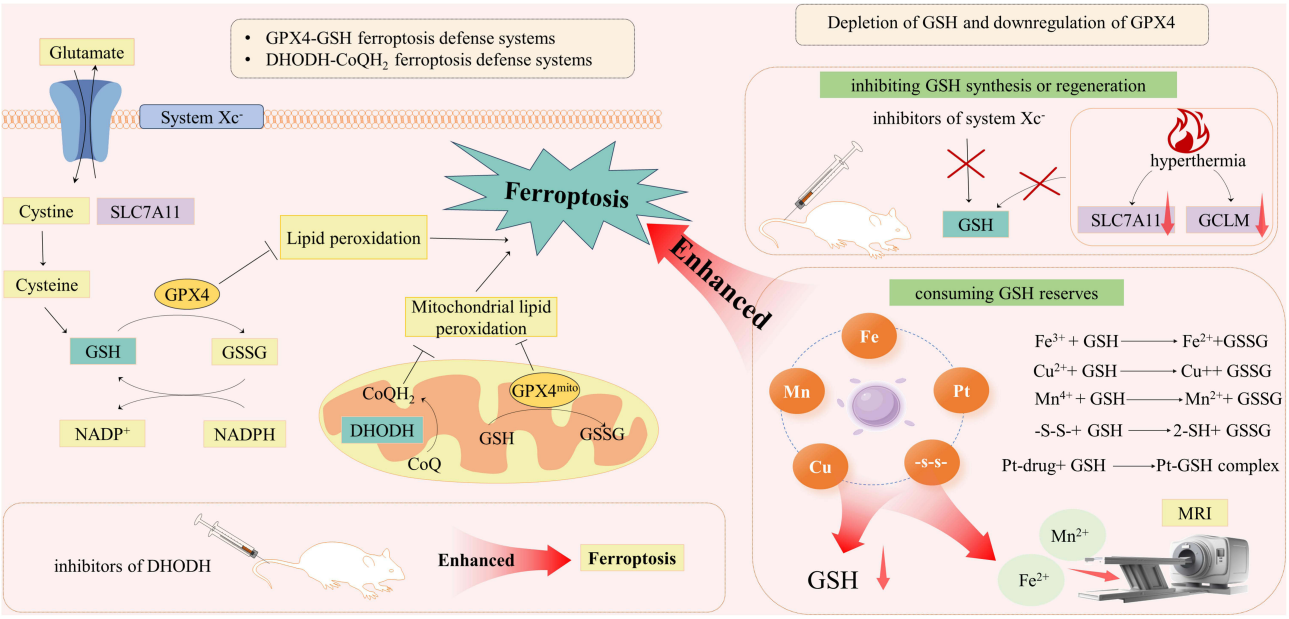

Figure 10 Schematic diagram of the mechanism of disrupting iron death defense pathways.

nano-diagnostic and therapeutic agent, SA-SFN-FGNP. This nano-agent leverages specific conditions in the tumor microenvironment—such as acidity, GSH levels, H_2O_2 content, and GPX4 activity—to trigger the responsive release or activation of nanoparticles. This mechanism creates a self-sustaining cycle of ROS generation within tumor cells, allowing for efficient therapeutic effects at low doses, while enhancing treatment specificity and safety. Additionally, SA-SFN-FGNP exhibits a high longitudinal relaxation rate (r1, 33.43 mM^{-1} s^{-1}, 3.0 T), enabling MRI visualization of ferroptosis in tumors.[143] Building on the foundation of FGNPs, the team designed a new composite nanoparticle, FGNPs@TA-Fe/Ca. Under the influence of the tumor microenvironment, FGNPs@TA-Fe/Ca releases iron and calcium ions within cells, triggering a cycle that accelerates both ferroptosis and calcium-induced cell death, leading to efficient tumor suppression. These nanoparticles also demonstrate a high longitudinal relaxation rate (r1, 44.00 mM^{-1} s^{-1}, 3.0 T), presenting a novel approach for MRI-guided treatment of colorectal cancer.[144] In 2023, the team advanced their research on ROS generation strategies by developing a novel nanotheranostic agent, TAF-HMON-CuP@PPDG. This platform utilizes GSH in the tumor microenvironment to degrade HMON, releasing CuP, which generate Cu^{2+} and H_2O_2 in the tumor cells, enhancing intracellular acidification. The subsequent Fenton reaction between Cu^{2+} and H_2O_2, along with the reaction between Cu^{+} and H_2O_2, creates a cyclic catalytic process that produces large amounts of ROS, triggering an intracellular ROS storm. This strategy not only improves the efficiency of tumor treatment but also provides a new perspective for tumor diagnosis and treatment through T1-weighted MRI imaging.[145]

Tumor cells have developed complex defense mechanisms to resist ferroptosis, limiting the effectiveness of ferroptosis-based therapies. The GPX4 pathway is the most well-known defense against ferroptosis. GPX4 uses GSH to reduce lipid peroxides, preventing the oxidation of unsaturated fatty acids on the cell membrane and halting ferroptosis.[130,146–148] Another critical mechanism involves dihydroorotate dehydrogenase (DHODH), which catalyzes the production of CoQH2 in the inner mitochondrial membrane.[149–151] CoQH2 is a powerful antioxidant that inhibits lipid peroxidation reactions in the mitochondria. By targeting and inhibiting the activity of key enzymes such as GPX4 and DHODH, the sensitivity of tumor cells to ferroptosis can be significantly enhanced.

Various strategies have been developed to deplete GSH and enhance ferroptosis. These strategies include using inhibitors to block GSH synthesis or regeneration, developing nano-drugs that consume GSH, or employing compounds like cinnamaldehyde to directly deplete GSH reserves in combination with chemotherapy.[152–154] Luo et al synthesized FCS/GCS by chelating Fe^{3+}/Gd^{3+} with polyphenols, loading a cinnamaldehyde prodrug (CA-OH), and grafting an amphiphilic polymer scaffold, P-SS-D. In the tumor environment, FCS/GCS releases Fe^{3+}/Gd^{3+} and cinnamaldehyde,

which consumes GSH, converting it to GSSG. Fe^{3+} catalyze the formation of •OH from H_2O_2, further reducing GSH levels, lowering GPX4 activity, promoting lipid peroxide accumulation in tumor cells, and initiating ferroptosis. Additionally, Gd^{3+} acts as a contrast agent for tumor-specific T1-weighted MRI imaging.[155] Manganese-based materials also play a vital role in consuming GSH in the tumor microenvironment. Wang et al developed arginine-rich manganese silicate nanobubbles (AMSNs) to deplete GSH and promote ferroptosis. The unique nanobubble structure and ultra-thin arginine-modified surface of AMSNs significantly enhance their GSH-consuming capability compared to solid MnO_2 nanoparticles. This depletion inactivates a large amount of GPX4, greatly improving ferroptosis efficacy. Moreover, the manganese ions released during GSH consumption further enhance the T1-weighted MRI signal, providing a novel approach for designing nano-drugs for tumor-targeted diagnosis and therapy.[156] Modifying external conditions to weaken the GPX4 defense mechanism is another promising strategy. Xie et al proposed inhibiting tumor ferroptosis defenses through heat stress and developed iron oxide nanoparticles (Fe_3O_4 NPs) to test their effectiveness. The study found that moderate heat treatment (45°C) significantly reduced GSH synthesis and suppressed the antioxidant response of tumors, amplifying reactive oxygen species damage.[157]

While the research on the DHODH antioxidant system is not as advanced as studies on the GPX4 pathway, this area is gaining increasing academic attention. Chen et al developed a layered double hydroxide (LDH)-based nanotheranostic agent that incorporates ferroptosis inducers (iron oxide nanoparticles, IONs) and DHODH inhibitors (siRs).[158] The siR/IONs@LDH agent is designed to release IONs and siRs in a pH-responsive manner, efficiently generating toxic ROS via the Fe²-mediated Fenton reaction, thereby synergistically inducing cancer cell death and promoting the accumulation of LPOs. In vivo therapeutic evaluations demonstrated that the siR/IONs@LDH nanomedicine platform effectively inhibited tumor growth with no significant side effects. Furthermore, siR/IONs@LDH also showed potential as a T1-weighted MRI contrast agent, enabling monitoring of nanoparticle accumulation at the tumor site and guiding subsequent ferroptosis therapy.

Dual Combination Therapy

Combination therapy offers several advantages over single-agent treatments by integrating two or more anti-tumor strategies to achieve synergistic effects—where the combined therapeutic outcome surpasses the sum of individual effects. This approach enables distinct mechanisms of action to complement one another, thereby enhancing overall therapeutic efficacy and reducing the likelihood of drug resistance in cancer cells. For instance, combining PTT with CDT not only amplifies their individual therapeutic effects but also promotes immunogenic cell death and activates an adaptive immune response, which can target a broader spectrum of tumor cells. This article systematically analyzes the benefits and limitations of various anti-tumor modalities, with particular emphasis on the superior performance of combination strategies (Figure 11).

Combined Therapy of PTT/MHT and CDT

Studies have shown that combining PTT with MHT enhances CDT effectiveness. Local tumor heating through photothermal or magnetothermal agents accelerates Fenton or Fenton-like reactions.[159–162] At the same time CDT enhances PTT efficacy by inhibiting the upregulation of heat shock proteins through ROS generation.[163–166] To maximize this synergy in cancer treatment, many studies have focused on combining Fenton or Fenton-like reagents with photothermal or magnetothermal agents and imaging agents to create multifunctional diagnostic and therapeutic platforms, improving tumor-targeting efficacy while minimizing damage to normal tissues.

Tang et al pioneered a nano-cube named FeS_2-PEG based on pyrite (FeS_2).[167] In the TME, the nano-cube undergoes surface oxidation, generating hydroxyl radicals to induce cell death via CDT. This oxidation also alters the iron valence state on the surface, enhancing both T1 and T2 relaxivity for MRI. Specifically, the longitudinal relaxivity (r1) increased from 0.34 to 1.0 mM^{-1} s^{-1}, and the transverse relaxivity (r2) increased from 2.18 to 18.14 mM^{-1} s^{-1}, raising the r2/r1 ratio from 6.41 to 18.14. This self-enhancement of MRI signals provides greater contrast and clarity, improving tumor diagnosis and treatment. Furthermore, upon exposure to near-infrared (NIR-I) laser irradiation, FeS_2-PEG generates localized heat, which accelerates Fenton-like reactions within the tumor site, achieving a synergistic therapeutic effect combining photothermal therapy (PTT) and CDT. The in vivo therapeutic efficacy of FeS_2-PEG was comprehensively demonstrated in a 4T1 tumor-bearing mouse model. As shown in (Figure 12a), infrared thermal imaging revealed

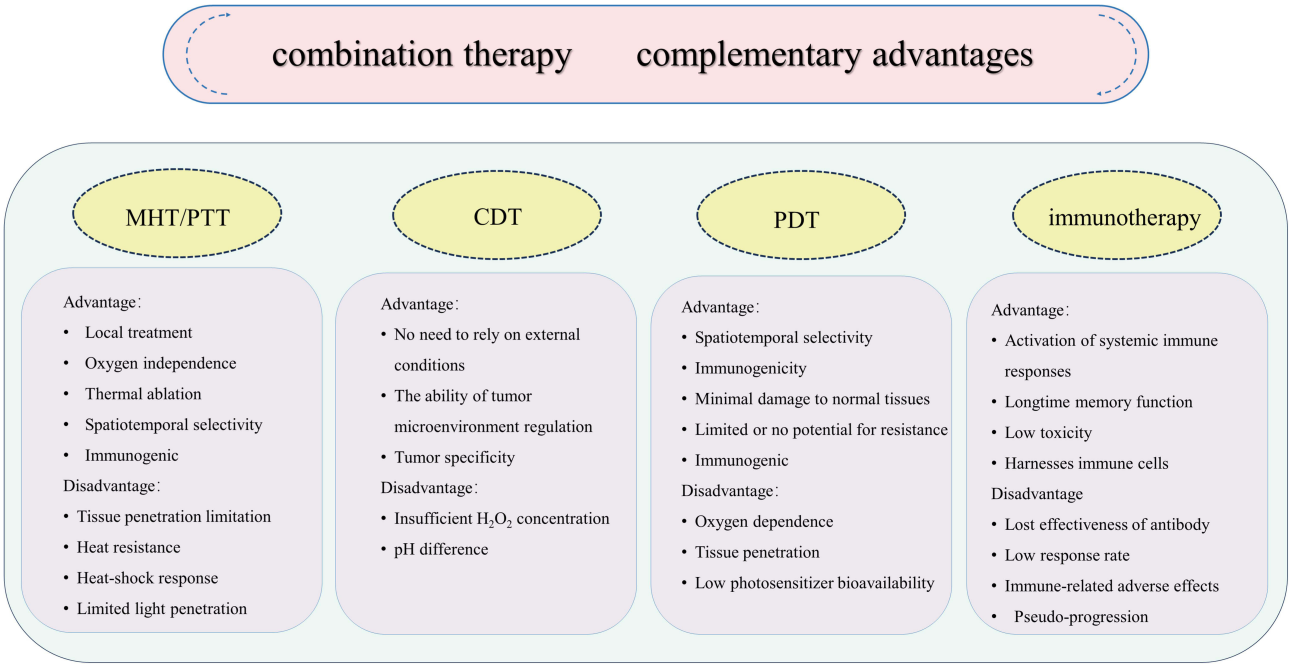

Figure 11 Comparison of advantages and disadvantages of different anticancer therapies.

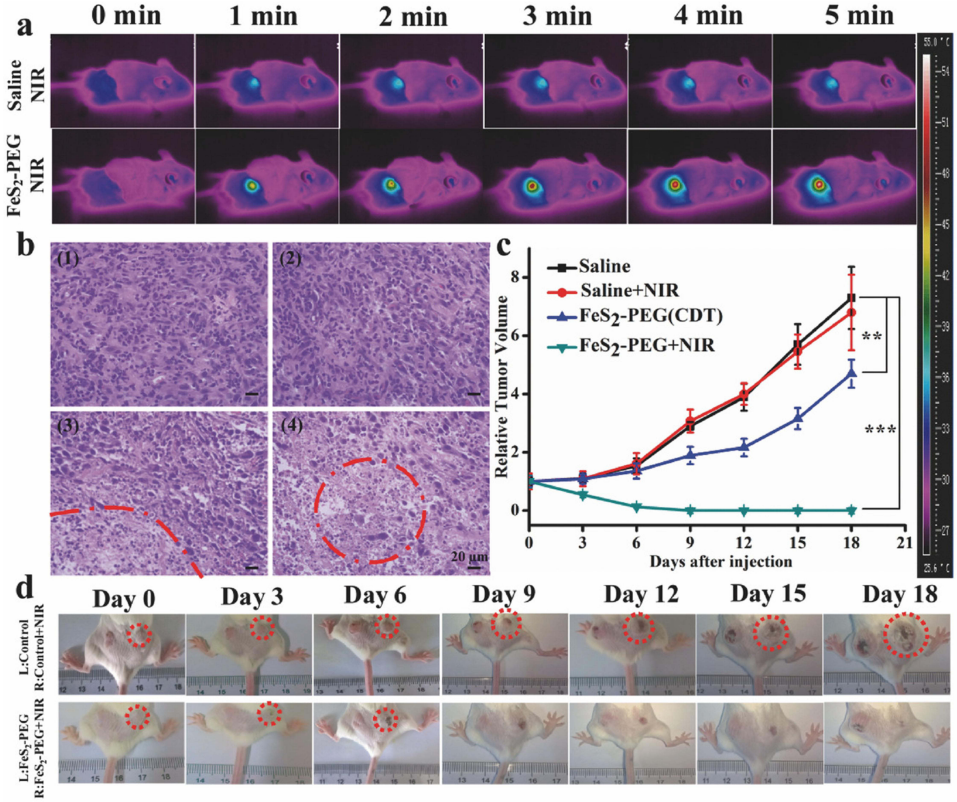

Figure 12 In vivo photothermal and chemodynamic therapy efficacy of FeS_2-PEG. (**a**) Representative infrared thermal images of 4T1 tumor-bearing mice at 1 h post-intravenous injection of saline or FeS_2-PEG (50 mg Fe kg^{-1}), followed by 808 nm laser irradiation (1.5 W cm^{-2}). (**b**) H&E staining of tumor sections collected 12 h after various treatments: (1) saline, (2) saline + laser, (3) FeS_2-PEG, and (4) FeS_2-PEG + laser. Red dotted circles highlight areas of apoptosis. Scale bar in (**b**) represents 20 μm. (**c**) Relative tumor volume changes over time in different treatment groups (n = 6, mean ± s.d., **P < 0.01, ***P < 0.001). (**d**) Representative photographs of bilateral 4T1 tumor-bearing Balb/c mice at different time points post-treatment. Reproduced from Tang ZM, Zhang HL, Liu YY et al. Antiferromagnetic Pyrite as the Tumor Microenvironment-Mediated Nanoplatform for Self-Enhanced Tumor Imaging and Therapy. *Advanced Materials*. 2017;29(47) with permission from John Wiley and Sons.[167]

pronounced temperature elevation in the tumor region following FeS_2-PEG administration and NIR-I laser exposure, confirming effective photothermal conversion. Histological examination (Figure 12b) indicated extensive tumor cell apoptosis and necrosis, particularly in the combined treatment group. In addition, longitudinal monitoring of tumor volume (Figure 12c) and macroscopic tumor photographs (Figure 12d) confirmed significant tumor suppression, underscoring the potent therapeutic synergy and translational potential of FeS_2-PEG for integrated cancer treatment. Liu et al further advanced this approach by developing a one-dimensional iron phosphide nanorod (FP NRs), which serves as a potent Fenton reagent for cancer treatment when combined with NIR-II (1064 nm) laser and ultrasound (US).[168] Due to the strong tissue penetration of the NIR-II laser and the exceptional properties of FP NRs, these nanorods exhibited a high photothermal conversion efficiency of 56.6%, significantly raising the temperature at the tumor site and intensifying the Fenton reaction, effectively killing cancer cells. FP NRs also demonstrated a high transverse relaxivity (r2) of up to 277.79 mM-1 s-1, allowing for precise tumor diagnosis.

Compared to PTT, MHT is not constrained by tissue penetration depth. When combined with CDT, MHT produces a synergistic effect similar to PTT, making it an ideal partner for CDT. Shen et al proposed a mitochondrial-targeting magnetothermal enzyme (Ir@MnFe2O4 NPs) for efficient cancer treatment.[169] Under an AMF, Ir@MnFe2O4 NPs induce local tumor heating via the magnetothermal effect, which accelerates the conversion of Fe^{3+} to Fe^{2+} and H_2O_2 to ·OH, thereby enhancing the efficacy of CDT. In turn, the enhanced CDT disrupts the redox homeostasis of cells, increasing their sensitivity to MHT. Notably, this nano-platform integrates two-photon microscopy (TPM) and MRI technologies, offering robust technical support for the precision and effective cancer treatment.

Combined Therapy of PTT and PDT

Both photodynamic therapy (PDT) and photothermal therapy (PTT) utilize laser irradiation to generate reactive oxygen species (ROS) or localized heat at the tumor site, enabling precise spatiotemporal elimination of cancer cells. Despite their distinct mechanisms of action, the cell death pathways they induce are complementary. Notably, PTT can improve tumor oxygenation, thereby creating a more favorable microenvironment for PDT.[170,171] Conversely, the ROS generated by PDT can damage tumor blood vessels, which may amplify the thermal effect of PTT.[172] Currently, MRI nanotheranostic agents used in PTT/PDT combination therapies can be categorized into single-photon and dual-photon nanotheranostic agents. Single-photon nanotheranostic agents contain a photoactive monomer capable of serving as both a PDT and PTT agent, allowing both therapies to be performed under the same light conditions (Figure 13a). This design offers time efficiency and cost-effectiveness; however, the optimal activation times for PDT and PTT may vary, and the lack of precise light exposure control can result in suboptimal therapeutic efficacy. In contrast, dual-light nanotheranostic agents utilize two independent light sources to separately activate PTT and PDT, thereby overcoming the limitations of single-light systems. Nevertheless, studies indicate that the synergistic effects of PTT and PDT are influenced by the order in which these therapies are administered (Figure 13b).[173] Therefore, further investigation into the optimal sequence of PTT and PDT is necessary to refine and enhance the effectiveness of this combined treatment approach.

Indocyanine green (ICG) and porphyrin are among the most widely used single-optical active molecules, exhibiting strong potential for combined PTT and PDT applications.[174–178] Sun et al developed a dual-modal imaging PTT/PDT therapeutic nanotheranostic agent using honeycomb manganese dioxide with peroxidase-like activity.[179] This nanotheranostic agent effectively integrates CuS nanoparticles and ICG molecules. Upon exposure to an 808 nm laser, both CuS NPs and ICG exhibit potent PTT effects. Simultaneously, the degradation of the manganese dioxide carrier releases oxygen, alleviating tumor hypoxia. The released ICG molecules then induce a strong PDT effect under the same irradiation, enhancing tumor cell destruction. Furthermore, the fluorescence recovery of ICG and the release of Mn^{2+} enable high-resolution fluorescence imaging and T1-weighted MRI, facilitating precise image-guided synergistic phototherapy. Li and Wang's research team has focused on the development of porphyrin-based nanomaterials, successfully creating COF-366 NPs and an integrated "nanoporphyrin" platform, both of which have shown significant effects in PTT/PDT combination therapy.[180,181] Despite the widespread interest in ICG and porphyrin for their favorable properties, their photostability still requires enhancement. Polypyrrole (PP), a novel biomaterial, is currently being developed for PTT/PDT due to its excellent photostability, biocompatibility, and strong light absorption in the near-infrared region.[182–184]

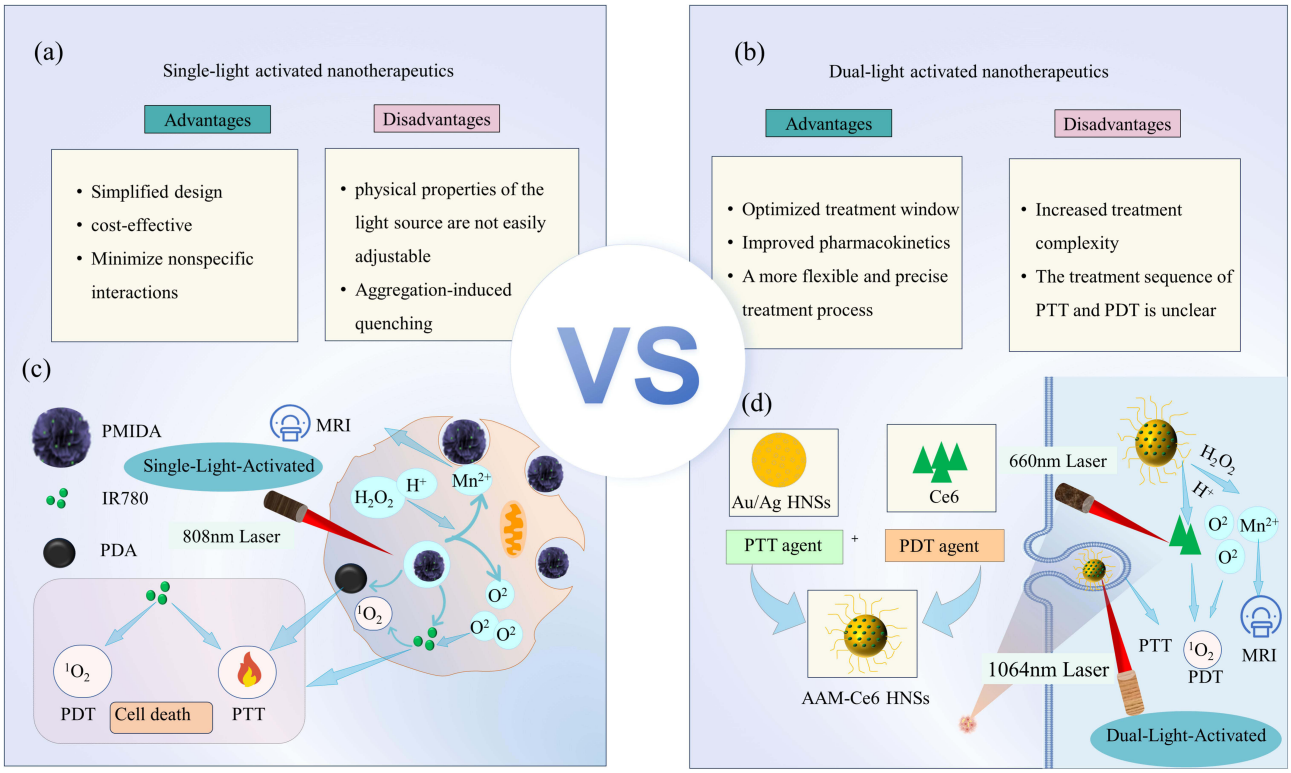

Figure 13 Comparison of advantages and disadvantages of single-light and dual-light nano-therapeutic agents, as well as examples of their applications. (**a**) Advantages and disadvantages of single-light-activated nano-therapeutic agents. (**b**) Advantages and disadvantages of dual-light-activated nano-therapeutic agents. (**c**) Representative application of single-light activation: PMIDA enables both PTT and PDT under 808 nm laser irradiation. (**d**) Representative application of dual-light activation: AAM-Ce6 HNSs generate singlet oxygen for PDT upon 660 nm laser excitation and induce heat generation under 1064 nm laser irradiation to achieve PTT.

Double-light nano-therapeutic agents integrate two or more materials within a single nanoparticle, where one component provides photosensitization and the other ensures high photothermal conversion. Gold nanostructures are the most traditional and extensively studied class of plasmonic nanomaterials for PTT. When combined with photosensitizers, they can produce a substantial synergistic effect in combined PTT/PDT treatment. Wu and colleagues designed a multifunctional diagnostic and therapeutic nano-platform AAM-Ce6 HNSs (Figure 13d).[185] This platform shows a significant photothermal conversion capability in the NIR-II (1064 nm) window. Within the TME, the manganese dioxide nanoparticles catalyze the conversion of endogenous hydrogen peroxide into oxygen while releasing a large amount of Mn^{2+} ions, which helps to relieve tumor hypoxia and generates a strong T1-weighted MRI signal. Concurrently, the Ce6 in the cavity, upon exposure to a 660 nm laser, produces a substantial amount of reactive oxygen species, demonstrating a potent PDT effect.

PDA is an emerging photothermal conversion agent that not only acts as a carrier and linker for delivering photosensitizers but also enhances the stability, biocompatibility, and imaging capabilities of nanoparticles through its unique chemical and physical properties. PDA plays a crucial role in achieving effective PDT and PTT and is widely utilized in designing both single-light and dual-light nano-therapeutic agents.[54,57,186–188] Yan et al applied the principles of single-light nanotheranostic agent design to create a multifunctional phototherapeutic diagnostic nanoplatform, PMIDA, based on a combination of PDA, MnO_2, and IR780 iodide, for effective magnetic resonance imaging-guided synergistic photodynamic and photothermal therapy (Figure 13c).[189] In this nano-platform, PDA functions as both a carrier and a connector, efficiently loading the tumor-targeting photothermal molecule IR780 and integrating MnO_2. It also acts as a "gatekeeper", preventing the leakage of IR780 into normal tissues and thereby minimizing side effects. Furthermore, it ensures the specific degradation of PMIDA in the tumor microenvironment, which not only addresses tumor hypoxia but also enhances PDT efficacy and achieves T1-weighted MRI.

A notable example of PDA in the development of dual-light nano-therapeutic agents is the design of Fe_3O_4 @PDA@Pt-PEG-Ce6 nanoparticles.[190] When it exposed to a combination of 660 nm and 808 nm lasers, cell viability significantly dropped, especially at a concentration of 60 μg/mL, where only 18.6% of the cells remained alive, highlighting the stronger anti-tumor effects of the combined treatment. Additionally, the presence of Fe_3O_4 and the yolk-shell hollow cavity enabled enhanced ultrasound (US) and magnetic resonance imaging (MRI), with stronger T2-weighted imaging signals detected in the liver and tumor areas of mice at 2, 4, and 8 hours post-administration. The inclusion of Ce6 and Pt further facilitated the breakdown of endogenous H_2O_2 in the tumor microenvironment, boosting oxygen production and significantly enhancing the efficacy of photodynamic therapy.

Combined Therapy of PDT and CDT

Both PDT and CDT are ROS-based treatments that can effectively combat the ongoing threat of malignant tumors.[191–193] Research has shown that the Fenton reaction during CDT not only produces ·OH through the disproportionation of H_2O_2 but also generates additional oxygen, thereby alleviating tumor hypoxia and enhancing the effectiveness of PDT.[194–196] Moreover, combining PDT agents with Fenton reagents can significantly increase ROS production, directly targeting tumor cells and damaging blood vessels, which in turn can trigger immunogenic cell death, further improving the efficiency of anti-cancer therapies.[197,198] The use of MRI technology offers more precise guidance for these integrated therapies. Consequently, developing high-performance Fenton-photosensitizers that can either reduce GSH levels in the TME or increase hydrogen peroxide and oxygen concentrations within tumor cells, while leveraging the benefits of MRI-directed combined PDT and CDT (Figure 14).[192]

Metal-organic frameworks (MOFs) and MOF-based nanoplatforms offer a range of advantages, such as imaging capabilities, large surface areas, ease of functionalization, and biocompatibility, making them highly suitable for the design of nanotheranostic agents.[199–202] Comprising metal ions and organic ligands, MOFs can be tailored for efficient cancer diagnosis and therapy by integrating different components. Iron-based and manganese-based MOFs, in particular, are commonly utilized in nano-diagnosis and therapy due to their ability to mediate Fenton reactions for CDT, as well as their roles in regulating the TME and enhancing imaging and tumor treatment.[199,203] UCNPs as another innovative approach in PDT/CDT due to their unique optical properties and imaging capabilities.[204–206] Lanthanide-doped UCNPs can convert low-energy near-infrared light into high-energy visible or ultraviolet light, allowing deep tissue penetration while minimizing damage to normal tissues.[207–210] Additionally, the high-energy ultraviolet light can promote Fenton reactions to produce hydroxyl radicals, providing a dual mechanism for attacking tumor cells.[211] Xu et al developed a multifunctional nano-diagnostic and therapeutic agent, PEG/LDNPs@CMSN, which incorporates lanthanum-doped nanoparticles coated with copper/manganese silicate nanospheres (CMSN). This agent exhibits strong upconversion (UC) and downconversion (DC) NIR-II emission, demonstrating exceptional antitumor effects in combined CDT/PDT therapy.[212] In the TME, PEG/LDNPs@CMSN serves a dual function: the CMSNs layer decomposes H_2O_2 to generate oxygen, mitigating tumor hypoxia and producing singlet oxygen for PDT under NIR laser excitation. Concurrently, CMSN degradation releases Cu^+ and Mn^{2+} ions, which generate hydroxyl radicals through a Fenton-like reaction for CDT, thereby providing necessary ROS and enhancing PDT efficacy. Moreover, the cycling of Cu^{2+} and Cu^+ via photoreduction ensures the continuous progression of the Fenton reaction, greatly increasing ·OH production and boosting CDT effectiveness. The incorporation of rare earth metals and copper/manganese also enables multimodal imaging, including NIR-II FL/CT/MRI, thus providing robust imaging guidance for precise tumor diagnosis and treatment. Given the significant benefits of combining PDT and CDT, many studies have explored integrating MOFs with UCNPs to further enhance their therapeutic efficacy. For instance, Ling et al developed UCNPs@MOFs, a novel nano-diagnostic and therapeutic agent that involves coating upconversion nanoparticles with an iron-based MOF on a $NaGdF_4$, Yb, Er@$NaGdF_4$, Yb, Tm@$NaYF_4$ core@shell@shell structure.[213] This agent generates singlet oxygen for PDT by absorbing UV-visible light emitted by UCNPs through Fe-MOFs, while Fe^{3+} catalyzes H_2O_2 to produce oxygen and ·OH, which are utilized in CDT. The resulting synergistic effects of singlet oxygen and hydroxyl radicals inhibit tumor growth. Additionally, the unique optical properties of UCNPs and the inclusion of gadolinium facilitate tumor cell imaging and T1-weighted MRI in the NIR region, aiding both in vitro and in vivo treatment guidance.

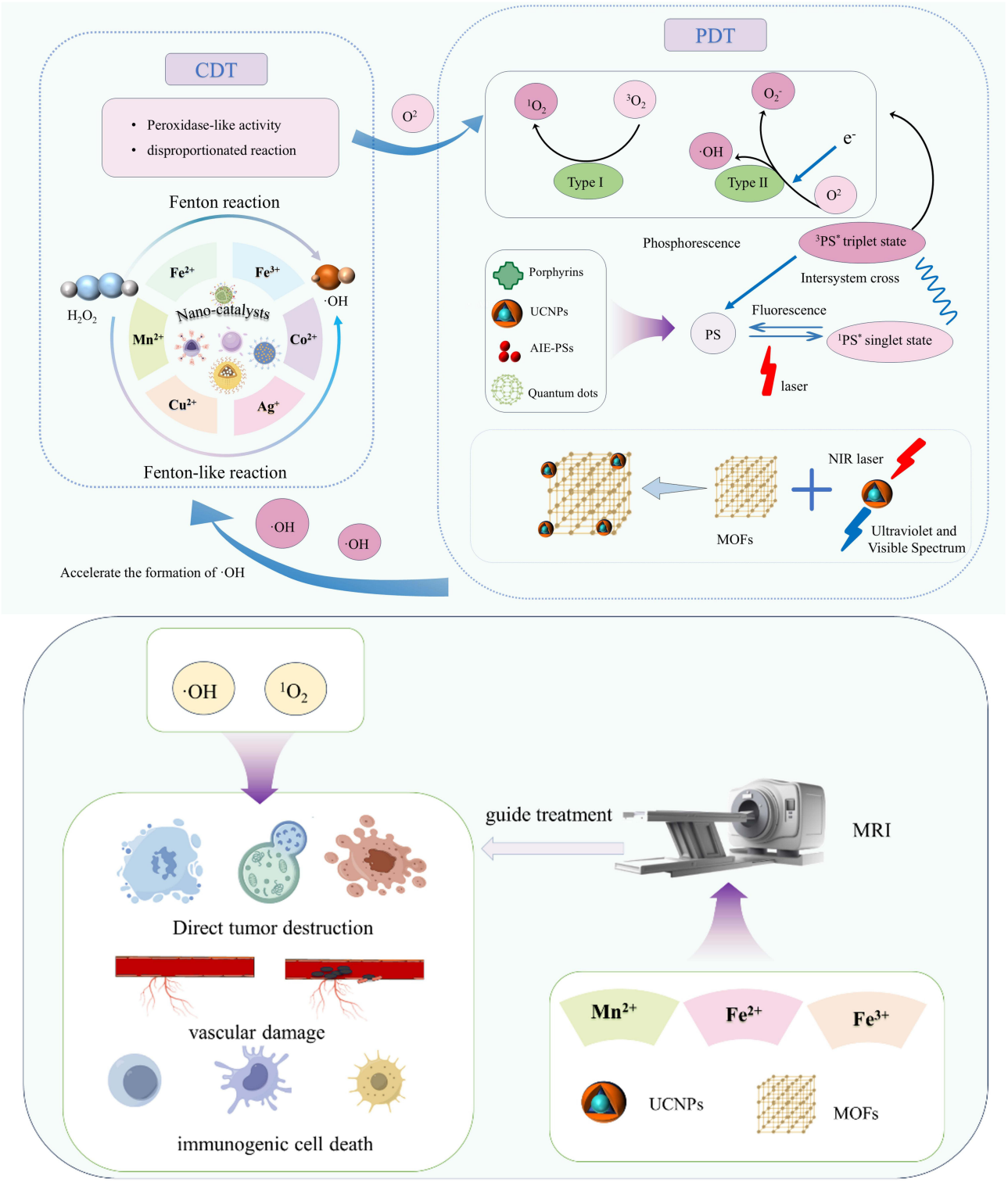

Figure 14 Schematic diagram of PDT and CDT combination therapy. CDT uses nano-catalysts to promote hydroxyl radical (·OH) production via Fenton-like reactions. PDT generates reactive oxygen species (ROS) through photosensitizer excitation and energy transfer. The combined ROS induce tumor destruction and immune activation. MRI enables treatment guidance via metal-based contrast agents.
Note: ^{1}PS* and ^{3}PS* indicate singlet and triplet excited states of the photosensitizer, not statistical significance*.

Significant progress has been made in utilizing nano-enzymes for constructing nanotheranostic agents for combined PDT/CDT therapies. Nano-enzymes composed of metal-based nanomaterials (such as Mn, Fe, Pt, etc) have demonstrated the ability to efficiently convert H_2O_2 into O_2, effectively alleviating tumor hypoxia and greatly enhancing PDT efficacy. Additionally, these nano-enzymes release metal ions that play a crucial role in CDT through the Fenton reaction, while also providing clear imaging results in MRI.[214] Wang et al were the first to synthesize a novel carbon dot nano-enzyme (Mn-CD) using toluene blue (TB) and manganese for MRI-guided combined CDT/PDT therapy.[215] The manganese doping of this nano-enzyme enhanced its responsiveness within the tumor microenvironment, significantly improving its magnetic resonance imaging capabilities and photostability under the combined activation of pH and GSH. The study found that, compared to a neutral environment, the r1 and r2 relaxation rates of Mn-CD increased by 224% and 249%, respectively. The depletion of GSH promoted ROS accumulation, substantially enhancing the anti-tumor capabilities of Mn-CD. Additionally, Mn-CDs displayed high peroxidase (POD)-like activity, catalyzing the production of hydroxyl radicals and oxygen from hydrogen peroxide. Under light conditions, the POD activity of Mn-CDs increased, leading to a significant rise in reactive oxygen species and oxygen production, thereby achieving better therapeutic outcomes. Similarly, Zhao et al developed an iron oxide nano-enzyme (IMOP) surface-engineered with Mn(II) and the photosensitizer pyropheophorbide-a (PPa) as an efficient Fenton-photosensitizer for anti-tumor therapy.[216] This nano-enzyme exhibited high catalase-like and glutathione peroxidase-like activity within the tumor microenvironment. Once concentrated in tumors, it acted as a CDT agent by catalyzing the production of oxygen and toxic hydroxyl radicals from hydrogen peroxide and increasing singlet oxygen generation through PPa-mediated PDT. Furthermore, its glutathione peroxidase-like activity helped reduce the GSH concentration in tumors, minimizing the consumption of active ROS during treatment. The presence of Mn(II) also enabled IMOP to monitor CDT/PDT progress via T1-weighted MRI.

Immunotherapy Combined with PTT/MHT Treatment

As discussed earlier, cancer immunotherapy has gained significant attention for its ability to activate the immune system to target and eliminate cancer cells. However, the effectiveness of standalone immunotherapy is often limited by the tumor microenvironment and immune evasion strategies of cancer cells. Studies have shown that combining immunotherapy with MHT or photothermal therapy PTT can significantly enhance anti-tumor effects.[217,218]

PTT and MHT can amplify immune responses by inducing immunogenic cell death or by reversing the immunosuppressive environment within the TME.[219–222] Additionally, combining immunotherapy with PTT/MHT can address their limitations in targeting distant metastatic lesions, thereby improving the treatment of both primary tumors and metastases, and ultimately extending patient survival.

Combining immune checkpoint inhibitors with photothermal or magnetothermal agents is a common strategy for enhancing the effectiveness of immunotherapy with PTT or MHT. Fang and colleagues developed a biomimetic nanosystem, $FePSe_3$@APP@CCM NSs, which combines the immune checkpoint blocker anti-PD-1 peptide (APP) with photothermal converter $FePSe_3$ nanosheets for magnetic resonance imaging and photoacoustic imaging-guided antitumor therapy. The photothermal effect generated by $FePSe_3$@APP@CCM NSs NIR laser irradiation can not only directly kill tumor cells but also act as an immune stimulant, promoting the maturation and activation of dendritic cells, which further activate T cells and enhance the immune response against tumors.[223] Li and his team explored an intelligent, responsive nanotheranostic agent, FA-P(MZF@Gd/JQ1), based on magnetic resonance enhancement technology (MRET).[224] This nano-agent integrates an MRET probe containing $Mn_{0.6}Zn_{0.4}Fe_2O_4$ (MZF@Gd) with magnetothermal effects, a PD-L1 inhibitor (JQ1), a thermosensitive copolymer, and a surface-targeting molecule, folic acid. Under an AMF, $Mn_{0.6}Zn_{0.4}Fe_2O_4$ generates localized heat to directly kill tumor cells, while the thermosensitive copolymer changes its hydrophobicity at a specific temperature, triggering the release of the PD-L1 inhibitor JQ1. As JQ1 release coincides with the activation of the anti-tumor immune response via magnetothermal therapy, the immune response within the tumor microenvironment is further enhanced, enabling the immune system to more effectively target and destroy tumor cells. Additionally, MRET technology can be used to assess therapeutic efficacy by measuring changes in granzyme B levels through alterations in T1-weighted signals before and after immune checkpoint blockade treatment, thereby guiding further treatment decisions.

PTT agents like Prussian blue, indocyanine green (ICG), and polydopamine can be combined with immunoadjuvants in nanomaterials to achieve synergistic immuno-photothermal therapy. Recently, Zeng and colleagues developed a multifunctional nano-platform called SMP@Mn by using MPDA as a carrier to load the STING agonist MSA-2 and chelate Mn^{2+} ions.[225] MSA-2 activates the STING pathway, and in combination with the thermal therapy, enhances the infiltration of dendritic cells and cytotoxic T cells into the tumor, while reducing the proportion of regulatory T cells. This dual action effectively inhibits tumor growth and metastasis in a 4T1 orthotopic breast cancer mouse model. Additionally, Mn^{2+} ions act as both a sensitizer for the STING pathway, further enhancing the immune response, and as a T1-weighted MRI contrast agent, allowing for real-time tracking of the nano-platform. This innovative strategy has demonstrated high efficiency in suppressing both primary and metastatic tumors, inducing a robust tumor-specific immune response, and offering new approaches for combination cancer therapy. Imiquimod (R837), an FDA-approved immunoadjuvant known for its safety and ability to activate DCs and stimulate the secretion of various pro-inflammatory factors, also shows promising anti-tumor activity.[226–228] Several nanocomposites, such as EV@Gd-MCNs-R837 and magnetite magnetic nanoparticle cores loaded with ICG and R837, have been developed for MRI-guided photothermal and immunotherapy, exhibiting significant potential in treating both primary and metastatic tumors.[229,230]

Multi-Therapeutic Combination Treatment

Chemotherapy, a common cancer treatment, is highly effective but often comes with various systemic side effects.[20,231,232] Thus, a key focus in current cancer research is how to effectively combine chemotherapy with other therapeutic modalities to create a comprehensive treatment plan. Among these, the combination of chemotherapy with PTT and CDT is the most extensively studied. Numerous nanotheranostic agents have been developed for this combined approach, including Fe-GA /BSA@DOX,[233] HMNCs,[234] CuS@mSiO_2@MnO_2/DOX,[235] HSPMH-DOX,[236] and AMGDC.[237] These nanoparticles typically integrate photothermal materials with metals possessing Fenton reaction catalytic activity to create hollow nanostructures, allowing for the loading of chemotherapeutic drugs like doxorubicin (DOX). By incorporating tumor-specific release mechanisms, these nanoparticles can accurately deliver chemotherapeutic drugs to the tumor site, ensuring targeted chemotherapy. Simultaneously, they also combine PTT and CDT treatments to enhance overall therapeutic efficacy. Additionally, the inclusion of iron and manganese metals provides these nanoparticle platforms with MRI imaging capabilities, enabling real-time monitoring and precise targeting throughout the treatment process.

Beyond the combination of chemotherapy, PTT, and CDT, some studies have explored integrating chemotherapy with PTT and PDT.[238,239] Wu et al developed a biodegradable nanoparticle platform H-MnO_2/DOX/BPQDs. This multifunctional platform is designed for dual-modal fluorescence imaging (FLI) and MRI, as well as combined chemotherapy/PTT/PDT. The H-MnO_2 component offers T1-weighted MRI imaging and the ability to convert hydrogen peroxide, allowing precise tumor localization and reducing tumor hypoxia. Meanwhile, the loaded doxorubicin (DOX) facilitates fluorescence imaging for visual tracking and acts as a chemotherapeutic agent to effectively kill cancer cells. Notably, under 630 nm laser irradiation, the BPQDs in this platform generate singlet oxygen ($^1O_2$) for PDT, and under 808 nm laser irradiation, they achieve excellent photothermal conversion efficiency for PTT. This dual-laser-triggered combination of chemotherapy, PTT, and PDT significantly enhances therapeutic effectiveness, presenting new possibilities for cancer treatment.

With ongoing advancements in research, the benefits of immunotherapy in cancer treatment are becoming increasingly evident, solidifying its role as a crucial component of combination therapies. For instance, Geng et al developed a "multi-in-one" core–shell metal–organic nanoplatform (DCMNs) by integrating Mn^{2+} with doxorubicin (DOX) and chlorin e6 (Ce6) to enhance the antitumor effects of α-PD-1 immunotherapy.[240] The Mn^{2+} core contributes to a strong signal in T1-weighted MRI, aiding in tumor tissue imaging. Additionally, DOX in the core and Ce6 in the shell demonstrate potent chemotherapy and PDT effects in vivo. DCMNs not only directly inhibit tumor cells but also promote T lymphocyte infiltration, significantly enhancing the anti-tumor response to anti-PD-1 therapy. Similarly, Kong, He, and colleagues designed iron-based micelles containing the photothermal agent indigo carmine (ICG) and targeting peptide cRGD (ICG@SANPs-cRGD), as well as smart manganese dioxide nanocomposite materials (SRCM) for MRI-guided triple combination therapy involving immunotherapy, PTT, and PDT, demonstrating remarkable anti-tumor effects.[241,242] The CRISPR/Cas system, a powerful gene-editing tool, has proven effective in modulating genes in

tumors or immune cells, making it an essential technology for gene therapy and immunotherapy in cancer.[243,244] Liu et al utilized this tool to create a self-assembled manganese sulfide (MnS) nanoparticle loaded with CRISPR/Cas9 and encapsulated with a hybrid membrane (MCRT) for targeted MRI contrast enhancement and synergistic gene, immunotherapy, and CDT treatments.[245] MCRT's unique structure and cationic surface enable efficient CRISPR/Cas9 loading. The pH-responsive MCRT decomposes into H_2S and Mn^{2+}, where H_2S enhances Mn^{2+}-mediated CDT by increasing intracellular H_2O_2 levels and works with CRISPR/Cas9 to downregulate the anti-apoptotic protein survivin, thereby achieving self-enhanced gene therapy and inducing immunogenic cell death. This process triggers a strong anti-tumor immune response, promoting tumor cell apoptosis, and inhibiting proliferation, thereby achieving excellent synergistic therapeutic effects (Figure 15). Moreover, MCRT exhibits efficient tumor accumulation and significant T1-weighted MRI contrast enhancement, demonstrating its great potential as a multifunctional therapeutic-imaging platform (Figure 16).

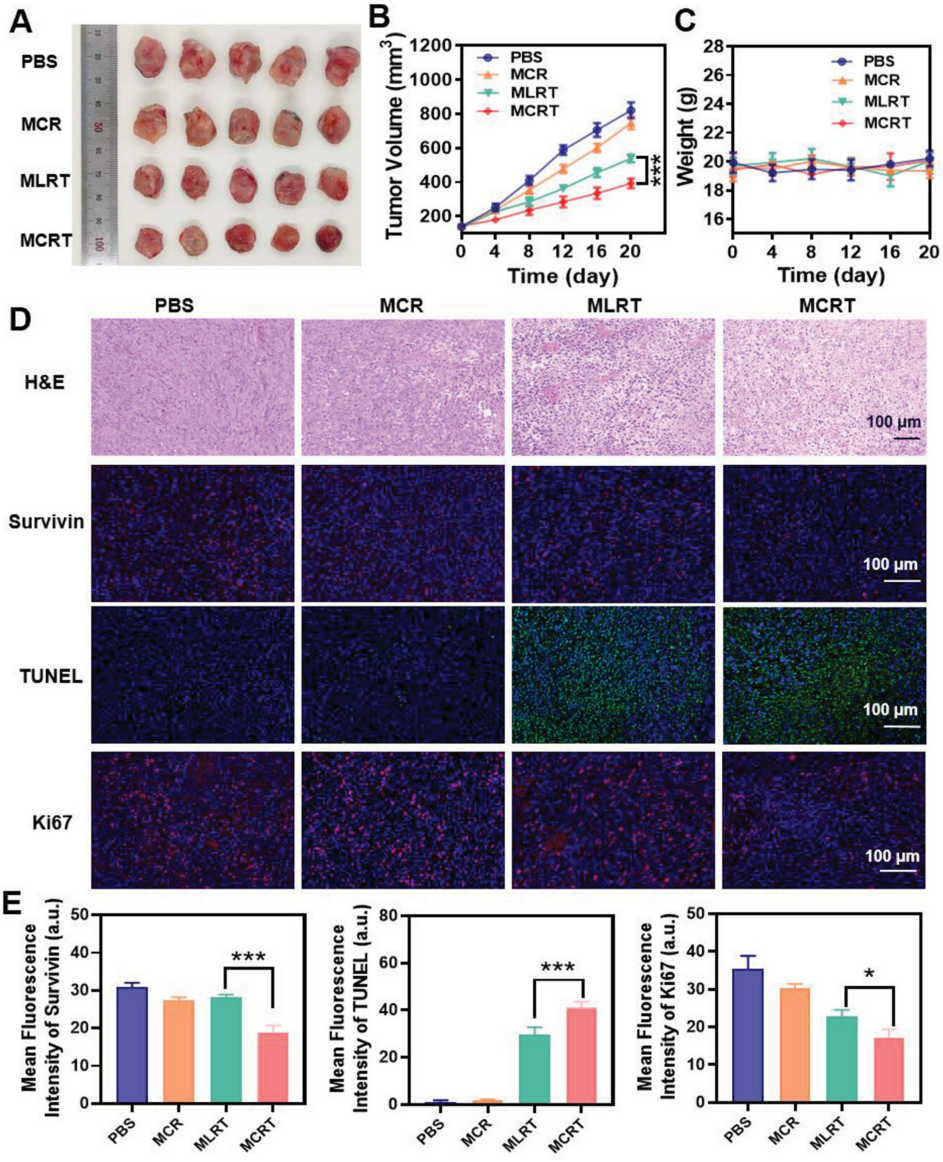

Figure 15 Antitumor efficacy of different treatments in 4T1 tumor-bearing mice. (**A**) Representative ex vivo tumor tissues collected at the end of treatment (n = 5). (**B**) Tumor volume progression curves during treatment. (**C**) Body weight variations of mice throughout treatment, reflecting systemic tolerance. (**D**) Histological (H&E) and immunofluorescence staining of tumor tissues, showing survivin expression (green), TUNEL-positive apoptotic cells (green), and Ki67 proliferation marker (red); nuclei were counterstained with DAPI (blue). Scale bar = 100 μm. (**E**) Quantitative analysis of survivin, TUNEL, and Ki67 fluorescence intensity in each group (n = 3). Data are presented as mean ± SD. Statistical analysis was performed by one-way ANOVA. *p < 0.05. ***p < 0.001. Reproduced from Liu H, Mu MY, Hou YB et al. A Novel CRISPR/Cas9-Encapsulated Biomimetic Manganese Sulfide Nanourchins for Targeted Magnetic Resonance Contrast Enhancement and Self-Enhanced Chemodynamics-Gene-Immune Synergistic Tumor Therapy. Copyright 2024, John Wiley and Sons.[245]

https://doi.org/10.2147/IJN.S529003

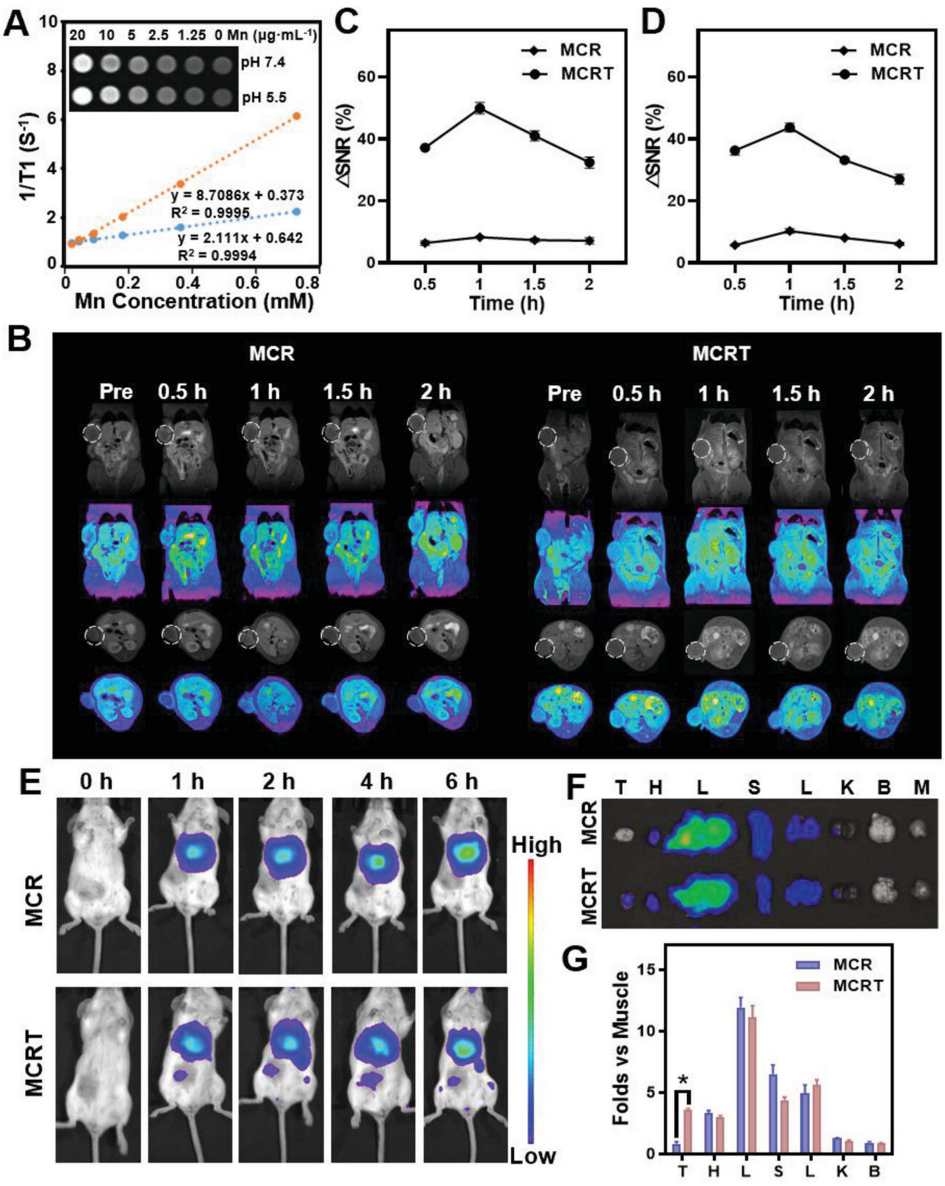

Figure 16 In vivo MRI and fluorescence imaging of MCR and MCRT in 4T1 tumor-bearing mice. (**A**) T1 relaxation rates and T1-weighted phantom images of MnS nanourchins at pH 7.4 and pH 5.5. (**B**) Coronal and axial T1-weighted MRI images at different time points post-injection of MCR or MCRT; tumor regions are marked with white dashed circles. (**C**–**D**) Quantification of signal-to-noise ratio (SNR) in the tumor regions from coronal (**C**) and axial (**D**) MRI images over time. (**E**) In vivo fluorescence imaging of Cy5.5-labeled MCR and MCRT in mice at 0–6 h post-injection. (**F**) Ex vivo fluorescence imaging of excised major organs 6 h post-injection (T: tumor; H heart; L liver; S spleen; K kidney; B brain; M muscle). (**G**) Quantitative analysis of fluorescence intensity in major organs relative to muscle (n = 3). Statistical analysis was performed by one-way ANOVA. *p < 0.05. Reproduced from Liu H, Mu MY, Hou YB et al. A Novel CRISPR/Cas9-Encapsulated Biomimetic Manganese Sulfide Nanourchins for Targeted Magnetic Resonance Contrast Enhancement and Self-Enhanced Chemodynamics-Gene-Immune Synergistic Tumor Therapy. Copyright 2024, John Wiley and Sons.[245]

Discussion

MRI-based theranostic technology enhances the precision and synergistic effects of therapy while significantly minimizing side effects. This technology is poised to play a crucial role in advancing cancer diagnosis and treatment. Currently, the rational design, development, and testing of various multifunctional nanotheranostic agents are being intensively explored, leading to several innovative outcomes. However, numerous challenges and unresolved issues remain. In this discussion, we examine several critical issues that should be considered as priorities for future research (Figure 17).

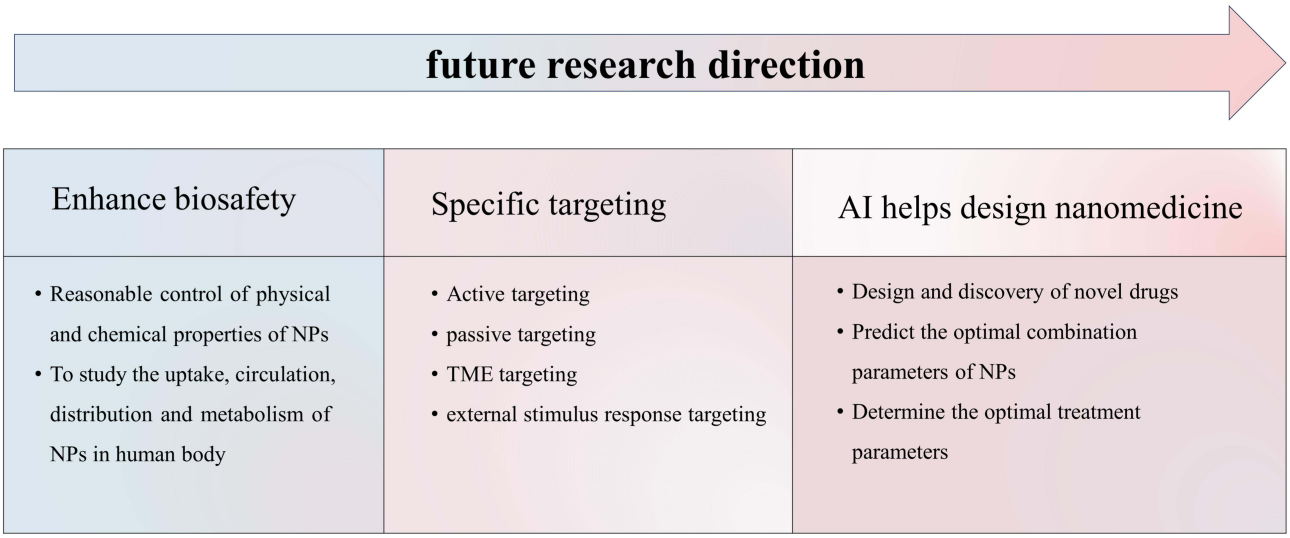

Figure 17 Future research directions for MRI-based nanotheranostic agents.

(1) Bio-safety Concerns. The primary goal of developing nanotheranostic agents is to improve human health, making bio-safety the top priority. However, due to the varying particle sizes, shapes, charges, compositions, and active modifications of nanoparticles, their behavior in the body—including distribution, cellular uptake, and metabolism—can differ greatly, complicating the resolution of potential safety issues. To address this, nanoparticles can be specifically surface-modified to enhance their stability and biocompatibility, preventing prolonged circulation in the bloodstream and unwanted accumulation in normal tissues. Additionally, precise control over the size of nanomaterials, and close attention to their behavior in vivo are crucial. Another promising approach involves developing a new generation of non-toxic or low-toxic nanoparticles or innovative construction strategies. For example, many studies now explore manganese-based alternatives to gadolinium-based contrast agents to reduce toxicity, while others are investigating bio-synthetic methods instead of chemical synthesis to improve bio-safety.

(2) Specific targeting and precise treatment. The accumulation of nanotheranostic agents at the tumor site is crucial for both imaging performance and therapeutic efficacy. Effective diagnosis and treatment depend on precise localization and concentration within the tumor, while minimizing damage to healthy tissues. Three primary strategies are employed to enhance the targeting and specificity of these agents. The first involves optimizing their size to take advantage of the unique pathophysiological characteristics of tumors, thereby increasing their accumulation through the enhanced EPR effect. Another strategy is to conjugate or encapsulate cell-specific ligands (such as antibodies, peptides, nucleic acid aptamers, polysaccharides, or small biomolecules) onto the surface of nano-therapeutic agents to recognize specific receptors on tumor cells, enabling active targeting. Another promising strategy is stimulus-responsive targeting, which has been previously mentioned. This method targets tumors by designing MRI nanotheranostic agents that respond to specific tumor microenvironment conditions (such as low pH and high GSH levels) or external stimuli (such as magnetic fields, light, or heat). This approach improves the tumor microenvironment by alleviating hypoxia, increasing hydrogen peroxide levels, depleting glutathione to enhance therapeutic effects, or modulating MRI signal responses.

(3) Artificial intelligence aids in nano-drug design. In recent years, artificial intelligence (AI) has advanced rapidly and found applications across numerous scientific fields, demonstrating considerable potential. Similarly, AI is playing an increasingly vital role in the development and application of nanotheranostic agents.[246–248] Currently, the scientific community lacks a comprehensive understanding of the formation and metabolism mechanisms of multifunctional nanotheranostic agents. This gap in systematic knowledge and design principles represents a major bottleneck in optimizing nanomedicine for various applications. AI, with its ability to learn from basic characteristics and make relevant predictions, offers promising solutions to many of the challenges in constructing

Table 1 Nano-Therapeutics Used in Different Cancer Therapies

Ther-agent	Ther-method	Therapeutic Component	Imaging Component	B_0(T)	Rela- (mM^{-1} s^{-1})		Functions and Innovations	Cell line	Refs.
					r1	r2			
Fe_3O_4@PLA-PEG /curcumin	MHT	Fe_3O_4 curcumin	Fe_3O_4			364.75	MHT; T2 MRI; Magnetic controlled release curcumin	Sarcoma 180	[37]
VNFG	MHT	Fe_3O_4	Gd_2O_3 Fe_3O_4	3.0	25.02	138.4	T1/T2 dual-modal MRI; MHT	4T1	[45]
FePt@MMT-MIT	MHT Chem-	FePt@MMT-MIT	FePt	7.0		41.835	MMT optimizes T2 MRI and heat effect; MHT; Chem-	SK-Hep-1	[46]
Au@Fe-PEG NPs	MHT PTT	Au Fe	Fe	9.4		60.5	T2 MRI; Remarkable energy conversion capability under NIR light and AMF		[47]
AuNWs	PTT	Au	ES-MIONs		3.20		T1 MRI/PA dual-mode imaging; PTT; GSH response	U87MG	[53]
Fe_3O_4@PDA	PTT	Fe_3O_4 PDA	Fe_3O_4			337.8	MRI; PTT	4T1	[57]
Gd/CuS@PEI-FA-PS NGs	PTT	CuS	Gd^{3+}		11.66		Absorption properties of NIR-II; FA targeting; MRI/PA dual-mode imaging	KB	[63]
$Zn_{0.2}Fe_{2.8}O_4$ @PDA@MnO_2	PTT	$Zn_{0.2}Fe_{2.8}O_4$ @PDA@ MnO_2	$Zn_{0.2}Fe_{2.8}O_4$ MnO_2	0.5	7.47	169.71	T1/T2 dual-modal MRI; GSH response; PTT	4T1	[67]
GdPz2	PDT	Porphyrin	Gd^{3+}	9.4	0.40		FL/MRI imaging; PDT	CT26	[82]
MUM NPs	PDT	AIE- PSs MnO_2 UCNPs	Mn^{2+}		6.89 pH5.5		AIE characteristics PSs; UCNPs increases the penetration depth of NIR tissue; MnO_2 shell responds to GSH to generating oxygen; achieves MRI	4T1	[87]
GMCD	PDT	DVDMS CAT GOx	Mn^{2+}		8.10 pH6.5		Cascade catalytic reaction produces O_2 and •OH; pH-responsive drug release, fluorescence imaging and TME-activated MRI imaging	4T1	[88]
GOx-MnCaP NPs	CDT	Gox Mn^{2+} DOX	Mn^{2+}	3.0	13.06 pH5.0		CDT; T1 MRI; CDT was enhanced by GOx cascade reaction; pH response degradation; H_2O_2formation	4T1	[100]
MMF-Au	CDT	MMF-Au	Mn^{2+}	3.0	18.3 pH6.0		Au NPs mimics GOx activity to catalyze H_2O_2formation; pH response degradation; CDT; T1 MRI and PAI dual modal imaging	HeLa	[101]
MM@HMFe @BS	CDT	HMFe BS	HMFe				Exposure of highly active atoms of HMFe enhanced CDT; Hollow load; Tumor targeting; pH regulation; T2 MRI	4T1	[102]
MnF@ASO	CDT	MnF@ASO	Mn^{2+}	7.0	5.62 pH5.0		pH modulation enhanced CDT and MRI; TME-triggered cascade catalysis is combined with tumor metabolic reprogramming	PC3	[103]
APPAM @U-104	Immu-	USIONs U-104	USIONs		2.67 pH6.5	16.2 pH7.4	pH response to drug release and MRI signal switching from T1 to T2; Anti-pd-l1 immunotherapy; pH regulation	PDAC	[123]
BMI	Immu-	MnO_2 IPI549	Mn^{2+}	3.0	9.76 pH6.8 +H_2O_2	50.64 pH6.8 + H_2O_2	Remodeling TIME activates the immune system; MnO_2 TME responds by releasing oxygen and achieving MRI; Inhibition of PI3Kγ of MDSCs promotes polarization of M1-type macrophages	4T1	[124]
MCCS	Immu-	MCCS	Mn^{2+}	3.0	9.588		MRI; Tumor targeting; cGAS-STING pathway activation; Anti-ctla-4 immunotherapy	A549	[127]
OMPN	Immu-PTT	OVA MnO_2 PDA	Mn^{2+}		31.07		PTT enhances the effect of immunotherapy; MnO_2 acts as MRI contrast agent and immune adjuvant	B16-OVA	[128]
Mn_{1-x}FexCO3@OVA	Immu-	Mn1−xFexCO_3	Mn^{2+} Fe^{3+}	3.0	1.95 pH5.3	65.5 pH5.3	T1-T2 dual-modal MRI guides vaccination; STING activation; CO_2 production promotes antigen cross-presentation	B16-OVA	[129]

SA-SFN-FGNP4	FT	SFN $Fe^{2+/3+}$	Gd_2O_3	3.0	33.43		Low pH response; Cycling accelerates ROS generation; T1 MRI	4T1	[143]
FGNPs@TA-Fe3/Ca4	FT	Fe^{3+}/Ca^{2+}	Gd_2O_3	3.0	44.00		Cycloacceleration of ferroptosis and calcicoptosis; pH responsiveness; T1 MRI	CT 26	[144]
TAF-HMON-CuP @PPDG	FT	TAF CuP	Gd^{3+}	3.0	13.9 pH6.7 +GSH		TME triggers ROS generation; TAF reduces tumor pH and promotes Fenton reaction; T1 MRI	4T1	[145]
FCS/GCS	FT	P-SS-D CA-OH Fe^{3+}/Gd^{3+}	Gd^{3+}	3.0	22.56		TME amplifies oxidative stress and promotes iron death; GSH consumption produces H_2O_2; T1 MRI	4T1	[155]
AMSNs	FT	Manganese silicate nanobubbles; Surface arginine	Mn^{2+}	3.0	4.59 pH5.0+ GSH		The structure of nanobubble and the ultra-thin surface arginine layer can effectively deplete GSH to promote iron death; pH/ GSH-responsive T1 MRI	MDA-MB 231; Huh7	[156]
GBP@ Fe_3O_4	FT	Fe_3O_4 1H-PFP	Fe_3O_4	0.5		56.498	Heat stress combined with Fe_3O_4destroyed tumor REDOX balance, and triggered 1H-PFP phase transition to promote Fe_3O_4 to produce ROS, amplifying oxidative damage; Metabolic reprogramming; T2 MRI	C42	[157]
siR/IONs @LDH	FT	IONs siR	IONs		14.01 pH6.8		IONs and siR Are released in response to pH, promoting ROS generation and blocking LPO clearance; T1 MRI	4T1	[158]
FeS_2-PEG	PTT CDT	FeS_2-PEG	FeS_2-PEG	7.0	1.0	18.14	The change of surface valence of iron ions promotes MRI and CDT	4T1	[167]
Fe_2P	PTT CDT	Fe_2P	Fe_2P		277.7		NIR II high-light thermal conversion efficiency; PTT and US responses promote CDT; PAI / MRI dual modal imaging	U14	[168]
Ir@$MnFe_2O_4$ NPs	MHT CDT	Ir@$MnFe_2O_4$ NPs	$MnFe_2O_4$	1.0		56.97	Coordination of MHT and CDT; Mitochondrial targeting; Fe (III) depletes GSH to Fe (II) to promote CDT; T2 MRI	HeLa	[169]
MCIH	PTT PDT	CuS NPs ICG	Mn^{2+}; ICG	9.4	16.24 pH6.5		Honeycomb MnO_2 catalyzes H_2O_2 to O_2; Tumor targeting; FL/T1 MR Dual modal imaging.	U14	[179]
AAM HNSs	PTT PDT	Au/Ag MnO_2 Ce6	Mn^{2+}		9.22		NIR-II light absorption capacity; MnO_2 catalyzes H_2O_2 to generate O_2 and promote PDT; FL/PAI/T1 MRI three-modal imaging	HeLa	[185]
PMIDA NPs	PTT PDT	PDA MnO_2 IR780	Mn^{2+}	3.0	4.58 pH6.5		PTT/PDT; T1 MRI; O_2 generation; PDA-IR780 double photothermal agent	4T1	[189]
Fe_3O_4@PDA@Pt-PEG-Ce6	PDT PTT	Pt Ce6 PDA	Fe_3O_4	0.5		128.32	Pt produced O_2 alleviating tumor hypoxia; Ce6 enhances singlet O_2 generation; cavity structure and Fe_3O_4 provide US and MRI	4T1	[190]
PEG/LDNPs @CMSN	CDT/ PDT	CMSNs LDNPs	LDNP Mn^{2+}	1.5	7.99 pH6.5+ GSH		TME regulation, bimetallic silicate photosensitizer, Fenton-like nano-catalyst and NIL-II /MR/ CT contrast agent	HeLa	[212]
UCNPs @MOFs	CDT/ PDT	UCNPs @MOFs	Gd^{3+}				FL/ MRI dual modal imaging; UCNPs optical conversion; Fe-MOFs catalyzes H_2O_2 to produce O_2 and promote CDT/PDT	HeLa	[213]
Mn-CDs	CDT/ PDT	Mn-CDs	Mn^{2+}	3.0	6.138 pH5.0 +GSH	43.13 pH5.0 + GSH	Manganese doping improves light stability and $^1O_2$; T1/T2 MRI dual modal imaging enhanced by acid and glutathione response; POD activity promotes therapy	4T1	[215]

(*Continued*)

Table 1 (Continued).

Ther-agent	Ther-method	Therapeutic Component	Imaging Component	B_0(T)	Rela- (mM^{-1} s^{-1})		Functions and Innovations	Cell line	Refs.
					r1	r2			
IMOP	CDT/ PDT	IMOP	Mn^{2+}	1.0	17.8		Highly efficient catalase-like and glutathione peroxidase activities, and fenton-like catalytic activities; Relieve tumor hypoxia	4T1	[216]
$FePSe_3$@APP@CCM	PTT Immu-	APP $FePSe_3$	$FePSe_3$	1.5	8.77		PAI/MRI dual modal imaging; Anti-pd-1 peptide enhanced immunotherapy; tumour targeting	CT26	[223]
FA-P	Immu- MHT	MZF-MNPs JQ-1	Gd-DTPA				MRET activates T1 MRI; Tumor targeting; MHT synergistic immu-	CT26; 4T1	[224]
SMP@Mn	PTT Immu-	MSA-2 Mn^{2+} MPDA	Mn^{2+}	1.0	14.24		pH/ thermal response drug release; MSA-2 and Mn^{2+} activate STING pathway; T1 MRI; Tumor targeting; PTT synergistic immu-	4T1	[225]
EV@Gd-MCNs-R837	PTT Immu-	R837 Gd-MCNs	Gd-MCNs	3.0	32.5		Efficient drug loading; Tumor targeting; PTT synergistic immunotherapy	4T1	[229]
MIRDs	PTT Immu-	ICG R837	Fe				Fe_3O_4core drug-carrying ICG; DPA-PEG coating loaded R837; Tumor targeting; Multimodal imaging	4T1	[230]
Fe–GA/BSA @DOX	Chem- PTT CDT	DOX Fe–GA	Fe				pH response releases DOX; Using consumed GSH to convert Fe(III) to Fe(II) to promote CDT; Efficient PTT;T1/T2 MRI dual modal imaging	C6	[233]
HMNCs	Chem- PTT CDT	HMNCs DOX	HMNCs			62.97	NIR-II responsiveness; Cavities are loaded with DOX and pH responsive release	Hela	[234]
CuS@$mSiO_2$ @ MnO_2 /DOX NCs	Chem- PTT CDT	CuS MnO_2 DOX	Mn^{2+}		1.963 pH6.5 +GSH		NIR and TME respond to drug controlled release; MnO_2 catalyzes the production of O_2 and •OH	HeLa	[235]
HSPMH-DOX	Chem- PTT CDT	PDA MnO_2 HA DOX	Mn^{2+}	3.0	9.73 pH5.5 +GSH		pH/GSH and NIR irradiation response; MnO_2 nano-enzyme properties enhance MRI and CDT	4T1	[236]
AMGDC NPs	Chem- PTT CDT	AuNR MnO_2 GOD DOX	Mn^{2+}	3.0	8.344 pH5.5 +GSH		Tumor targeting; MnO_2 generates Mn^{2+} in response to GSH enhancing CDT; GOD catalyzes the production of H_2O_2 from glucose in tumor and enhances CDT; NIR-II promotes PTT and enhances CDT; PAI/MRI dual modal imaging	U87MG	[237]
H-MnO_2 /DOX/ BPQDs	Chem- PTT PDT	DOX BPQDs H-MnO_2	Mn^{2+}				FL/MRI dual modal imaging; DOX was released in response to TME; Unloaded medicine; MnO_2 alleviates the hypoxic environment of the tumor	HepG2	[239]
DCMNs	Chem- PDT Immu-	DOX Ce6	Mn^{2+}				Efficient drug loading; pH responsive release; Erythrocyte membrane coating improves cycle time and stability; Enhance anti-PD-1 anti-tumor response	4T1; HeLa	[240]
ICG@SANPs-cRGD	PTT PDT Immu-	ICG	Fe_3O_4				Tumor targeting; FL/MRI dual modal imaging; Combined treatment with ICD/ICB/PTT/PDT	4T1	[241]
SRCM	PTT PDT Immu-	MnO_2 Ce6	Mn^{2+}	3.0	4.68 pH5.5 +GSH		Intelligently targeting TME and adjusting pH/GSH/H_2O_2 and hypoxia environment to improve efficacy; Promote immune cell infiltration, activate antigen presenting cells (APC), induce ICD	4T1	[242]
MCRT	Gene- Immu- CDT	CRISPR/ Cas9 MnS	Mn^{2+}		8.70 pH5.5		pH-responsive CRISPR/Cas9 release; H_2S self-enhanced CDT; H_2S and released CRISPR/ Cas9 synergistic self-augmentation gene therapy; H_2S-enhanced CDT-gene therapy simultaneously induces ICD	4T1	[245]

Notes: Ther-agent refers to Therapeutic agents; Ther-method refers to Therapeutic methods; Rela- indicates relaxivity; Chem- indicates Chemotherapy; Immu- indicates Immunotherapy.

nanotheranostic agents. Firstly, AI can facilitate the identification and prediction of new drug molecules with diagnostic and therapeutic potential by building and analyzing extensive databases, thereby aiding the development of novel nano-therapeutic agents. Secondly, AI can help design nanoparticles with specific attributes or optimize the performance of nanotheranostic agents by modeling various parameters such as particle size, shape, and anisotropy to identify the most effective combinations. Furthermore, statistical analysis of nanoparticle trajectories within the body can be employed to discern the distribution patterns of nano-drugs, enhancing their transport and targeting capabilities, or to better understand the interactions between nano-carriers and the biological environment, thereby improving drug safety. Finally, predictive models can be developed to determine optimal drug dosages, administration frequencies, and treatment timings, increasing the success rates of clinical trials and accelerating clinical translation.

Summary and Outlook

This article comprehensively reviews the design strategies, therapeutic mechanisms, and applications of MRI-based multifunctional nanotheranostic agents across a wide range of cancer treatment modalities, including monotherapies and combinational therapies, and offers a comprehensive summary of several developed MRI nanotheranostic agents (Table 1). Through the integration of imaging and therapy within a single nanoplatform, these agents demonstrate substantial potential in enhancing tumor diagnosis precision, guiding therapeutic delivery, and minimizing systemic toxicity. The progress across various imaging-guided strategies, including magnetic hyperthermia, photothermal and photodynamic therapy, chemodynamic therapy, immunotherapy, and ferroptosis, reflects the growing emphasis on precise, synergistic, and real-time tumor treatment.

Despite significant advances, major challenges remain in clinical translation. Future research should prioritize the development of nanoplatforms with well-defined safety profiles, improved targeting specificity, and enhanced responsiveness to tumor microenvironment cues. In particular, rational material design that enables controllable biodegradation and minimal off-target effects is essential. Moreover, there is a need to establish robust, standardized evaluation systems and scalable GMP-compliant production processes. Multi-modal integration—combining MRI with fluorescence, photoacoustic, or nuclear imaging—will further facilitate personalized, adaptive treatment regimens. Additionally, incorporating artificial intelligence into nanoparticle design and therapeutic modeling holds promise for optimizing formulation parameters, predicting in vivo behavior, and improving clinical decision-making.

Looking ahead, several transformative trends are emerging that are expected to shape the next decade of MRI-guided nanotheranostics. A comprehensive bibliometric analysis of anti-tumor therapy literature over the past 20 years (Figure 18) reveals that ferroptosis research has experienced particularly rapid growth, indicating its increasing

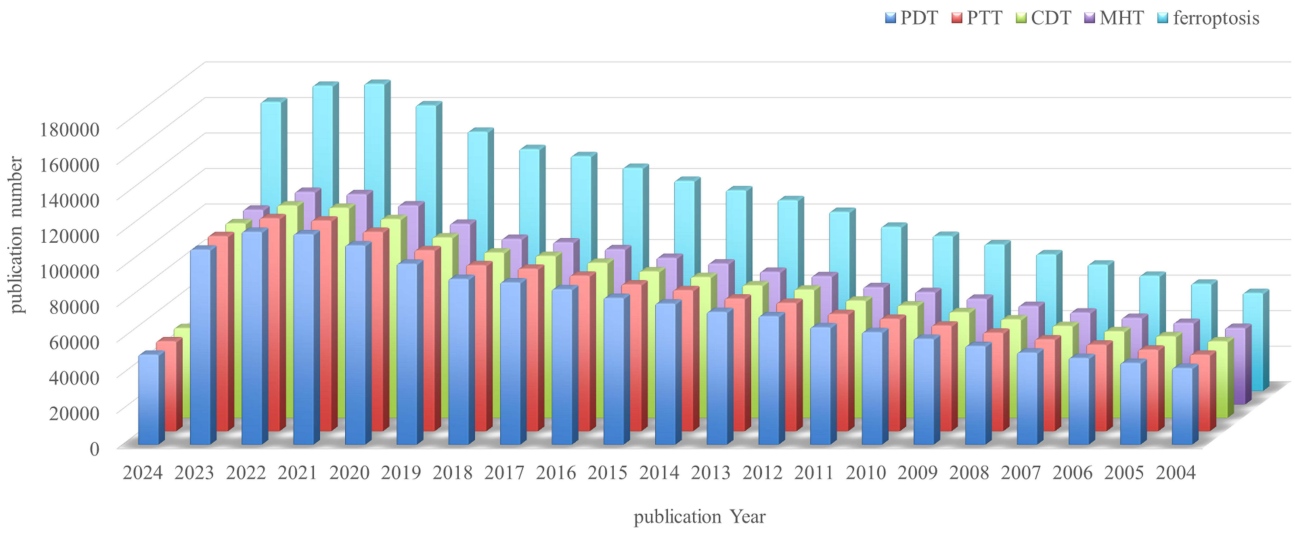

Figure 18 Analysis of the trends in publication volumes of different anti-tumor therapies over the past 20 years.

https://doi.org/10.2147/IJN.S529003

prominence as a therapeutic strategy. In parallel, the convergence of nanomedicine with immunotherapy, gene-editing technologies (eg, CRISPR), and AI-driven design suggests the formation of a new generation of intelligent, immune-responsive, and genetically programmable nanotheranostic systems. These interdisciplinary innovations are poised to revolutionize the future of precision oncology by offering safer, more effective, and highly individualized treatment solutions.

Acknowledgments

The authors gratefully acknowledge the use of the Figure platform (www.figdraw.com) for the preparation of the figures in this manuscript. This work was financially supported by the Guangxi Science and Technology Major Program (Guike AA23023002); the Special project of local science and technology development funds guided by the central government (GuikeZY21195012); the Guangxi Key Laboratory of Traditional Chinese Medicine Quality Standards (Guangxi Institute of Traditional Medical and Pharmaceutical Sciences) (guizhongzhongkai201703) and the Foundation of Key Laboratory of Trusted Software (No. kx201703).

Author Contributions

All authors made a significant contribution to the work reported, whether that is in the conception, study design, execution, acquisition of data, analysis and interpretation, or in all these areas; took part in drafting, revising or critically reviewing the article; gave final approval of the version to be published; have agreed on the journal to which the article has been submitted; and agree to be accountable for all aspects of the work.

Disclosure

The authors have declared that no competing interest exists.

References

1. Bray F, Laversanne M, Sung HYA, et al. Global cancer statistics 2022: GLOBOCAN estimates of incidence and mortality worldwide for 36 cancers in 185 countries. *Ca-a Cancer J Clin*. 2024;74(3):229–263. doi:10.3322/caac.21834
2. Chang MY, Hou ZY, Wang M, et al. Cu_2MoS_4/au heterostructures with enhanced catalase-like activity and photoconversion efficiency for primary/metastatic tumors eradication by phototherapy-induced immunotherapy. *Small*. 2020;16(14). doi:10.1002/smll.201907146.
3. Feng LL, Xie R, Wang CQ, et al. Magnetic targeting, tumor microenvironment-responsive intelligent nanocatalysts for enhanced tumor ablation. *Acs Nano*. 2018;12(11):11000–11012. doi:10.1021/acsnano.8b05042
4. Ye ZY, Bao Y, Chen ZF, et al. Recent advances in the metal/organic hybrid nanomaterials for cancer theranostics. *Coord Chem Rev*. 2024;504:215654.
5. Ma YF, Huang J, Song SJ, Chen HB, Zhang ZJ. Cancer-targeted nanotheranostics: recent advances and perspectives. *Small*. 2016;12 (36):4936–4954. doi:10.1002/smll.201600635
6. Lim EK, Kim T, Paik S, Haam S, Huh YM, Lee K. Nanomaterials for theranostics: recent advances and future challenges. *Chem Rev*. 2015;115 (1):327–394. doi:10.1021/cr300213b
7. Chen HM, Zhang WZ, Zhu GZ, Xie J, Chen XY. Rethinking cancer nanotheranostics. *Nature Rev Mater*. 2017;2(7). doi:10.1038/natrevmats.2017.24
8. Zhou ZJ, Yang LJ, Gao JH, Chen XY. Structure-relaxivity relationships of magnetic nanoparticles for magnetic resonance imaging. *Adv Mater*. 2019;31(8):1804567.
9. Hsieh V, Okada S, Wei H, et al. Neurotransmitter-responsive nanosensors for T2-weighted magnetic resonance imaging. *J Am Chem Soc*. 2019;141(40):15751–15754. doi:10.1021/jacs.9b08744
10. Zhang H, Liu XL, Fan HM. Advances in magnetic nanoparticle-based magnetic resonance imaging contrast agents. *Nano Res*. 2023;16 (11):12531–12542. doi:10.1007/s12274-023-6214-9
11. Wang ZL, Xue XD, Lu HW, et al. Two-way magnetic resonance tuning and enhanced subtraction imaging for non-invasive and quantitative biological imaging. *Nature Nanotechnol*. 2020;15(6):482. doi:10.1038/s41565-020-0678-5
12. Jeon M, Halbert MV, Stephen ZR, Zhang MQ. Iron oxide nanoparticles as T_1 contrast agents for magnetic resonance imaging: fundamentals, challenges, applications, and prospectives. *Adv Mater*. 2021;33(23). doi:10.1002/adma.201906539
13. Lu H, Chen A, Zhang X, et al. A pH-responsive T1-T2dual-modal MRI contrast agent for cancer imaging. *Nat Commun*. 2022;13(1). doi:10.1038/s41467-022-35655-x.
14. Lu Z-R, Laney V, Li Y. Targeted contrast agents for magnetic resonance molecular imaging of cancer. *Acc Chem Res*. 2022;55(19):2833–2847. doi:10.1021/acs.accounts.2c00346
15. Kircher MF, Willmann JK. Molecular body imaging: MR imaging, CT, and US. Part I. Principles. *Radiology*. 2012;263(3):633–643. doi:10.1148/radiol.12102394

16. Direrса WB, Kan T-C, Getachew G, et al. Preclinical assessment of enhanced chemodynamic therapy by an FeMnOx<-based nanocarrier: tumor-microenvironment-mediated fenton reaction and ros-induced chemotherapeutic for boosted antitumor activity. *ACS Appl Mater Interfaces*. 2023;15(48):55258–55275. doi:10.1021/acsami.3c10733
17. Korupalli C, Kuo CC, Getachew G, et al. Multifunctional manganese oxide-based nanocomposite theranostic agent with glucose/light--responsive singlet oxygen generation and dual-modal imaging for cancer treatment. *J Colloid Interface Sci*. 2023;643:373–384. doi:10.1016/j.jcis.2023.04.049
18. Getachew G, Korupalli C, Rasal AS, Direrса WB, Fahmi MZ, Chang JY. Highly luminescent, stable, and red-emitting CsMg(x)Pb(1-x)I(3) quantum dots for dual-modal imaging-guided photodynamic therapy and photocatalytic activity. *ACS Appl Mater Interfaces*. 2022;14(1):278–296. doi:10.1021/acsami.1c19644
19. Zhou W, Pan T, Cui H, Zhao Z, Chu PK, Yu X-F. Black phosphorus: bioactive nanomaterials with inherent and selective chemotherapeutic effects. *Angew Chem-Int Ed*. 2019;58(3):769–774. doi:10.1002/anie.201810878
20. Senapati S, Mahanta AK, Kumar S, Maiti P, Li C, Ren J. Controlled drug delivery vehicles for cancer treatment and their performance. *Sign Transduc Targeted Therapy*. 2018;3:3. doi:10.1038/s41392-017-0003-4
21. Wang C, Fan W, Zhang Z, Wen Y, Xiong L, Chen X. Advanced nanotechnology leading the way to multimodal imaging-guided precision surgical therapy. *Adv Mater*. 2019;31(49):1904329.
22. Song M, Liu N, He L, et al. Porous hollow palladium nanoplatform for imaging-guided trimodal chemo-, photothermal-, and radiotherapy. *Nano Res*. 2018;11(5):2796–2808. doi:10.1007/s12274-017-1910-y
23. Hao XY, Wu JY, Xiang DX, Yang YY. Recent advance of nanomaterial-mediated tumor therapies in the past five years. *Front Pharmacol*. 2022;13:846715.
24. Zhu XD, Li SL. Nanomaterials in tumor immunotherapy: new strategies and challenges. *Mol Cancer*. 2023;22(1):94.
25. Shi JJ, Kantoff PW, Wooster R, Farokhzad OC. Cancer nanomedicine: progress, challenges and opportunities. *Nat Rev Cancer*. 2017;17(1):20–37. doi:10.1038/nrc.2016.108
26. Xu Y, Luo C, Wang J, et al. Application of nanotechnology in the diagnosis and treatment of bladder cancer. *J Nanobiotechnol*. 2021;19(1). doi:10.1186/s12951-021-01104-y.
27. Chan MH, Li CH, Chang YC, Hsiao MC. Iron-based ceramic composite nanomaterials for magnetic fluid hyperthermia and drug delivery. *Pharmaceutics*. 2022;14(12):2584. doi:10.3390/pharmaceutics14122584
28. Alromi DA, Madani SY, Seifalian A. Emerging application of magnetic nanoparticles for diagnosis and treatment of cancer. *Polymers*. 2021;13(23):4146. doi:10.3390/polym13234146
29. Zhu XJ, Feng W, Chang J, et al. Temperature-feedback upconversion nanocomposite for accurate photothermal therapy at facile temperature. *Nat Commun*. 2016;7:10437.
30. Xie G, Guo S, Li B, et al. Nonmetallic graphite for tumor magnetic hyperthermia therapy. *Biomaterials*. 2024;306:122498.
31. Gu Y, Pinol R, Moreno-Loshuertos R, et al. Local temperature increments and induced cell death in intracellular magnetic hyperthermia. *Acs Nano*. 2023;17(7):6822–6832. doi:10.1021/acsnano.3c00388
32. Gong J, Hu J, Yan X, et al. Injectable hydrogels including magnetic nanosheets for multidisciplinary treatment of hepatocellular carcinoma via magnetic hyperthermia. *Small*. 2024;20(3). doi:10.1002/smll.202300733.
33. Gobbo OL, Sjaastad K, Radomski MW, Volkov Y, Prina-Mello A. Magnetic nanoparticles in cancer theranostics. *Theranostics*. 2015;5(11):1249–1263. doi:10.7150/thno.11544
34. Dadfar SM, Roemhild K, Drude NI, et al. Iron oxide nanoparticles: diagnostic, therapeutic and theranostic applications. *Adv Drug Delivery Rev*. 2019;138:302–325. doi:10.1016/j.addr.2019.01.005
35. Soetaert F, Korangath P, Serantes D, Fiering S, Ivkov R. Cancer therapy with iron oxide nanoparticles: agents of thermal and immune therapies. *Adv Drug Delivery Rev*. 2020;163:65–83. doi:10.1016/j.addr.2020.06.025
36. Lartigue L, Hugounenq P, Alloyeau D, et al. Cooperative organization in iron oxide multi-core nanoparticles potentiates their efficiency as heating mediators and MRI contrast agents. *Acs Nano*. 2012;6(12):10935–10949. doi:10.1021/nn304477s
37. Thong PQ, Huong LT, Tu ND, et al. Multifunctional nanocarriers of Fe3O4@PLA-PEG/curcumin for MRI, magnetic hyperthermia and drug delivery. *Nanomedicine*. 2022;17(22):1677–1693. doi:10.2217/nnm-2022-0070
38. Laha SS, Thorat ND, Singh G, et al. Rare-earth doped iron oxide nanostructures for cancer theranostics: magnetic hyperthermia and magnetic resonance imaging. *Small*. 2022;18(11). doi:10.1002/smll.202104855.
39. Hu FQ, Zhao YS. Inorganic nanoparticle-based T1 and T1/T2 magnetic resonance contrast probes. *Nanoscale*. 2012;4(20):6235–6243. doi:10.1039/c2nr31865b
40. Lastovina TA, Budnyk AP, Kudryavtsev EA, et al. Solvothermal synthesis of Sm3+-doped Fe3O4 nanoparticles. *Mater Sci Eng C-Mater Biol Appl*. 2017;80:110–116. doi:10.1016/j.msec.2017.05.087
41. Lunin AV, Sokolov IL, Zelepukin IV, et al. Spindle-like MRI-active europium-doped iron oxide nanoparticles with shape-induced cytotoxicity from simple and facile ferrihydrite crystallization procedure. *RSC Adv*. 2020;10(12):7301–7312. doi:10.1039/C9RA10683A
42. Osial M, Rybicka P, Pekala M, Cichowicz G, Cyranski MK, Krysinski P. Easy synthesis and characterization of holmium-doped SPIONs. *Nanomaterials*. 2018;8(6):430. doi:10.3390/nano8060430
43. Chen J, Xiang HH, Zhao ZZ, Wu YK, Fei MY, Song MM. An ultra-sensitiveT2-weighted MR contrast agent based on Gd3+ ion chelated Fe3O4 nanoparticles. *RSC Adv*. 2020;10(31):18054–18061. doi:10.1039/D0RA01807D
44. McKiernan EP, Moloney C, Chaudhuri TR, et al. Formation of hydrated PEG layers on magnetic iron oxide nanoflowers shows internal magnetisation dynamics and generates high in-vivo efficacy for MRI and magnetic hyperthermia. *Acta Biomater*. 2022;152:393–405. doi:10.1016/j.actbio.2022.08.033
45. Bao JF, Guo SS, Zu XY, et al. Magnetic vortex nanoring coated with gadolinium oxide for highly enhanced T1-T2 dual-modality magnetic resonance imaging-guided magnetic hyperthermia cancer ablation. *Biomed Pharmacother*. 2022;150:112926.
46. Hu ZF, Wei QL, Zhang HM, et al. Advances in FePt-involved nano-system design and application for bioeffect and biosafety. *J Mat Chem B*. 2022;10(3):339–357. doi:10.1039/D1TB02221K
47. Christou E, Pearson JR, Beltrán AM, et al. Iron-gold nanoflowers: a promising tool for multimodal imaging and hyperthermia therapy. *Pharmaceutics*. 2022;14(3). doi:10.3390/pharmaceutics14030636.

48. Luo S, Qin SJ, Oudeng G, Zhang L. Iron-based hollow nanoplatforms for cancer imaging and theranostics. *Nanomaterials*. 2022;12(17):3023. doi:10.3390/nano12173023
49. Xiong Y, Rao Y, Hu J, Luo Z, Chen C. Nanoparticle-based photothermal therapy for breast cancer noninvasive treatment. *Adv Mater*. 2023:230514.
50. Zou L, Wang H, He B, et al. Current approaches of photothermal therapy in treating cancer metastasis with nanotherapeutics. *Theranostics*. 2016;6(6):762–772. doi:10.7150/thno.14988
51. Liu YJ, Bhattarai P, Dai ZF, Chen XY. Photothermal therapy and photoacoustic imaging via nanotheranostics in fighting cancer. *Chem Soc Rev*. 2019;48(7):2053–2108. doi:10.1039/c8cs00618k
52. Du L, Chen W, Zhong J, et al. Dopamine multivalent-modified polyaspartic acid for MRI-guided near-infrared photothermal therapy. *Regene Biomate*. 2023;10:rbad022.
53. Liu YJ, Yang Z, Huang XL, et al. Glutathione-responsive self-assembled magnetic gold nanowreath for enhanced tumor imaging and imaging-guided photothermal therapy. *Acs Nano*. 2018;12(8):8129–8137. doi:10.1021/acsnano.8b02980
54. Wu D, Duan XH, Guan QQ, et al. Mesoporous polydopamine carrying manganese carbonyl responds to tumor microenvironment for multimodal imaging-guided cancer therapy. *Adv Func Mater*. 2019;29(16):1900095.
55. Zhu ML, Shi Y, Shan YF, et al. Recent developments in mesoporous polydopamine-derived nanoplatforms for cancer theranostics. *J Nanobiotechnol*. 2021;19(1). doi:10.1186/s12951-021-01131-9.
56. Cheng W, Zeng XW, Chen HZ, et al. Versatile polydopamine platforms: synthesis and promising applications for surface modification and advanced nanomedicine. *Acs Nano*. 2019;13(8):8537–8565. doi:10.1021/acsnano.9b04436
57. Li B, Gong TT, Xu NN, et al. Improved stability and photothermal performance of polydopamine-modified Fe3O4 nanocomposites for highly efficient magnetic resonance imaging-guided photothermal therapy. *Small*. 2020;16(45). doi:10.1002/smll.202003969.
58. Meng X, Pang X, Zhang K, et al. Recent advances in near-infrared-II fluorescence imaging for deep-tissue molecular analysis and cancer diagnosis. *Small*. 2022;18(31). doi:10.1002/smll.202202035.
59. Chang M, Hou Z, Wang M, et al. Single-atom PD nanozyme for ferroptosis-boosted mild-temperature photothermal therapy. *Angew Chem-Int Ed*. 2021;60(23):12971–12979. doi:10.1002/anie.202101924
60. Wang P, Li J, Wei M, et al. Tumor-microenvironment triggered signal-to-noise boosting nanoprobes for NIR-IIb fluorescence imaging guided tumor surgery and NIR-II photothermal therapy. *Biomaterials*. 2022;287:121636.
61. Li C, Chen G, Zhang Y, Wu F, Wang Q. Advanced fluorescence imaging technology in the near-infrared-II window for biomedical applications. *J Am Chem Soc*. 2020;142(35):14789–14804.
62. Luo H, Gao S. Recent advances in fluorescence imaging-guided photothermal therapy and photodynamic therapy for cancer: from near-infrared-I to near-infrared-II. *J Control Release*. 2023;362:425–445. doi:10.1016/j.jconrel.2023.08.056
63. Zhang CC, Sun WJ, Wang Y, et al. Gd-/CuS-loaded functional nanogels for MR/PA imaging-guided tumor-targeted photothermal therapy. *ACS Appl Mater Interfaces*. 2020;12(8):9107–9117. doi:10.1021/acsami.9b23413
64. Ma GC, Liu ZK, Zhu CG, et al. H2O2-responsive NIR-II AIE nanobomb for carbon monoxide boosting low-temperature photothermal therapy. *Angew Chem-Int Ed*. 2022;61(36). doi:10.1002/anie.202207213.
65. Birbo B, Madu EE, Madu CO, Jain A, Lu Y. Role of HSP90 in cancer. *Int J Mol Sci*. 2021;22(19):10317. doi:10.3390/ijms221910317
66. Yang G, Song T, Zhang H, et al. Stimulus-detonated biomimetic "nanobomb" with controlled release of HSP90 inhibitor to disrupt mitochondrial function for synergistic gas and photothermal therapy. *Adv Healthcare Mater*. 2023;12(26). doi:10.1002/adhm.202300945.
67. Yao JL, Zheng F, Yang F, et al. An intelligent tumor microenvironment responsive nanotheranostic agent for T1/T2 dual-modal magnetic resonance imaging-guided and self-augmented photothermal therapy. *Biomater Sci*. 2021;9(22):7591–7602. doi:10.1039/D1BM01324F
68. Sarbadhikary P, George BP, Abrahamse H. Recent advances in photosensitizers as multifunctional theranostic agents for imaging-guided photodynamic therapy of cancer. *Theranostics*. 2021;11(18):9054–9088. doi:10.7150/thno.62479
69. Correia JH, Rodrigues JA, Pimenta S, Dong T, Yang ZC. Photodynamic therapy review: principles, photosensitizers, applications, and future directions. *Pharmaceutics*. 2021;13(9):1332. doi:10.3390/pharmaceutics13091332
70. Sun ZH, Liu J, Li YY, et al. Aggregation-induced-emission photosensitizer-loaded nano-superartificial dendritic cells with directly presenting tumor antigens and reversed immunosuppression for photodynamically boosted immunotherapy. *Adv Mater*. 2023;35(3).
71. Sun X, Cao ZY, Mao KR, et al. Photodynamic therapy produces enhanced efficacy of antitumor immunotherapy by simultaneously inducing intratumoral release of sorafenib. *Biomaterials*. 2020;240:119845.
72. Alzeibak R, Mishchenko TA, Shilyagina NY, Balalaeva IV, Vedunova MV, Krysko DV. Targeting immunogenic cancer cell death by photodynamic therapy: past, present and future. *J ImmunoTherapy Cancer*. 2021;9(1):e001926. doi:10.1136/jitc-2020-001926
73. Hu TT, Wang ZD, Shen WC, Liang RZ, Yan D, Wei M. Recent advances in innovative strategies for enhanced cancer photodynamic therapy. *Theranostics*. 2021;11(7):3278–3300. doi:10.7150/thno.54227
74. Akbar A, Khan S, Chatterjee T, Ghosh M. Unleashing the power of porphyrin photosensitizers: illuminating breakthroughs in photodynamic therapy. *J Photochem Photobiol B*. 2023;248:112796.
75. Tian J, Huang B, Nawaz MH, Zhang W. Recent advances of multi-dimensional porphyrin-based functional materials in photodynamic therapy. *Coord Chem Rev*. 2020;420:213410.
76. Pareek Y, Ravikanth M, Chandrashekar TK. Smaragdyrins: emeralds of expanded porphyrin family. *Acc Chem Res*. 2012;45(10):1801–1816. doi:10.1021/ar300136s
77. Chen H, Wang Y, Wang W, et al. High-yield porphyrin production through metabolic engineering and biocatalysis. *Nature Biotechnol*. 2024.
78. Li Q, Zhao NN, Bai F. Size- and shape-dependent photocatalysis of porphyrin nanocrystals. *Mrs Bulletin*. 2019;44(3):172–177. doi:10.1557/mrs.2019.41
79. Shao S, Rajendiran V, Lovell JF. Metalloporphyrin nanoparticles: coordinating diverse theranostic functions. *Coord Chem Rev*. 2019;379:99–120. doi:10.1016/j.ccr.2017.09.002
80. Calvete MJF, Pinto SMA, Pereira MM, Geraldes C. Metal coordinated pyrrole-based macrocycles as contrast agents for magnetic resonance imaging technologies: synthesis and applications. *Coord Chem Rev*. 2017;333:82–107. doi:10.1016/j.ccr.2016.11.011
81. Zou TJ, Zhen MM, Chen DQ, et al. The positive influence of fullerene derivatives bonded to manganese(III) porphyrins on water proton relaxation. *Dalton Trans*. 2015;44(19):9114–9119. doi:10.1039/C4DT03482A

82. Yuzhalcova DV, Lermontova SA, Grigoryev IS, et al. In vivo multimodal tumor imaging and photodynamic therapy with novel theranostic agents based on the porphyrazine framework-chelated gadolinium (III) cation. *Biochim Biophys Acta-Gen Subj*. 2017;1861(12):3120–3130. doi:10.1016/j.bbagen.2017.09.004
83. Schmitt J, Jenni S, Sour A, et al. A porphyrin dimer-GdDOTA conjugate as a theranostic agent for one- and two-photon photodynamic therapy and MRI. *Bioconjugate Chem*. 2018;29(11):3726–3738. doi:10.1021/acs.bioconjchem.8b00634
84. Lou XY, Zhang G, Song N, Yang YW. Supramolecular materials based on AIEgens for photo-assisted therapy. *Biomaterials*. 2022;286:121595.
85. Ni JC, Wang YJ, Zhang HK, Sun JZ, Tang BZ. Aggregation-induced generation of reactive oxygen species: mechanism and photosensitizer construction. *Molecules*. 2021;26(2):268. doi:10.3390/molecules26020268
86. Hu R, Qin A, Tang BZ. AIE polymers: synthesis and applications. *Prog Polym Sci*. 2020;100:101176.
87. Wang YW, Li YM, Zhang ZJ, Wang L, Wang D, Tang BZ. Triple-jump photodynamic theranostics: mnO_2 combined upconversion nanoplatforms involving a type-I photosensitizer with aggregation-induced emission characteristics for potent cancer treatment. *Adv Mater*. 2021;33(41):2103748.
88. Fu LH, Wan YL, Li CY, et al. Biodegradable calcium phosphate nanotheranostics with tumor-specific activatable cascade catalytic reactions-augmented photodynamic therapy. *A*. 2021;31(14).
89. Yu Q, Li X, Wang J, Guo LP, Gao WY, Huang LQ. Recent advances in reprogramming strategy of tumor microenvironment for rejuvenating photosensitizers-mediated photodynamic therapy. *Small*. 2024;20(16).
90. Zhong X, Wang X, Li J, Hu J, Cheng L, Yang X. ROS-based dynamic therapy synergy with modulating tumor cell-microenvironment mediated by inorganic nanomedicine. *Coord Chem Rev*. 2021;437.
91. Zhao PR, Li HY, Bu WB. A forward vision for chemodynamic therapy: issues and opportunities. *Angew Chem-Int Ed*. 2023;62(7).
92. Li S-L, Chu X, Dong H-L, Hou H-Y, Liu Y. Recent advances in augmenting Fenton chemistry of nanoplatforms for enhanced chemodynamic therapy. *Coord Chem Rev*. 2023;479:215004.
93. Fu L-H, Wan Y, Qi C, et al. Nanocatalytic theranostics with glutathione depletion and enhanced reactive oxygen species generation for efficient cancer therapy. *Adv Mater*. 2021;33(7). doi:10.1002/adma.202006892.
94. Tian QW, Xue FF, Wang YR, et al. Recent advances in enhanced chemodynamic therapy strategies. *Nano Today*. 2021;39:101162.
95. Sun Q, Wang Z, Liu B, et al. Recent advances on endogenous/exogenous stimuli-triggered nanoplatforms for enhanced chemodynamic therapy. *Coord Chem Rev*. 2022;451.
96. Zhang X, He C, Chen Y, et al. Cyclic reactions-mediated self-supply of H_2O_2 and O_2 for cooperative chemodynamic/starvation cancer therapy. *Biomaterials*. 2021;275.
97. Deng F, Fan G, Yuan P, et al. A self-accelerated biocatalyst for glucose-initiated tumor starvation and chemodynamic therapy. *Chem Commun*. 2020;56(93):14633–14636. doi:10.1039/D0CC06483A
98. Guo Y, Jia H-R, Zhang X, et al. A glucose/oxygen-exhausting nanoreactor for starvation- and hypoxia-activated sustainable and cascade chemo-chemodynamic therapy. *Small*. 2020;16(31).
99. Glorieux C, Liu S, Trachootham D, Huang P. Targeting ROS in cancer: rationale and strategies. *Nat Rev Drug Discov*. 2024;23(8):583–606. doi:10.1038/s41573-024-00979-4
100. Fu LH, Hu YR, Qi C, et al. Biodegradable manganese-doped calcium phosphate nanotheranostics for traceable cascade reaction-enhanced anti-tumor therapy. *Acs Nano*. 2019;13(12):13985–13994. doi:10.1021/acsnano.9b05836
101. Jiang C, He T, Tang QA, et al. Nanozyme catalyzed cascade reaction for enhanced chemodynamic therapy of low- H_2O_2 tumor. *Appl Mater Today*. 2022;26.
102. Zuo WB, Chen WB, Liu JX, et al. Macrophage-mimic hollow mesoporous fe-based nanocatalysts for self-amplified chemodynamic therapy and metastasis inhibition via tumor microenvironment remodeling. *ACS Appl Mater Interfaces*. 2022;14(4):5053–5065. doi:10.1021/acsami.1c22432
103. Chen H, Wu PY, Xiao ZZ, et al. Engineering a self-fueling and self-reported theranostic nanocatalyst for amplified cancer imaging and chemodynamic therapy. *Nano Today*. 2024;54.
104. Di XJ, Pei ZC, Pei YX, James TD. Tumor microenvironment-oriented MOFs for chemodynamic therapy. *Coord Chem Rev*. 2023;484.
105. Song WT, Musetti SN, Huang L. Nanomaterials for cancer immunotherapy. *Biomaterials*. 2017;148:16–30. doi:10.1016/j.biomaterials.2017.09.017
106. Zhang W, Wang F, Hu C, Zhou Y, Gao H, Hu J. The progress and perspective of nanoparticle-enabled tumor metastasis treatment. *Acta Pharmaceutica Sinica B*. 2020;10(11):2037–2053. doi:10.1016/j.apsb.2020.07.013
107. Abbott M, Ustoyev Y. Cancer and the immune system: the history and background of immunotherapy. *Semin Oncol Nurs*. 2019;35(5):150923. doi:10.1016/j.soncn.2019.08.002
108. Zhang Y, Zhang Z. The history and advances in cancer immunotherapy: understanding the characteristics of tumor-infiltrating immune cells and their therapeutic implications. *Cell Mol Immunol*. 2020;17(8):807–821. doi:10.1038/s41423-020-0488-6
109. Ribas A, Wolchok JD. Cancer immunotherapy using checkpoint blockade. *Science*. 2018;359(6382):1350. doi:10.1126/science.aar4060
110. Sahin U, Tureci O. Personalized vaccines for cancer immunotherapy. *Science*. 2018;359(6382):1355–1360. doi:10.1126/science.aar7112
111. Kroemer G, Galassi C, Zitvogel L, Galluzzi L. Immunogenic cell stress and death. *Nat Immunol*. 2022;23(4):487–500. doi:10.1038/s41590-022-01132-2
112. Samson N, Ablasser A. The cGAS-STING pathway and cancer. *Nat Cancer*. 2022;3(12):1452–1463. doi:10.1038/s43018-022-00468-w
113. Liu J, Cabral H, Song B, et al. Nanoprobe-based magnetic resonance imaging of hypoxia predicts responses to radiotherapy, immunotherapy, and sensitizing treatments in pancreatic tumors. *Acs Nano*. 2021;15(8):13526–13538. doi:10.1021/acsnano.1c04263
114. Liu XM, Wang MK, Jiang YC, et al. Magnetic resonance imaging nanoprobe quantifies nitric oxide for evaluating M1/M2 macrophage polarization and prognosis of cancer treatments. *Acs Nano*. 2023;17(24):24854–24866. doi:10.1021/acsnano.3c05627
115. Carter BW, Bhosale PR, Yang WT. Immunotherapy and the Role of Imaging. *Cancer*. 2018;124(14):2906–2922. doi:10.1002/cncr.31349
116. Zhang K, Qi C, Cai KY. Manganese-based tumor immunotherapy. *Adv Mater*. 2023;35(19).
117. Lv M, Chen M, Zhang R, et al. Manganese is critical for antitumor immune responses via cGAS-STING and improves the efficacy of clinical immunotherapy. *Cell Res*. 2020;30(11):966–979. doi:10.1038/s41422-020-00395-4

118. Liu LJ, Pan YW, Zhao CC, Huang P, Chen XY, Rao L. Boosting checkpoint immunotherapy with biomaterials. *Acs Nano*. 2023;17(4):3225–3258. doi:10.1021/acsnano.2c11691
119. Korman AJ, Garrett-Thomson SC, Lonberg N. The foundations of immune checkpoint blockade and the ipilimumab approval decennial. *Nat Rev Drug Discov*. 2022;21(2):163. doi:10.1038/s41573-022-00393-8
120. Huber V, Camisaschi C, Berzi A, et al. Cancer acidity: an ultimate frontier of tumor immune escape and a novel target of immunomodulation. *Semi Cancer Biol*. 2017;43:74–89. doi:10.1016/j.semcancer.2017.03.001
121. Bader JE, Voss K, Rathmell JC. Targeting metabolism to improve the tumor microenvironment for cancer immunotherapy. *Molecular Cell*. 2020;78(6):1019–1033. doi:10.1016/j.molcel.2020.05.034
122. Cappellesso F, Orban MP, Shirgaonkar N, et al. Targeting the bicarbonate transporter SLC4A4 overcomes immunosuppression and immunotherapy resistance in pancreatic cancer. *Nat Cancer*. 2022;3(12):1464–1483. doi:10.1038/s43018-022-00470-2
123. Fan K, Yang X, Tian FZ, et al. Acidic tumor microenvironment-activated MRI nanoprobes for modulation and visualization of anti-PD-L1 immunotherapy. *Nano Today*. 2024;54.
124. Yu M, Duan XH, Cai YJ, et al. Multifunctional nanoregulator reshapes immune microenvironment and enhances immune memory for tumor immunotherapy. *Adv Sci*. 2019;6(16). doi:10.1002/advs.201900037.
125. Chang CC, Dinh TK, Lee YA, et al. Nanoparticle delivery of MnO_2 and antiangiogenic therapy to overcome hypoxia-driven tumor escape and suppress hepatocellular carcinoma. *ACS Appl Mater Interfaces*. 2020;12(40):44407–44419. doi:10.1021/acsami.0c08473
126. Butterfield LH, Najjar YG. Immunotherapy combination approaches: mechanisms, biomarkers and clinical observations. *Nat Rev Immunol*. 2024;24(6):399–416. doi:10.1038/s41577-023-00973-8
127. Huang ZX, Wang YJ, Su C, et al. Mn-anti-CTLA4-CREKA-sericin nanotheragnostics for enhanced magnetic resonance imaging and tumor immunotherapy. *Small*. 2023.
128. Xiao B, Li DD, Xu HX, et al. An MRI-trackable therapeutic nanovaccine preventing cancer liver metastasis. *Biomaterials*. 2021;274.
129. Huang W, Shi SJ, Jiang YL, et al. Universal Fe/Mn nanoadjuvant with T1/T2 MRI self-navigation and gas generation for ideal vaccines with precise tracking. *Acs Nano*. 2023;17(16):15590–15604. doi:10.1021/acsnano.3c02309
130. Stockwell BR. Ferroptosis turns 10: emerging mechanisms, physiological functions, and therapeutic applications. *Cell*. 2022;185(14):2401–2421. doi:10.1016/j.cell.2022.06.003
131. Nie T, Zou W, Meng Z, et al. Bioactive iridium nanoclusters with glutathione depletion ability for enhanced sonodynamic-triggered ferroptosis-like cancer cell death. *Adv Mater*. 2022;34(45). doi:10.1002/adma.202206286.
132. Dixon SJ, Lemberg KM, Lamprecht MR, et al. Ferroptosis: an iron-dependent form of nonapoptotic cell death. *Cell*. 2012;149(5):1060–1072. doi:10.1016/j.cell.2012.03.042
133. Liu Y, Jiang Y, Zhang M, Tang Z, He M, Bu W. Modulating hypoxia via nanomaterials chemistry for efficient treatment of solid tumors. *Acc Chem Res*. 2018;51(10):2502–2511. doi:10.1021/acs.accounts.8b00214
134. Jiang XJ, Peng Q, Peng MJ, et al. Cellular metabolism: a key player in cancer ferroptosis. *Cancer Commun*. 2024;44(2):185–204. doi:10.1002/cac2.12519
135. Lei G, Zhuang L, Gan BY. Targeting ferroptosis as a vulnerability in cancer. *Nat Rev Cancer*. 2022;22(7):381–396. doi:10.1038/s41568-022-00459-0
136. Yang H, Yao X, Liu Y, Shen X, Li M, Luo Z. Ferroptosis nanomedicine: clinical challenges and opportunities for modulating tumor metabolic and immunological landscape. *Acs Nano*. 2023;17(16):15328–15353. doi:10.1021/acsnano.3c04632
137. Zhang C, Liu XY, Jin SD, Chen Y, Guo RH. Ferroptosis in cancer therapy: a novel approach to reversing drug resistance. *Mol Cancer*. 2022;21(1). doi:10.1186/s12943-022-01530-y
138. Chen X, Kang R, Kroemer G, Tang D. Broadening horizons: the role of ferroptosis in cancer. *Nat Rev Clin Oncol*. 2021;18(5):280–296. doi:10.1038/s41571-020-00462-0
139. Wang WM, Green M, Choi JE, et al. CD8+ T cells regulate tumor ferroptosis by targeting the system xc- during cancer immunotherapy. *J Immunol*. 2019;202(1):137.11. doi:10.4049/jimmunol.202.Supp.137.11
140. Zhang C, Bu W, Ni D, et al. Synthesis of iron nanometallic glasses and their application in cancer therapy by a localized fenton reaction. *Angew Chem-Int Ed*. 2016;55(6):2101–2106. doi:10.1002/anie.201510031
141. Chi H, Zhu G, Yin Y, et al. Dual-Responsive multifunctional "core-shell" magnetic nanoparticles promoting Fenton reaction for tumor ferroptosis therapy. *Int J Pharm*. 2022;622:121898. doi:10.1016/j.ijpharm.2022.121898
142. Xu W, Guan G, Yue R, et al. Chemical design of magnetic nanomaterials for imaging and ferroptosis-based cancer therapy. *Chem Rev*. 2025;125(4):1897–1961. doi:10.1021/acs.chemrev.4c00546
143. Zhou HM, Lu XY, Du C, et al. Cycloacceleration of reactive oxygen species generation based on exceedingly small magnetic iron oxide nanoparticles for tumor ferroptosis therapy. *Small*. 2022;18(35). doi:10.1002/smll.202202705.
144. Guo SA, Li ZH, Feng J, et al. Cycloacceleration of ferroptosis and calcicoptosis for magnetic resonance imaging-guided colorectal cancer therapy. *Nano Today*. 2022;47.
145. Huang L, Zhu JY, Xiong W, et al. Tumor-generated reactive oxygen species storm for high-performance ferroptosis therapy. *Acs Nano*. 2023;17(12):11492–11506. doi:10.1021/acsnano.3c01369
146. Yang WS, SriRamaratnam R, Welsch ME, et al. Regulation of ferroptotic cancer cell death by GPX4. *Cell*. 2014;156(1–2):317–331. doi:10.1016/j.cell.2013.12.010
147. Stockwell BR, Jiang X, Gu W. Emerging mechanisms and disease relevance of ferroptosis. *Trends Cell Biol*. 2020;30(6):478–490. doi:10.1016/j.tcb.2020.02.009
148. Seibt TM, Proneth B, Conrad M. Role of GPX4 in ferroptosis and its pharmacological implication. *Free Radic Biol Med*. 2019;133:144–152. doi:10.1016/j.freeradbiomed.2018.09.014
149. Mao C, Liu XG, Zhang YL, et al. DHODH-mediated ferroptosis defence is a targetable vulnerability in cancer. *Nature*. 2021;593(7860):586. doi:10.1038/s41586-021-03539-7
150. Wang F, Min J. DHODH tangoing with GPX4 on the ferroptotic stage. *Sign Transduc Targeted Therapy*. 2021;6(1). doi:10.1038/s41392-021-00656-7
151. Mao C, Liu X, Zhang Y, et al. DHODH-mediated ferroptosis defence is a targetable vulnerability in cancer. *Nature*. 2021;593(7860):586.

152. Ling X, Chen X, Riddell IA, et al. Glutathione-scavenging poly(disulfide amide) nanoparticles for the effective delivery of Pt(IV) prodrugs and reversal of cisplatin resistance. *Nano Lett*. 2018;18(7):4618–4625. doi:10.1021/acs.nanolett.8b01924
153. Ju E, Dong K, Chen Z, et al. Copper(II)–graphitic carbon nitride triggered synergy: improved ros generation and reduced glutathione levels for enhanced photodynamic therapy. *Angewandte Chemie International Edition*. 2016;55(38):11467–11471. doi:10.1002/anie.201605509
154. Li J, Dirisala A, Ge Z, et al. Therapeutic Vesicular Nanoreactors with Tumor-Specific Activation and Self-Destruction for Synergistic Tumor Ablation. *Angew Chem-Int Ed*. 2017;56(45):14025–14030. doi:10.1002/anie.201706964
155. Luo SW, Ma D, Wei RL, et al. A tumor microenvironment responsive nanoplatform with oxidative stress amplification for effective MRI-based visual tumor ferroptosis. *Acta Biomater*. 2022;138:518–527. doi:10.1016/j.actbio.2021.11.007
156. Wang SF, Li FY, Qiao RR, et al. Arginine-rich manganese silicate nanobubbles as a ferroptosis-inducing agent for tumor-targeted theranostics. *Acs Nano*. 2018;12(12):12380–12392. doi:10.1021/acsnano.8b06399
157. Xie SW, Sun WS, Zhang CF, et al. Metabolic control by heat stress determining cell fate to ferroptosis for effective cancer therapy. *Acs Nano*. 2021;15(4):7179–7194. doi:10.1021/acsnano.1c00380
158. Chen SJ, Yang J, Liang ZY, et al. Synergistic functional nanomedicine enhances ferroptosis therapy for breast tumors by a blocking defensive redox system. *ACS Appl Mater Interfaces*. 2023;15(2).
159. Ying W, Zhang Y, Gao W, et al. Hollow magnetic nanocatalysts drive starvation-chemodynamic-hyperthermia synergistic therapy for tumor. *Acs Nano*. 2020;14(8):9662–9674. doi:10.1021/acsnano.0c00910
160. An P, Fan F, Gu D, Gao Z, Hossain AMS, Sun B. Photothermal-reinforced and glutathione-triggered *in Situ* cascaded nanocatalytic therapy. *J Control Release*. 2020;321:734–743. doi:10.1016/j.jconrel.2020.03.007
161. Zhang Q, Guo Q, Chen Q, Zhao X, Pennycook SJ, Chen H. Highly efficient 2D NIR-II photothermal agent with fenton catalytic activity for cancer synergistic photothermal-chemodynamic therapy. *Adv Sci*. 2020;7(7).
162. Manivasagan P, Thambi T, Joe A, et al. Progress in nanomaterial-based synergistic photothermal-enhanced chemodynamic therapy in combating bacterial infections. *Pro Mater Sci*. 2024;144.
163. Pidamaimaiti G, Huang XY, Pang K, Su Z, Wang F. A microenvironment-mediated Cu_2O-MoS_2 nanoplatform with enhanced Fenton-like reaction activity for tumor chemodynamic/photothermal therapy. *New J Chem*. 2021;45(23):10296–10302. doi:10.1039/D1NJ01272J
164. Cao W, Jin MY, Yang K, et al. Fenton/Fenton-like metal-based nanomaterials combine with oxidase for synergistic tumor therapy. *J Nanobiotechnol*. 2021;19(1). doi:10.1186/s12951-021-01074-1.
165. Ying WW, Zhang Y, Gao W, et al. Hollow magnetic nanocatalysts drive starvation-chemodynamic-hyperthermia synergistic therapy for tumor. *Acs Nano*. 2020;14(8):9662–9674.
166. Wang M, Chen Q, Xu D, et al. Self-cycling redox nanoplatform in synergy with mild magnetothermal and autophagy inhibition for efficient cancer therapy. *Nano Today*. 2022;43.
167. Tang ZM, Zhang HL, Liu YY, et al. Antiferromagnetic pyrite as the tumor microenvironment-mediated nanoplatform for self-enhanced tumor imaging and therapy. *Adv Mater*. 2017;29(47). doi:10.1002/adma.201701683.
168. Liu Y, Zhen WY, Wang YH, et al. One-dimensional Fe_2P acts as a fenton agent in response to NIR II light and ultrasound for deep tumor synergetic theranostics. *Angew Chem-Int Ed*. 2019;58(8):2407–2412. doi:10.1002/anie.201813702
169. Shen JC, Rees TW, Zhou ZG, Yang SP, Ji LN, Chao H. A mitochondria-targeting magnetothermogenic nanozyme for magnet-induced synergistic cancer therapy. *Biomaterials*. 2020;251.
170. Cheng L, Yuan C, Shen SD, et al. Bottom-up synthesis of metal-ion-doped WS_2 nanoflakes for cancer theranostics. *Acs Nano*. 2015;9(11):11090–11101. doi:10.1021/acsnano.5b04606
171. Yang S, Sun B, Liu F, et al. NIR-ii imaging-guided mitochondrial-targeting organic nanoparticles for multimodal synergistic tumor therapy. *Small*. 2023;19(26).
172. Li XS, Lovell JF, Yoon J, Chen XY. Clinical development and potential of photothermal and photodynamic therapies for cancer. *Nat Rev Clin Oncol*. 2020;17(11):657–674. doi:10.1038/s41571-020-0410-2
173. Kim JY, Choi WI, Kim M, Tae G. Tumor-targeting nanogel that can function independently for both photodynamic and photothermal therapy and its synergy from the procedure of PDT followed by PTT. *J Control Release*. 2013;171(2):113–121. doi:10.1016/j.jconrel.2013.07.006
174. Sun R, Liu M, Lu J, et al. Bacteria loaded with glucose polymer and photosensitive ICG silicon-nanoparticles for glioblastoma photothermal immunotherapy. *Nat Commun*. 2022;13(1).
175. Liu B, Li C, Chen G, et al. Synthesis and optimization of MoS_2@Fe_3O_4-ICG/Pt(IV) nanoflowers for MR/IR/PA bioimaging and combined PTT/PDT/chemotherapy triggered by 808 nm laser. *Adv Sci*. 2017;4(8). doi:10.1002/advs.201600540.
176. Guo B, Feng G, Manghnani PN, et al. A porphyrin-based conjugated polymer for highly efficient in vitro and in vivo photothermal therapy. *Small*. 2016;12(45):6243–6254. doi:10.1002/smll.201602293
177. Liu H, Gao C, Xu P, et al. Biomimetic gold nanorods-manganese porphyrins with surface-enhanced Raman scattering effect for photoacoustic imaging-guided photothermal/photodynamic therapy. *Small*. 2024.
178. Hayashi K, Nakamura M, Miki H, et al. Photostable iodinated silica/porphyrin hybrid nanoparticles with heavy-atom effect for wide-field photodynamic/photothermal therapy using single light source. *A*. 2014;24(4):503–513.
179. Sun QQ, Wang Z, Liu B, et al. Self-generation of oxygen and simultaneously enhancing photodynamic therapy and MRI effect: an intelligent nanoplatform to conquer tumor hypoxia for enhanced phototherapy. *Chem Engine J*. 2020;390.
180. Li YP, Lin TY, Luo Y, et al. A smart and versatile theranostic nanomedicine platform based on nanoporphyrin. *Nat Commun*. 2014;5.
181. Wang DW, Zhang Z, Lin L, et al. Porphyrin-based covalent organic framework nanoparticles for photoacoustic imaging-guided photodynamic and photothermal combination cancer therapy. *Biomaterials*. 2019;223.
182. Akakuru OU, Xu C, Liu C, et al. Metal-free organo-theranostic nanosystem with high nitroxide stability and loading for image-guided targeted tumor therapy. *Acs Nano*. 2021;15(2):3079–3097. doi:10.1021/acsnano.0c09590
183. Song XJ, Liang C, Gong H, Chen Q, Wang C, Liu Z. Photosensitizer-conjugated albumin-polypyrrole nanoparticles for imaging-guided in vivo photodynamic/photothermal therapy. *Small*. 2015;11(32):3932–3941. doi:10.1002/smll.201500550
184. Zha ZB, Yue XL, Ren QS, Dai ZF. Uniform polypyrrole nanoparticles with high photothermal conversion efficiency for photothermal ablation of cancer cells. *Adv Mater*. 2013;25(5):777–782. doi:10.1002/adma.201202211

185. Wu K, Zhao HH, Sun ZQ, et al. Endogenous oxygen generating multifunctional theranostic nanoplatform for enhanced photodynamic-photothermal therapy and multimodal imaging. *Theranostics*. 2019;9(25):7697–7713. doi:10.7150/thno.38565
186. Xu PP, Liao GF. A novel fluorescent biosensor for adenosine triphosphate detection based on a metal-organic framework coating polydopamine layer. *Materials*. 2018;11(9).
187. Wang D, Wu H, Lim WQ, et al. A mesoporous nanoenzyme derived from metal-organic frameworks with endogenous oxygen generation to alleviate tumor hypoxia for significantly enhanced photodynamic therapy. *Adv Mater*. 2019;31(27).
188. Jiang Q, Pan M, Hu J, et al. Regulation of redox balance using a biocompatible nanoplatform enhances phototherapy efficacy and suppresses tumor metastasis. *Chem Sci*. 2021;12(1):148–157. doi:10.1039/D0SC04983B
189. Mo ZM, Qiu MJ, Zhao K, et al. Multifunctional phototheranostic nanoplatform based on polydopamine-manganese dioxide-IR780 iodide for effective magnetic resonance imaging-guided synergistic photodynamic/photothermal therapy. *J Colloid Interface Sci*. 2022;611:193–204. doi:10.1016/j.jcis.2021.12.071
190. Yan K, Mu CL, Zhang C, et al. Pt nanoenzyme decorated yolk-shell nanoplatform as an oxygen generator for enhanced multi-modality imaging-guided phototherapy. *J Colloid Interface Sci*. 2022;616:759–768. doi:10.1016/j.jcis.2022.02.042
191. Jia CY, Guo YX, Wu FG. Chemodynamic therapy via fenton and fenton-like nanomaterials: strategies and recent advances. *Small*. 2022;18(6). doi:10.1002/smll.202103868
192. Wang YD, Gao FC, Li XF, et al. Tumor microenvironment-responsive fenton nanocatalysts for intensified anticancer treatment. *J Nanobiotechnol*. 2022;20(1).
193. Zhang L, Fan Y, Yang Z, Yang M, Wong C-Y. NIR-II-driven and glutathione depletion-enhanced hypoxia-irrelevant free radical nanogenerator for combined cancer therapy. *J Nanobiotechnol*. 2021;19(1).
194. Liu Y, Zhen WY, Jin LH, et al. All-in-one theranostic nanoagent with enhanced reactive oxygen species generation and modulating tumor microenvironment ability for effective tumor eradication. *Acs Nano*. 2018;12(5):4886–4893. doi:10.1021/acsnano.8b01893
195. Zhang C, Bu WB, Ni DL, et al. Synthesis of iron nanometallic glasses and their application in cancer therapy by a localized fenton reaction. *Angew Chem-Int Ed*. 2016;55(6):2101–2106.
196. Dai YL, Yang Z, Cheng SY, et al. Toxic reactive oxygen species enhanced synergistic combination therapy by self-assembled metal-phenolic network nanoparticles. *Adv Mater*. 2018;30(8). doi:10.1002/adma.201704877.
197. Zhu HM, Cao GD, Qiang C, et al. Hollow ferric-tannic acid nanocapsules with sustained $O_2$and ROS induction for synergistic tumor therapy. *Biomater Sci*. 2020;8(14):3844–3855. doi:10.1039/D0BM00533A
198. Sheng S, Liu F, Lin L, et al. Nanozyme-mediated cascade reaction based on metal-organic framework for synergetic chemo-photodynamic tumor therapy. *J Control Release*. 2020;328:631–639. doi:10.1016/j.jconrel.2020.09.029
199. Liu Z, Yan ZW, Di YF, et al. Current advances in metal-organic frameworks for cancer nanodynamic therapies. *Coord Chem Rev*. 2023;497.
200. Tan -L-L, Li H, Qiu Y-C, et al. Stimuli-responsive metal-organic frameworks gated by pillar 5 arene supramolecular switches. *Chem Sci*. 2015;6 (3):1640–1644. doi:10.1039/C4SC03749A
201. Wu M-X, Gao J, Wang F, et al. Multistimuli responsive core-shell nanoplatform constructed from Fe_3O_4@MOF equipped with pillar 6 arene nanovalves. *Small*. 2018;14(17). doi:10.1002/smll.201704440.
202. Cai W, Wang J, Chu C, Chen W, Wu C, Liu G. Metal organic framework-based stimuli-responsive systems for drug delivery. *Adv Sci*. 2019;6 (1). doi:10.1002/advs.201801526
203. Ye YY, Zhao YF, Sun Y, Cao J. Recent progress of metal-organic framework-based photodynamic therapy for cancer treatment. *Int J Nanomed*. 2022;17:2367–2395. doi:10.2147/IJN.S362759
204. Yang L, Yu S, Yan Y, Bi S, Zhu -J-J. Upconversion nanoparticle@Au core–satellite assemblies for *in situ* amplified imaging of MicroRNA in living cells and combined cancer phototherapy. *Anal Chem*. 2022;94(19):7075–7083. doi:10.1021/acs.analchem.2c00477
205. Song X, Li F, Tian F, et al. Upconversion nanoparticle-based optogenetic nanosystem for photodynamic therapy and cascade gene therapy. *Acta Biomater*. 2023;157:538–550. doi:10.1016/j.actbio.2022.12.002
206. Song N, Fan X, Guo X, et al. A DNA/upconversion nanoparticle complex enables controlled co-delivery of CRISPR-Cas9 and photodynamic agents for synergistic cancer therapy. *Adv Mater*. 2024.
207. Wang YH, Song SY, Zhang ST, Zhang HJ. Stimuli-responsive nanotheranostics based on lanthanide-doped upconversion nanoparticles for cancer imaging and therapy: current advances and future challenges. *Nano Today*. 2019;25:38–67. doi:10.1016/j.nantod.2019.02.007
208. Cen D, Zheng Q, Zheng BZ, et al. A near-infrared light-responsive ROS cascade nanoplatform for synergistic therapy potentiating antitumor immune responses. *A*. 2023;33(9).
209. Wen S, Zhou J, Zheng K, Bednarkiewicz A, Liu X, Jin D. Advances in highly doped upconversion nanoparticles. *Nat Commun*. 2018;9(1):9. doi:10.1038/s41467-017-01881-x
210. Li Y, Chen G. Upconversion nanoparticles for cancer therapy. *Adv Nanobiomed Res*. 2022;2(12). doi:10.1002/anbr.202200092
211. Hu P, Wu T, Fan WP, et al. Near infrared-assisted Fenton reaction for tumor-specific and mitochondrial DNA-targeted photochemotherapy. *Biomaterials*. 2017;141:86–95. doi:10.1016/j.biomaterials.2017.06.035
212. Xu JT, Shi RP, Chen GY, et al. All-in-one theranostic nanomedicine with ultrabright second near-infrared emission for tumor-modulated bioimaging and chemodynamic/photodynamic therapy. *Acs Nano*. 2020;14(8):9613–9625. doi:10.1021/acsnano.0c00082
213. Ling B, Wang YG, Mi R, et al. Multimodal imaging and synergetic chemodynamic/photodynamic therapy achieved using an $NaGdF_4$,Yb,Er@ NaGdF $NaGdF_4$,Yb,Tm@ $NaGdF_4$@Fe-MOFs nanocomposite. *Chem-Asian J*. 2022;17(14). doi:10.1002/asia.202200161.
214. Ai YJ, Hu ZN, Liang XP, Sun HB, Xin HB, Liang QL. Recent advances in nanozymes: from matters to bioapplications. *A*. 2022;32(14).
215. Chu DC, Qu H, Huang XP, et al. Manganese amplifies photoinduced ROS in toluidine blue carbon dots to boost MRI guided chemo/ photodynamic therapy. *Small*. 2024;20(4). doi:10.1002/smll.202304968.
216. Li MY, Huo LL, Zeng J, et al. Surface engineered iron oxide nanozyme for synergistic chemodynamic/ photodynamic therapy with glutathione depletion and hypoxia relief. *Chem Engine J*. 2022;440.
217. Ge R, Liu CW, Zhang X, et al. Photothermal-activatable Fe_3O_4 superparticle nanodrug carriers with PD-L1 immune checkpoint blockade for anti-metastatic cancer immunotherapy. *ACS Appl Mater Interfaces*. 2018;10(24):20342–20355. doi:10.1021/acsami.8b05876
218. Yan MM, Liu YJ, Zhu XH, et al. Nanoscale reduced graphene oxide-mediated photothermal therapy together with IDO inhibition and PD-L1 blockade synergistically promote antitumor immunity. *ACS Appl Mater Interfaces*. 2019;11(2):1876–1885. doi:10.1021/acsami.8b18751

219. Dias AMM, Courteau A, Bellaye PS, et al. Superparamagnetic iron oxide nanoparticles for immunotherapy of cancers through macrophages and magnetic hyperthermia. *Pharmaceutics*. 2022;14(11):2388. doi:10.3390/pharmaceutics14112388
220. Chang MY, Hou ZY, Wang M, et al. Recent advances in hyperthermia therapy-based synergistic immunotherapy. *Adv Mater*. 2021;33(4). doi:10.1002/adma.202004788.
221. Ma Y, Zhang Y, Li X, et al. Near-infrared II phototherapy induces deep tissue immunogenic cell death and potentiates cancer immunotherapy. *Acs Nano*. 2019;13(10):11967–11980. doi:10.1021/acsnano.9b06040
222. Huang L, Li Y, Du Y, et al. Mild photothermal therapy potentiates anti-PD-L1 treatment for immunologically cold tumors via an all-in-one and all-in-control strategy. *Nat Commun*. 2019;10(1):10. doi:10.1038/s41467-018-07709-6
223. Fang XY, Wu XL, Li ZD, et al. Biomimetic anti-PD-1 peptide-loaded 2D $FePSe_3$ nanosheets for efficient photothermal and enhanced immune therapy with multimodal MR/PA/thermal imaging. *Adv Sci*. 2021;8(2). doi:10.1002/advs.202003041.
224. Li MH, Lin C, Shen AJ, et al. A smart responsive nanotheranostic system for MRI of tumor response to immunotherapy and enhanced synergism of thermo-immunotherapy. *Adv Func Mater*. 2024.
225. Zeng WF, Li ZM, Huang QL, et al. Multifunctional mesoporous polydopamine-based systematic delivery of STING agonist for enhanced synergistic photothermal-immunotherapy. *A*. 2024;34(1).
226. Liu DC, Fu LY, Gong LL, et al. Proton-gradient-driven porphyrin-based liposome remote-loaded with imiquimod as in situ nanoadjuvants for synergistically augmented tumor photoimmunotherapy. *ACS Appl Mater Interfaces*. 2024;16(7):8403–8416. doi:10.1021/acsami.3c17133
227. Liu D, Fu L, Gong L, et al. Proton-gradient-driven porphyrin-based liposome remote-loaded with imiquimod as in situ nanoadjuvants for synergistically augmented tumor photoimmunotherapy. *ACS Appl Mater Interfaces*. 2024;16(7):8403–8416.
228. Wang H, Yang X, Hu C, et al. Programmed polymersomes with spatio-temporal delivery of antigen and dual-adjuvants for efficient dendritic cells-based cancer immunotherapy. *Chin Chem Lett*. 2022;33(9):4179–4184. doi:10.1016/j.cclet.2022.02.022
229. Song XX, Zhang C, Xing MY, et al. Immunological gadolinium-doped mesoporous carbon nanoparticles for tumor-targeted MRI and photothermal-immune co-therapy. *J Mat Chem B*. 2023;11(26):6147–6158. doi:10.1039/D3TB00595J
230. Zhang F, Lu GH, Wen XL, et al. Magnetic nanoparticles coated with polyphenols for spatio-temporally controlled cancer photothermal/immunotherapy. *J Control Release*. 2020;326:131–139. doi:10.1016/j.jconrel.2020.06.015
231. Qin S-Y, Cheng Y-J, Lei Q, Zhang A-Q, Zhang X-Z. Combinational strategy for high-performance cancer chemotherapy. *Biomaterials*. 2018;171:178–197. doi:10.1016/j.biomaterials.2018.04.027
232. Lu N, Huang P, Fan W, et al. Tri-stimuli-responsive biodegradable theranostics for mild hyperthermia enhanced chemotherapy. *Biomaterials*. 2017;126:39–48. doi:10.1016/j.biomaterials.2017.02.025
233. Liu CC, Li CC, Jiang S, Zhang C, Tian Y. pH-responsive hollow Fe-gallic acid coordination polymer for multimodal synergistic-therapy and MRI of cancer. *Nanoscale Adv*. 2021;4(1):173–181. doi:10.1039/D1NA00721A
234. Wang XY, Li CW, Qian JC, et al. NIR-II responsive hollow magnetite nanoclusters for targeted magnetic resonance imaging-guided photothermal/chemo-therapy and chemodynamic therapy. *Small*. 2021;17(31). doi:10.1002/smll.202100832.
235. Zhang MY, Liu XJ, Luo Q, et al. Tumor environment responsive degradable CuS@mSiO2@MnO2/DOX for MRI guided synergistic chemo-photothermal therapy and chemodynamic therapy. *Chem Engine J*. 2020;389.
236. Shi YP, Zhou MY, Zhang Y, Wang YF, Cheng JL. MRI-guided dual-responsive anti-tumor nanostructures for synergistic chemo-photothermal therapy and chemodynamic therapy. *Acta Biomater*. 2023;158:571–582. doi:10.1016/j.actbio.2022.12.053
237. Pan YB, Zhu Y, Xu CX, et al. Biomimetic yolk-shell nanocatalysts for activatable dual-modal-image-guided triple- augmented chemodynamic therapy of cancer. *Acs Nano*. 2022;16(11):19038–19052. doi:10.1021/acsnano.2c08077
238. Wang Y, Zhang F, Lin HM, Qu FY. Biodegradable hollow $MoSe_2/Fe_3O_4$ nanospheres as the photodynamic therapy-enhanced agent for multimode CT/MR/IR imaging and synergistic antitumor therapy. *ACS Appl Mater Interfaces*. 2019;11(47):43964–43975. doi:10.1021/acsami.9b17237
239. Wu YF, Chen ZX, Yao ZP, et al. Black phosphorus quantum dots encapsulated biodegradable hollow mesoporous MnO_2: dual-modality cancer imaging and synergistic chemo-phototherapy. *A*. 2021;31(41).
240. Geng ZM, Chen FJ, Wang XY, Wang L, Pang Y, Liu JY. Combining anti-PD-1 antibodies with Mn^{2+}-drug coordinated multifunctional nanoparticles for enhanced cancer therapy. *Biomaterials*. 2021;275.
241. He LY, Wang JF, Zhu PY, et al. Intelligent manganese dioxide nanocomposites induce tumor immunogenic cell death and remould tumor microenvironment. *Chem Engine J*. 2023;461.
242. Kong CQ, Xu BH, Qiu GH, et al. Multifunctional nanoparticles-mediated PTT/PDT synergistic immune activation and antitumor activity combined with anti-PD-L1 immunotherapy for breast cancer treatment. *Int J Nanomed*. 2022;17:5391–5411. doi:10.2147/IJN.S373282
243. Song XR, Liu C, Wang N, et al. Delivery of CRISPR/Cas systems for cancer gene therapy and immunotherapy. *Adv Drug Delivery Rev*. 2021;168:158–180. doi:10.1016/j.addr.2020.04.010
244. Ansari I, Chaturvedi A, Chitkara D, Singh S. CRISPR/Cas mediated epigenome editing for cancer therapy. *Semi Cancer Biol*. 2022;83:570–583. doi:10.1016/j.semcancer.2020.12.018
245. Liu H, Mu MY, Hou YB, et al. A novel CRISPR/Cas9-encapsulated biomimetic manganese sulfide nanourchins for targeted magnetic resonance contrast enhancement and self-enhanced chemodynamics-gene-immune synergistic tumor therapy. *Adv Func Mate*. 2024.
246. Tan P, Chen XT, Zhang H, Wei Q, Luo K. Artificial intelligence aids in development of nanomedicines for cancer management. *Semi Cancer Biol*. 2023;89:61–75. doi:10.1016/j.semcancer.2023.01.005
247. Mullowney MW, Duncan KR, Elsayed SS, et al. Artificial intelligence for natural product drug discovery. *Nat Rev Drug Discov*. 2023;22(11):895–916. doi:10.1038/s41573-023-00774-7
248. Liang GS, Fan WG, Luo H, Zhu X. The emerging roles of artificial intelligence in cancer drug development and precision therapy. *Biomed Pharmacother*. 2020;128.